Valorization of mixed polyolefin waste stream by addition of few-layer graphene

by

S M Nourin SULTANA

MANUSCRIPT-BASED THESIS PRESENTED TO ÉCOLE DE TECHNOLOGIE SUPÉRIEURE IN PARTIAL FULFILLEMENT FOR THE DEGREE OF DOCTOR OF PHILOSOPHY
Ph.D.

MONTREAL, AUGUST 7, 2024

ÉCOLE DE TECHNOLOGIE SUPÉRIEURE
UNIVERSITÉ DU QUÉBEC

BOARD OF EXAMINERS

THIS THESIS HAS BEEN EVALUATED

BY THE FOLLOWING BOARD OF EXAMINERS

Mrs. Nicole R. Demarquette, Thesis Supervisor
Department of Mechanical Engineering, at École de Technologie Supérieure

Mr. Éric David, Thesis Co-supervisor
Department of Mechanical Engineering, École de Technologie Supérieure

Mrs. Giovanna Gutiérrez, Thesis Co-supervisor
Research and Development, NanoXplore Inc.

Mrs. Emna Helal, Thesis Co-supervisor
Department of Mechanical Engineering, École de Technologie Supérieure

Mr. Bora Ung, President of the Board of Examiners
Department of Electrical Engineering, École de Technologie Supérieure

Mr. Ricardo Zednik, Member of the jury
Department of Mechanical Engineering, École de Technologie Supérieure

Mr. Denis Rodrigue, External Evaluator
Department of Chemical Engineering, Université Laval

THIS THESIS WAS PRENSENTED AND DEFENDED

IN THE PRESENCE OF A BOARD OF EXAMINERS AND PUBLIC

ON JULY 16, 2024

AT ÉCOLE DE TECHNOLOGIE SUPÉRIEURE

ACKNOWLEDGMENT

I would like to express my gratitude to my PhD thesis supervisor, Professor Nicole R. Demarquette, for her support, guidance, and encouragement throughout my PhD journey. I extend my sincere thanks to my co-supervisor, Professor Eric David, and my industrial co-supervisor, Dr. Emna Helal, for their continuous support and constructive feedback, which have been invaluable to my research.

I would also like to thank the members of the jury, Prof. Bora Ung and Prof. Ricardo Zednik from École de Technologie Supérieure, and Prof. Denis Rodrigue from Université Laval, for agreeing to evaluate this work during the defense.

I am grateful to the following organizations for their support, which has enabled me to continue this work: NanoXplore Inc., Natural Sciences and Engineering Research Council, PRIMA Quebec, Fonds de Recherche du Québec-Nature et Technologies, and Quebec Circular Economy Research Network.

I am profoundly grateful to my husband, Md. Shahnewaz Hossain, for his love, patience, and understanding, and to my son, Noaz Hossain, whose presence brought immense joy and motivation to my life during this challenging journey. My sincerest appreciation goes to my parents, whose prayers and moral support have been a constant source of strength for me.

I also wish to acknowledge the supporting professionals and facilities at ETS Montreal for providing the necessary resources and a conducive environment for my research. Finally, I am deeply thankful to my friends Daria, Camila, Samira, and Mitasha at ETS Montreal, for their friendship, support, and encouragement throughout this journey.

To all of you, thank you.

Valorisation d'un flux de déchets mixtes de polyoléfines par l'ajout de graphène à quelques couches

S M Nourin SULTANA

RESUME

Cette thèse vise à surcycler un flux de déchets de polyoléfines mélangés (MPWS) par l'ajout de graphène en quelques couches (FLG) disponible dans le commerce, produit par exfoliation mécanochimique du graphite.

L'étude a commencé par la conception de composites de mélanges de polyéthylène (PE)/polypropylène (PP)/FLG via un mélange à l'état fondu, afin d'avoir une vue d'ensemble de l'influence du FLG sur un système de mélange de polyoléfines contrôlé. La caractérisation des composites remplis de FLG comprenait l'analyse de la conductivité électrique, l'évolution morphologique en condition fondue et sous déformation induite par cisaillement, les propriétés mécaniques et la stabilité aux UV. Fait intéressant, une petite quantité de FLG, 4 % en poids et 5 % en poids de FLG a induit un comportement semi-conducteur dans les mélanges PE/PP - 60/40 et PE/PP - 20/80, respectivement. La déformation induite par cisaillement n'a pas affecté la conductivité électrique, indiquant la stabilité du réseau de FLG au sein du composite. De plus, seulement 1 % en poids de FLG a permis de maintenir les propriétés mécaniques d'origine dans les composites de polyoléfines exposés aux UV. Un effet stabilisant aux UV comparativement prononcé a été observé dans les mélanges riches en PE par rapport aux mélanges riches en PP.

Par la suite, l'impact de l'ajout de FLG sur la processabilité et les propriétés mécaniques du MPWS a été examiné. Les résultats ont indiqué que l'ajout de FLG a facilité le renforcement des composites MPWS sans compromettre la processabilité, une caractéristique notable mais inhabituelle des charges rigides. Une augmentation maximale de la résistance à la traction (de 9 %) et de la résistance à la flexion (de 23 %) a été observée dans les composés contenant MPWS, 4 % en poids de FLG et 9 % en poids de PP vierge. Des concentrations plus élevées de FLG (>4 % en poids) dans le MPWS ont conduit à des améliorations des propriétés de traction et de flexion tout en maintenant la résistance à l'impact. Notamment, 10 % en poids de FLG ont augmenté la résistance à l'impact de 9 %, attribuée à la résistance du FLG à la propagation des fissures.

Ensuite, l'effet photo-stabilisant du FLG a été examiné dans le MPWS et dans un mélange PE/PP vierge. Malgré l'état probablement pré-dégradé du MPWS, les composites exposés aux UV contenant 1, 4, 7 et 10 % en poids de FLG ont conservé environ 60 %, 70 %, 80 % et 90 % de la ductilité d'origine. Le MPWS non rempli n'a retenu que 20 % de sa ductilité d'origine après l'exposition aux UV. Pour les mélanges de polyoléfines vierges, la présence de 0,5 % en poids était suffisante pour maintenir la finition de surface et les propriétés mécaniques contre la photodégradation. Apparemment, le MPWS nécessitait des concentrations plus élevées de FLG pour atteindre une rétention de propriétés comparable, probablement en raison de la mauvaise dispersion du FLG dans le MPWS et des incertitudes associées telles que les impuretés, la pré-dégradation et la polydispersité. Par conséquent, le concept de préconditionnement des polyoléfines vierges avec une concentration minimale de FLG avant leur intégration dans des applications pratiques se pose, nécessitant une évaluation de faisabilité plus approfondie. Globalement, cette étude met en lumière le potentiel du FLG en tant qu'additif polyvalent pour améliorer les caractéristiques des mélanges de polyoléfines, offrant une solution prometteuse et économiquement viable pour atténuer la pollution plastique.

Mots-clés: graphène, conductivité électrique, polyoléfine, déchets, processabilité, photodégradation, photoprotection, propriétés mécaniques

Valorization of mixed polyolefin waste stream by addition of few-layer graphene

S M Nourin SULTANA

ABSTRACT

This thesis aimed at upcycling a mixed polyolefin waste stream (MPWS) by addition of commercially available few-layer graphene (FLG), produced via mechanochemical exfoliation of graphite.

The study commenced with designing polyethylene (PE)/ polypropylene (PP)/ FLG blend composites via melt-mixing, to have a basic overview of the influence of FLG on a controlled polyolefin blend system. Characterization of FLG-filled composites included the analysis of electrical conductivity, morphological evolution in molten condition and under shear-induced deformation, mechanical properties, and UV stability. Interestingly, a small amount of FLG, 4 wt.% and 5 wt.% of FLG induced electro dissipative behavior in PE/PP – 60/40 and PE/PP – 20/80 blends, respectively. Shear-induced deformation in molten condition did not affect the electrical conductivity, indicating the stability of the FLG network within the composite. Additionally, 1 wt.% of FLG maintained original mechanical properties in UV-exposed polyolefin composites. Comparatively pronounced UV stabilizing effect was observed in PE-rich blends than in PP-rich blends.

Thereafter, the impact of adding FLG on the processability and mechanical properties of MPWS was examined. Results indicated that the addition of FLG facilitated the reinforcement of MPWS composites without compromising processability, a notable but unusual feature of rigid fillers. A maximum increase in tensile strength (by 9%) and flexural strength (by 23%) was observed in compounds containing MPWS, 4 wt.% of FLG, and 9 wt.% of prime PP. Higher FLG concentrations (>4 wt.%) in MPWS led to improved tensile and flexural properties while maintaining impact strength. Notably, 10 wt.% of FLG increased impact strength by 9%, attributed to FLG's resistance to crack propagation.

Subsequently, the photo stabilizing effect of FLG was examined in both MPWS and a prime PE/PP blend. Despite the likely predegraded state of MPWS, UV-exposed composites containing 1, 4, 7, and 10 wt.% of FLG retained approximately 60%, 70%, 80%, and 90% of the original ductility, respectively. Unfilled MPWS retained only 20% of its original ductility after UV exposure. For prime polyolefin blends, presence of 0.5 wt.% was adequate to maintain surface finish and mechanical properties against photodegradation. Apparently, MPWS required higher FLG concentrations to achieve comparable property retention, possibly due to FLG's poor dispersion in MPWS and associated uncertainties such as impurities, pre-degradation, and polydispersity. Therefore, the concept of preconditioning prime polyolefins with a minimal concentration of FLG before their integration into practical applications arises, necessitating further feasibility assessment. Overall, this study highlights the potential of FLG as a versatile additive for improving the features of polyolefin blends, offering a promising and economically viable solution to mitigate plastic pollution.

Keywords: graphene, electrical conductivity, polyolefin, waste, processability, photodegradation, photoprotection, mechanical properties

TABLE OF CONTENTS

LIST OF TABLES

LIST OF FIGURES

LIST OF ABREVIATIONS

ABS	Acrylonitrile butadiene styrene
ABS-g-MAH	Maleic anhydride grafted ABS
ATR-FTIR	Attenuated total reflectance - Fourier transform infrared spectroscopy
BDS	broadband dielectric spectrometer
CB	Carbon black
CI	Carbonyl index
CNT	Carbon nanotubes
DSC	Differential scanning calorimetry
EB	Elongation at break
EMI	Electromagnetic interference
EPDM	Ethylene propylene diene monomer
EPR	Electron paramagnetic resonance
EVA	Ethylene vinyl acetate
FLG	Few-layer graphene
GNPs	Graphene nano plateletes
GO	Graphene oxide
GWP	Global warming potential
HDPE	High density polyethylene
HIPS	High impact polystyrene
IS	Impact strength
LDPE	Low-density polyethylene
LLDPE	Liner low-density polyethylene
MB	Master batch
MFI	Melt flow index
MPWS	Mixed polyolefins waste stream
PBAT	Polybutylene adipate terephthalate
PBT	Polybutylene terephthalate
PC	Polycarbonate

PCL	Polycaprolactone
PE	Polyethylene
PEMA	Poly(ethyl methacrylate)
PET	Polyethylene tetraphthalate
PLA	Polylactic acid
PP	Polypropylene
PS	Polystyrene
PVAc	Polyvinyl acetate
PVC	Polyvinyl chloride
PVDF	Polyvinylidene fluoride
PVME	Polyvinyl methyl ether
SAN	Styrene acrylonitrile
SAOS	Small amplitude oscillatory shear
SD	Standard deviation
SEBS	Styrene-ethylene-butylene-styrene
SEM	Scanning electron microscope
TEU	Total energy use
UV	Ultraviolet

LIST OF SYMBOLS

α	Interfacial tension
$\dot{\gamma}$	Applied shear rate
γ_{1-2}	Surface tensions of component 1 and component
ρ	Viscosity ratio
η_m	Viscosity of matrix phase
η_d	viscosity of dispersed phase
C_a	Capillary number
C_{ac}	Critical Capillary number
HO_2^o	Hydroperoxy radicals
O_2	Oxygen molecules
OH^o	Hydroxyl radicals
ΔH_m	Melting enthalpy
R^o	Alkyl radicals
RO^o	Alkyl oxy radical
ROO^o	Alkyl peroxyl radical
$ROOH$	Hydroperoxides
R_v	Volume average radius
W_{1-2}	Wetting coefficient

INTRODUCTION

0.1 Context of the Research

Nowadays, the reliance on plastic products has surged. This trend is driven by the lightweight, chemical inertness, easy moldability and processability of thermoplastics. As a result, plastic waste accumulation has skyrocketed. A survey (Petigny et al., 2019) by Deloitte on plastic waste management in Canada reported that the majority of the waste is just dumped into the environment, resulting in an acute plastic pollution and a loss of billions of dollars. Therefore, research initiatives (Fang et al., 2013; Karaagac et al., 2021; Kazemi et al., 2015; Khadri Diallo et al., 2022; Najafi et al., 2006) to upgrade the value of this plastic waste, with no base value or minimum worth, are indispensable. Any effective strategy to improve the properties of plastic waste to channel back to regular applications (Jubinville et al., 2020) would reduce the plastic waste accumulation, and demand for new plastic production. Thereby, it would be a potential step toward the protection and conservation of the environment.

Remarkably, around half of the global plastic waste comprises of the mixture of polyolefins (Singh et al., 2023). Since polyolefins are lighter than water, mixture of polyolefins can be easily separated from other waste plastics in a simple water-based float-sink tank (Ragaert et al., 2017). This separated polyolefin mixture is termed as mixed polyolefin waste stream (MPWS). Further separation of this mixture into individual polyethylene (PE) and polypropylene (PP) is not economically feasible due to the complications, related to their comparable densities. Therefore, blending the mixture and using them as is, appears to be the most straightforward recycling solution. However, this simple solution is not enough to overcome the detrimental effect of polymer aging, presence of impurities, variations in molecular structure and weight on the properties of MPWS. Hence, an effective strategy is imperative to improve the properties of MPWS. This would enable the utilization of a significant portion of plastic waste, with no commercial value and would otherwise be ended up in landfills. This is a serious environmental concern to address, which motivates this research work.

In this context, mechanical recycling emerges as the cheapest and most straightforward method to reintegrate waste streams into practical applications. Several studies are available in literature (Fang et al., 2013; Karaagac et al., 2021; Kazemi et al., 2015; Khadri Diallo et al., 2022; Najafi et al., 2006), involving the mixing of MPWS with prime polymers, copolymers, and a few rigid fillers. Besides, the incorporation of carbonaceous fillers (Chaudhuri et al., 2017; Chiu et al., 2021; Cui et al., 2016; dos Anjos et al., 2022; dos Anjos et al., 2022; Horrocks et al., 1999; Lago et al., 2020; López-Martínez et al., 2022; Nunes et al., 2021) into polymeric materials is a rapidly growing research field with immense potential for enhancing polymer properties. Among these fillers, graphene stands out as a highly promising candidate (Chakraborty & Hashmi, 2018; Choi et al., 2010; Kuilla et al., 2010) due to its two-dimensional geometry, outstanding reinforcing efficiency, excellent electrical conductivity, and antioxidant properties. However, commercializing nanographene on a large scale poses a significant challenge (Batista et al., 2019). To address this, mechanochemical exfoliation of graphite to produce graphene has been attempted by NanoXplore Inc. in compliance with Canadian environmental regulations. This process successfully produces low-cost few-layer graphene at a large scale (Moghimian et al., 2017). Additionally, recent studies have confirmed that few-layer graphene (FLG), with 6 to 10 layers, does not exhibit the adverse dermal, inhalation, and gene toxicity effects associated with other nanocarbons (Moghimian & Nazarpour, 2020). This grade of FLG has been reported to improve the electrical conductivity (Kurusu et al., 2018), mechanical strength (Batista et al., 2019; Ferreira Junior et al., 2022; Khadri Diallo et al., 2022), and photostability (Karimi et al., 2023) of prime thermoplastics.

However, the potential effect of adding FLG to improve the properties of a MPWS has not been thoroughly investigated. Therefore, this study aims to analyze the potential of commercially available FLG to enhance the properties of a mixed polyolefin waste stream.

0.2 Objectives

The main objective of this research was to improve the properties of MPWS by the addition of commercially available FLG. The primary objective of this study was divided into three secondary objectives, outlined as follows :

1. To examine the impact of a commercial FLG on the properties (morphology, electrical conductivity, mechanical properties, and resistance to photodegradation) of prime polyolefin blends.
2. To determine the influence of FLG, either alone or combined with prime polyolefins, on the morphology, processability, and reinforcement of MPWS.
3. To assess the photostabilizing effectiveness of FLG in both MPWS and prime PE/PP blends.

0.3 Approach and Methodology

To achieve the research objective, a systematic approach was implemented. Initially, an extensive investigation was conducted to examine the effects of adding FLG on the morphology, electrical conductivity, mechanical properties, and ultraviolet (UV) protection of control polyolefin blends. The independent variables of this study included the composition of the PE/PP blend, FLG concentration, and the order of FLG addition during melt-mixing. The results of this study are presented in Chapter 2 of this thesis.

Based on the findings of the initial study, FLG was introduced into MPWS to explore its impact on the properties of the polyolefin waste stream. Various concentrations of FLG, both individually and in combination with prime polymers, were melt-mixed with MPWS to investigate the mechanical reinforcement of the waste-recovered polyolefin composite. This investigation is detailed in Chapter 3 of the thesis and was subsequently published in the journal, Crystals.

In addition, the potential application of FLG as a photostabilizing agent was examined in MPWS and prime PE/PP blends to develop durable polyolefin composites suitable for outdoor applications, such as containers, bumpers, dashboards, garden furniture, playground equipment, bottle crates, etc. The findings of this study are presented in Chapter 4 of the thesis and were published in the Recycling journal. Figure 0.1 illustrates the approach of the PhD project in brief:

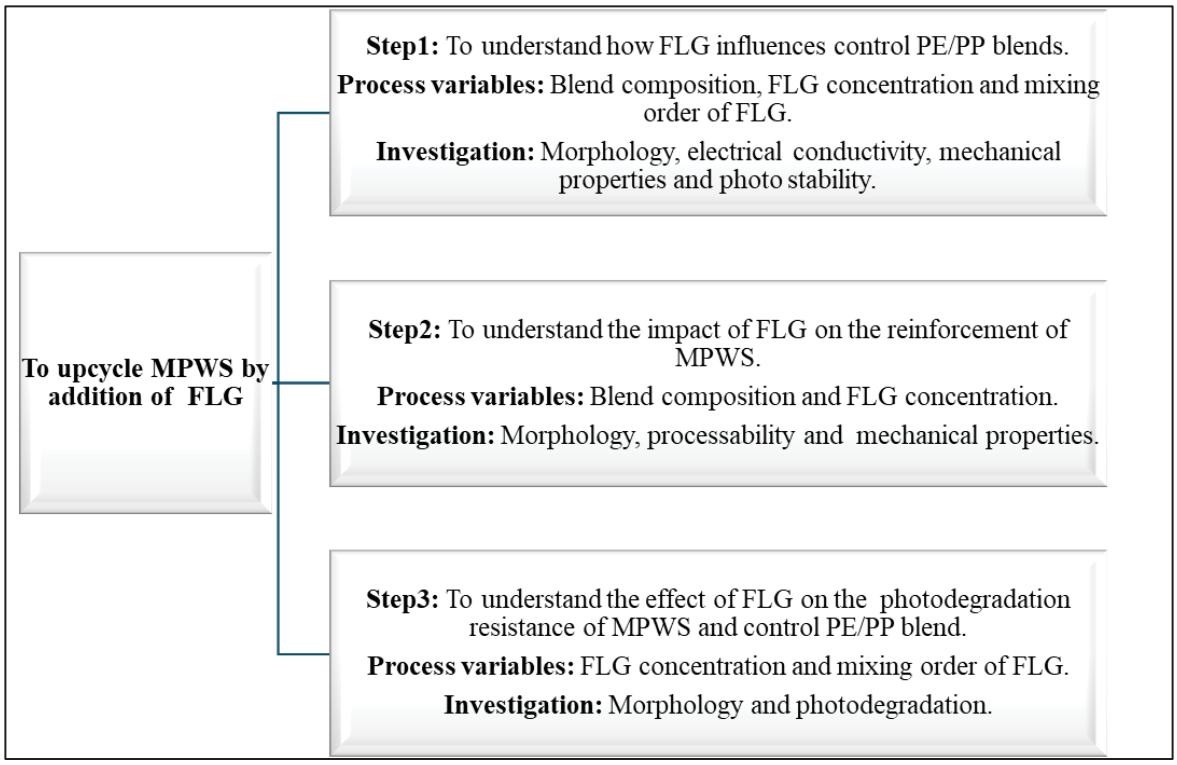

Figure 0.1 The outline of the PhD project

0.4 Organization of the PhD thesis

This thesis consists of six main chapters. After this Introduction, a brief literature review is presented. In that chapter, the importance and strategies of mechanical recycling of MPWS are discussed based on the findings from the literature. Moreover, the potential of graphene to improve the properties of polymer is also addressed. The next three chapters are articles which

correspond to the secondary objectives of this thesis. Finally, the conclusions of this investigation as well the recommendations for future work are reported at the end of this thesis.

Chapter 2 presents the paper titled “The Influence of a Commercial Few-Layer Graphene on Electrical Conductivity, Mechanical Properties, and Photodegradation Resistance of Polyolefin Blends,” which is submitted to Crystals for publication. This study examines the impact of FLG on the electrical conductivity, mechanical properties, and UV protection of polyolefin blend composites. The sample preparation involved mixing various concentrations of FLG with either the PE or PP phase, followed by melt blending with the corresponding phase.

Chapter 3 showcases the paper titled “Effect of Few-Layer Graphene on the Properties of Mixed Polyolefin Waste Stream”, published in Crystals. This study demonstrates the influence of FLG addition on the processability and mechanical properties of MPWS. Three types of compounds were investigated: MPWS with FLG; blends of MPWS with prime polyethylene (PE) or polypropylene (PP) or PP copolymer; and MPWS with both the prime polymer and FLG.

Chapter 4, details the paper titled “The Influence of a Commercial Few-Layer Graphene on the Photodegradation Resistance of a Waste Polyolefins Stream and Prime Polyolefin Blends”, published in Recycling. This study investigated the photostabilizing role of FLG in MPWS and prime polyolefin blends, with a focus on retarding the photodegradation of polyolefins through FLG addition.

In conclusion, a summary of the research findings, along with concluding remarks on the significance of the work are provided. This part also addresses research limitations and provides suggestions for the potential future studies to address these limitations.

Additionally, the thesis includes three annexes at the end, each providing supplementary information related to the articles discussed in chapters 2, 3, and 4, respectively.

CHAPTER 1

POTENTIALS OF GRAPHENE TOWARDS UPCYCLING OF MIXED POLYOLEFIN WASTE STREAM

Chapter outline: This chapter provides a comprehensive overview of the context of this work, starting with the motivation behind the study. It includes a detailed definition of mixed polyolefin waste streams (MPWS) and the fundamental concepts of immiscible polymer blend composites. The chapter then covers various aspects of MPWS recycling, with a particular focus on mechanical recycling. Following this, it delves into the possibilities offered by graphene, explaining the chemical structure and types of graphene. In addition, the potential benefits of incorporating graphene into polymer blend composites have been mentioned. The chapter concludes by outlining the approach taken in this study to investigate the influence of graphene in enhancing MPWS properties.

1.1 Motivation

Recently, polymers have garnered more attention than metals in both domestic and industrial applications due to their lighter weight, lower corrosiveness, and easier processability. However, once the shelf life or demand for plastic material diminishes, one of the common and straightforward disposal methods involves dumping them into landfills (Siddiqui & Pandey, 2013). Since most of the polymers are chemically inert, these wastes persist in the environment indefinitely (Phuong et al., 2016). Consequently, plastic pollution is an inevitable impact of the growing reliance on plastic materials. This escalating environmental concern stemming from plastic usage has sparked significant research interest in the recovery of plastic waste (Grigore, 2017; Maris et al., 2018; More Recycling for the Canadian Plastics Industry Association, 2018; Ragaert et al., 2017, 2020; Schyns & Shaver, 2020; Silva & Wiebeck, 2020). Recovery of plastic waste would increase the lifespan of plastic materials. In turn, the demand for new plastic and the accumulation of plastic waste would be reduced. Hence, scientific studies aimed at enhancing the properties of plastic waste with minimal intrinsic

value are gaining more attention. A brief review of MPWS, associated upcycling strategies, and the potential of graphene in the mechanical upcycling of MPWS has been presented.

1.2 Definition of MPWS

Once the plastic waste arrives at the sorting center, it undergoes initial manual sorting. Afterwards, this challenging mixture of plastic waste undergoes a series of treatments including washing, grinding, and separation (Ragaert et al., 2017). Primarily, the process commences by shredding the materials into small pieces. The waste then proceeds to a washer where rocks, metals, glass, and inorganic wastes are separated and removed. The shredded and washed particles are directed to a density-based float-sink separation facility. Float-sink separation, using water as a flotation agent, is a relatively cost-effective method for sorting shredded flakes (Wang et al., 2015). During this stage, polymers with densities below 1 g/cm^3 (such as unfilled PP and PE) float, while all other polymers (such as PS, PET, PVC, ABS, etc.) sink. The float fraction, comprising PP + PE, is referred to as a mixed polyolefin waste stream (MPWS) (Paben, 2016).

It is worth noting that nearly half of the global plastic waste (Singh et al., 2023) consists of MPWS. The polymers within MPWS are lighter than water, and their density ranges often overlap. Consequently, separating these polymers into mono-streams is seldom feasible and tends to be expensive (Ragaert et al., 2017). Thus, effectively upcycling of MPWS is financially more viable than upgrading individually recovered PE or PP. Additionally, typical uncertainties associated with MPWS include, but are not limited to, uncertain composition, unknown molecular weight distribution, phase separation, and the presence of impurities (Larsen et al., 2021). These uncertainties compromise the properties of MPWS, rendering it unsuitable for direct use. Hence, investigations to upcycle MPWS are necessary.

1.2.1 General Overview of Immiscible Polymer Blend Composites

Given that MPWS predominantly comprises immiscible polyethylene (PE) and polypropylene (PP), it is imperative to possess a foundational understanding of the key factors influencing the properties of immiscible polymer blend systems. The bend morphology and localization of filler in an immiscible blend composite are crucial factors in tailoring composites with desired properties. The final properties of composites are directly related to blend morphology and filler localization.

1.2.2 Blend Morphology

Depending on the composition, an immiscible polymer blend may form droplet-dispersed, co-continuous or lamellar type of morphology, as shown in Figure 1.1. This microstructure or phase morphology of polymer blend composite is directly related to the final properties of the system. For example, conductive filler-filled co-continuous blend morphology is suitable for obtaining improved electrical conductivity of the composite.

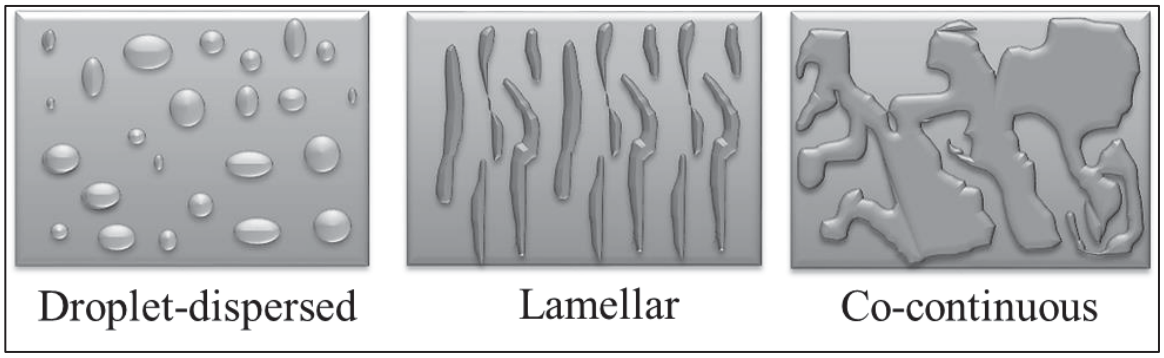

Figure 1.1 Typical obtainable morphology with an immiscible polymer blend

1.2.2.1 Localization of Filler

In an immiscible polymer blend composite, the filler may represent selective localization based on competing thermodynamic affinity. This selective localization of conductive filler in a co-

continuous blend composite has been reported to be beneficial in obtaining higher electrical conductivity at a lower concentration of filler. It is worth mentioning that the localization of filler is governed by the comparative thermodynamic and kinetic factors.

- **Thermodynamic Factor**

The Young-Laplace equation, originally proposed for a solid-liquid interface, is used as a basis to estimate the wettability co-efficient for a filler-polymer system. In this case, the harmonic or geometric mean correlation (S. Wu, 1971) for materials' surface tension can be combined in the equation 1.1. This equation has been used widely (Göldel et al., 2009; Pötschke et al., 2008; Masao Sumita et al., 1991) to predict the localization of solid/rigid fillers in an immiscible polymer blend system:

$$W_{1-2} = \frac{\gamma_{\text{polymer2-filler}} - \gamma_{\text{polymer1-filler}}}{\gamma_{\text{polymer1-polymer2}}} \quad (1.1)$$

Here, γ_{1-2} is surface tension, where 1 and 2 stand for the two different polymers. By employing equation 1.1, researchers (Elias et al., 2007; Masao Sumita et al., 1991; D. Wu et al., 2011) have reported that if $W_{1-2} > 1$, then the filler prefers polymer 1 as interfacial tension between filler and polymer 2 will be higher; if $W_{1-2} < -1$, then the filler prefers polymer 2; and if $-1 < W_{1-2} < 1$, the filler is predicted to be located at the interface. This theory is recommended for the systems at equilibrium with no chemical interaction between the components. Based on wetting co-efficient calculation, it has been reported (Tu et al., 2017a) that graphene thermodynamically prefers PE over PP in PE/PP blend system.

- **Kinetic Factor**

The order of mixing of the components of composite can critically influence dispersion and localization of filler. The researchers have (Gubbels et al., 1995; Gubbels et al., 1994; Gubbels & Jérôme, 1998) reported the effect of the order of mixing on the localization of carbon black

in PE/PS immiscible blend system. They noticed that the kinetic factor can influence the electrical percolation threshold of a blend nanocomposite. If nanofiller is premixed a less favourable phase, a chance remains for the fillers to move and travel across the interphace to migrate the more favourable phase. As a result, this strategy offers an opportunity to capture fillers at the interface of an immiscible polymer blend system.

1.2.3 Recycling of MPWS

Different approaches are followed to tackle MPWS, as mentioned in Figure 1.2.

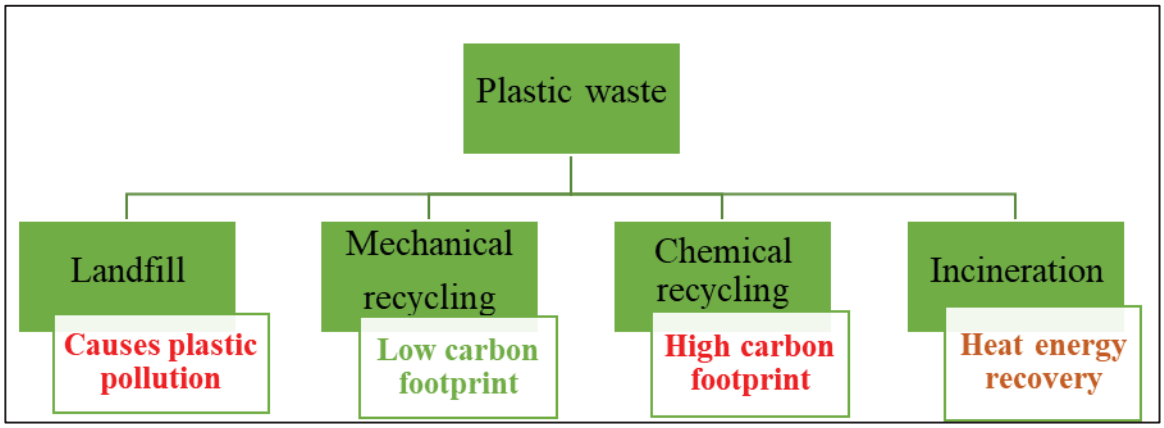

Figure 1.2 Approaches towards plastic waste management, modified from (Singh et al., 2023)

The landfilling approach to plastic waste disposal is often referred to as a zero approach because no byproduct can be obtained from this method (Davidson et al., 2021). Mechanical and chemical recycling are identified as the primary and secondary approaches, respectively, for handling MPWS. These two methods stand out as the interesting paths explored in plastic recycling (Grigore, 2017; Silva & Wiebeck, 2020). Mechanical recycling involves the collection of plastic waste followed by its reprocessing. Conversely, chemical recycling entails converting polymers back into monomer units by altering their chemical structure. Additionally, incineration provides another avenue for plastic recycling, where energy is recovered from the plastic. It is noteworthy that the global warming potential (GWP) and total

energy use (TEU) are crucial factors to consider when assessing the feasibility of waste management approaches. A study has reported (Ferdous et al., 2021) that recycling has a lesser impact on GWP and TEU compared to landfilling and incineration approaches.

In this study, the mechanical recycling approach, reviewed below, of MPWS has been chosen due to its wide acceptance in industrial applications, simplified processing steps, and minimal or no chemical involvement.

1.2.4 Mechanical Recycling of MPWS

As mentioned earlier, the separation of PP and PE presents challenges due to their similar physical properties and densities (Madi, 2013; Strapasson et al., 2005). To address these challenges and reduce recycling costs, it is more advisable to utilize the PE/PP blend obtained during recycling. However, these blends often exhibit compromised properties due to immiscibility, which can be improved by incorporating suitable compatibilizers, stabilizers, and fillers (Ghosh, 2021; Martikka & Kärki, 2019; Strapasson et al., 2005). Many researchers have explored the incorporation of copolymers and rigid fillers to enhance the properties of MPWS (Bertin & Robin, 2002; Fang et al., 2013; Fortelný et al., 2004; Garofalo et al., 2015; Kazemi et al., 2015; Khadri Diallo et al., 2022; Yousefi et al., 1998). Generally, the addition of copolymers improves the toughness of waste polyolefins at the expense of compromised strength. Conversely, inorganic rigid fillers typically strengthen the composites while reducing impact and tensile toughness. Therefore, a comprehensive investigation is necessary to improve the strength, toughness, and durability of MPWS.

1.3 Possibilities of Graphene

Among different types of carbonaceous filler particles, pure and an atomic-thin graphene is often dubbed as a "wonder material" owing to its extraordinary properties (Chakraborty & Hashmi, 2018; Choi et al., 2010; Kuilla et al., 2010). Ideally, graphene is incredibly strong, even though its thickness is comparable to an atom. Moreover, it serves as an outstanding

conductor of both heat and electricity. With its vast array of potential applications spanning electronics, energy storage, composites, and beyond, graphene holds immense promise for developing various industries. However, researchers have also investigated other carbonaceous fillers, such as carbon black (Im et al., 2009; Yi et al., 1998; Yui et al., 2006; Zaikin et al., 2007), carbon nanotube (CNT) (Alig et al., 2012; Navas et al., 2017; Rostami et al., 2015; Strugova et al., 2021; Verma et al., 2015) to improve the properties of polymeric materials. While carbon black is zero-dimensional (any dimension < 100 nm), carbon nanotube is one-dimensional (one dimension, length > 100 nm), and graphene is two-dimensional (two dimensions, length and width > 100 nm) (Afzal et al., 2016). This two-dimensional geometry of graphene remarkably reduces the extent of dermal effect, inhalation problem, and gene toxicity than that of carbon black or carbon nanotube (Moghimian & Nazarpour, 2020). Moreover, the mass production of CNT is both complex and expensive (Volder et al., 2013), while the production of carbon black is linked to significant carbon emissions and other environmental impacts (Aprianti et al., 2023). In contrast to the complications associated with the mass production of CNT and carbon black, large-scale production of graphene is feasible through mechanochemical exfoliation of graphite, with minimal impact on quality and the environment (Moghimian & Nazarpour, 2020).

The following section of this chapter provides a detailed discussion of the structure and intriguing properties of graphene, which are particularly promising for enhancing the properties of polymeric composites.

1.3.1 Generalities of Graphene

Graphene is a two-dimensional material composed of carbon atoms, arranged in a hexagonal lattice. The interesting chemical structure of graphene results in outstanding properties. The chemical structure of graphene has been illustrated in Figure 1.3. As can be seen, the hexagonal array of the graphene sheet is comprised sp^2 hybridized carbon atoms (Karimi et al., 2021). Due to sp^2 hybridization, each carbon atom can share three sigma bonds with the neighboring carbon atoms, and one π bond with one of the three neighboring carbon atoms. The presence

of these sigma bonds contributes to graphene's remarkable mechanical strength, while the π bonds facilitate its outstanding electrical conductivity (Mak et al., 2012). Moreover, the presence of conjugated π bonds in graphene's structure and its 2D geometry have gained attention for its potential as a UV stabilizing agent and barrier of small molecules, respectively.

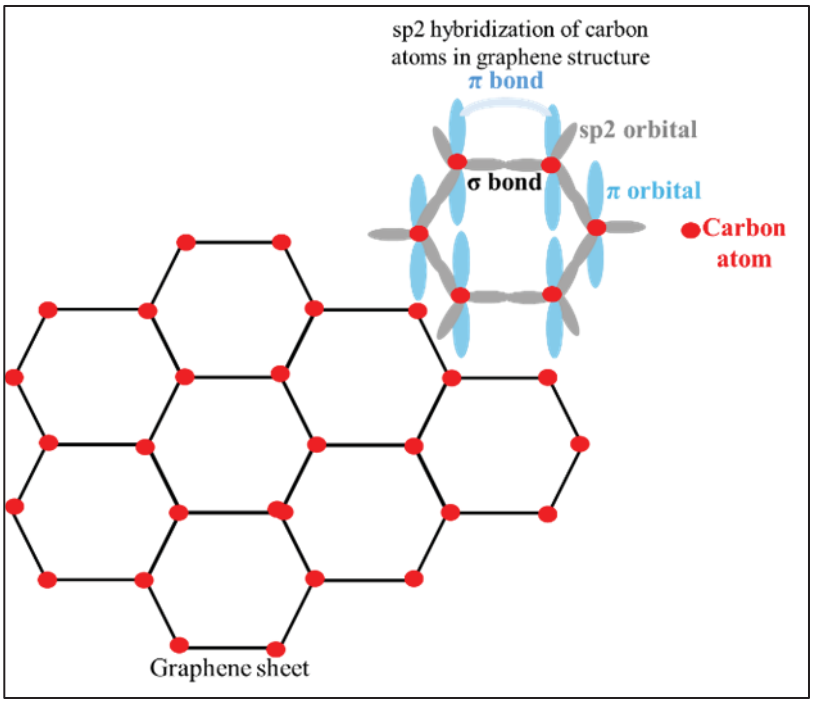

Figure 1.3 Schematic diagram of a graphene sheet; modified from (Wirth-Lima & Bezerra-Fraga, 2021)

1.3.2 Type of Graphene

Considering the remarkable properties of atomically thin pure graphene, it's evident that large-sized, defect-free, single-layered graphene is preferable for enhancing the properties of polymer matrices. However, commercializing graphene-based products on a large scale has posed challenges in terms of production scalability, cost-effectiveness, and integration into existing technologies. Nevertheless, ongoing research and development efforts in this field aim to produce thin and pure graphene at a large scale to unlock its full potential.

In this context, graphene is broadly categorized into two types: lab-grade graphene and commercial-grade few-layer graphene (FLG). FLG typically consists of five to ten layers of atomic graphene sheets. For instance, NanoXplore Inc, a Quebec-based Canadian company, produces FLG via mechanochemical exfoliation of graphite. This grade of graphene is often more cost-effective compared to lab-grade nanographene, which is produced in compliance with Canadian environmental regulations. FLG has demonstrated potential applications in reinforcing materials (Khadri Diallo et al., 2022), slowing down UV degradation (Karimi et al., 2023), and aiding in the processing (Genoyer et al., 2023) of plastic materials. However, the potential of FLG to enhance the properties of MPWS has not been reported in the literature prior to this work.

The influence of graphene from different suppliers, has been investigated by researchers (Cetiner et al., 2023; dos Anjos et al., 2022; Guo et al., 2020; Haghnegahdar et al., 2017; Khadri Diallo et al., 2022; Lago et al., 2020; Lou et al., 2016; Nunes et al., 2021; Tu et al., 2017a) on the properties of polymer matrix. In Table 1.1, the average thickness and particle size of graphene, confirmed by the providers, have been mentioned. This table has been provided to outline the physical structure of graphene, investigated in literature for different polymer blend systems. The influence of these grades of graphene has been mentioned in Table 1.2 and Table 1.3, presented in the subsequent sections of this chapter.

Table 1.1 Average thickness and particle size of different grades of graphene, explored in literature, to improve the properties of polymer materials

Source of graphene	**Average thickness**	**Average particle size**	**Ref.**
Avanzare Innovacion Tecnologica S.L., Spain	0.7 nm	50-500 μm	(Lago et al., 2020)
Angstron Materials, USA	1-1.2 nm	≤10 μm	(Haghnegahdar et al., 2017)
Lab processed	1.4 nm		(Tu et al., 2017a)

Source of graphene	Average thickness	Average particle size	Ref.
NanoXplore Inc., Canada **(provider of FLG of this work)**	6-10 atomic layer	1-2 µm	(Khadri Diallo et al., 2022)
GNPs H-5, XG Science, USA	15 nm	1-5 µm	(Guo et al., 2020)
C-750, XG Science, USA	15 nm	150 - 250 nm	(Guo et al., 2020)
Cheaptube, USA	8–15 nm	>2 µm	(dos Anjos et al., 2022)
Enerage Inc., Taiwan	50–100 nm	7 µm	(Lou et al., 2016)
Nanografen Co.,Turkey		50 nm	(Cetiner et al., 2023)
2DM Materials, Singapore		1 µm	(Nunes et al., 2021)

1.3.3 Potentials of Graphene in Polymer Blend Composites

1.3.3.1 Electrical Conductivity

Graphene stands out as a promising candidate for enhancing the conductivity of insulating polymer matrices. The electrical conductivity of nanocomposites primarily hinges on the establishment of an interconnected network of electrically conductive fillers. Theoretically, if such a network of interconnected graphene is achieved, the nanocomposite can exhibit electrical conductivity even at lower graphene loadings. This critical minimum loading of filler necessary to establish the network is termed as the percolation threshold. Beyond this threshold, the conductivity of the nanocomposite experiences a sharp increase. This phenomenon results in an S-shaped characteristic curve when electrical conductivity is plotted

as a function of filler loading in a log-log plot. Figure 1.4 provides a schematic representation of this S-shaped characteristic curve. This curve delineates three distinct zone: insulative, percolation, and conductive.

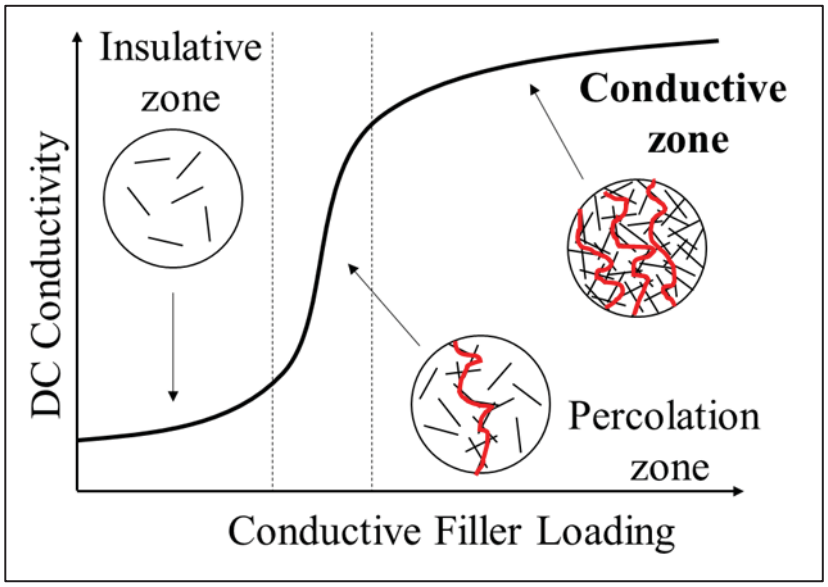

Figure 1.4 Characteristic conductivity vs. conductive filler loading curve of a conductive composite

The black lines inside the circle represent the presence of conductive fillers in the polymer matrix and the red line represents the possible conductive path of free electrons. Furthermore, the formation of filler network is critically related to the dispersion of filler in the composite. The extent of filler dispersion makes a huge difference. For example, 0.7 nm thin graphene with an average particle size of 50-500 um was expected to result in higher electrical conductivity in PC/ABS composite (Lago et al., 2020). However, poor dispersion of graphene, obtained by melt-mixing strategy, hindered the formation of an electrically conductive network. Contrarily, better dispersion of graphene by solution mixing strategy could result in higher electrical conductivity in the composite of the same composition (Lago et al., 2020). However, the solution mixing strategy (Sultana et al., 2019) is out of the scope of this work as this mixing strategy is neither viable for industrial application nor for polyolefin blend (the blend system of this work).

In addition, the electrical conductivity of graphene is a function of the layer number (Nirmalraj et al., 2011), and lateral size (Guo et al., 2020; Ma et al., 2017). It has been reported (Nirmalraj et al., 2011) that the electrical conductivity of graphene nanosheets decreases, as the layer number increases. This indicates that few-layer graphene is electrically less conductive than single-layered graphene. Initial findings (Galindo et al., 2014) has suggested that monolayer graphene exhibits ten times higher electrical conductivity than few-layer graphene. Moreover, it was reported that the conductivity of FLG with 14-16 layers approaches that of graphite. Additionally, the electrical conductivity of graphene demonstrates a linear increase with size (Guo et al., 2020) but becomes independent of size when the nanosheet size exceeds 2 μm (Ma et al., 2017). Furthermore, when the aspect ratio (Haghnegahdar et al., 2017; Rafeie et al., 2018) of graphene is very high, improved electrical conductivity is achievable at lower concentrations. Apart from the formation of an interconnected network and the extent of filler dispersion, the physical structure of the used graphene intensively influences the resulting electrical properties of a polymer composite. Table 1.2 lists the studies, that reported the electrical conductivity of melt-processed and graphene-filled polymer blend composite. Table 1.2 also reports the concentration of graphene, required to obtain an electrically dissipative (electrical conductivity from 10^{-8} S/cm to 1 S/cm) polymer blend composite.

Table 1.2 The electrical conductivity of melt-processed and graphene-filled polymer blend composite, reported in literature

Blend system	**Source of graphene**	**Graphene (wt.%)**	**Electrical conductivity (S/cm)**	**Ref.**
PVDF /PP	Angstron Materials, USA	0.9	1.00E-02	(Rafeie et al., 2018)
PP/EPDM	Angstron Materials, USA	1	1.00E-02	(Haghnegahdar et al., 2017)
PP/PET	Lab processed	1	1.00E-05	(Sadeghi et al., 2019)

Blend system	Source of graphene	Graphene (wt.%)	Electrical conductivity (S/cm)	Ref.
LLDPE/PP	Angstron Materials, USA	3	1.00E-05	(Mun et al., 2019)
LLDPE/PEMA	2DM Materials, Singapore	3	1.00E-04	(Nunes et al., 2021)
LLDPE/EVA	NanoXplore, Inc, CA	5	1.00E-04	(Helal et al., 2019)
PP/SEBS composites	Enerage Inc., Taiwan	5	1.00E-06	(Lou et al., 2016)
PP/EPDM	Shanghai Aladdin Biochemical Technology Co, China	4	1.00E-08	(Sarfraz et al., 2022)
PC/ABS	Cheaptubes, USA	5	1.00E-08	(dos Anjos et al., 2022)
PP/PE	XG Sciences,USA	11	1.00E-02	(Al-Saleh, 2016)
PLA/PBAT	XG Sciences,USA	10	1.00E-03	(Guo et al., 2020)
PC/SAN	XG Sciences,USA	10	1.00E-04	(Liebscher et al., 2020)

1.3.3.2 Reinforcement

The unique mechanical properties and two-dimensional nature of graphene offer opportunities to simultaneously strengthen (Haghnegahdar et al., 2017; Khadri Diallo et al., 2022; Parameswaranpillai et al., 2015; Tu et al., 2017a) and toughen (Bijarimi et al., 2019; dos Anjos

et al., 2022; Pour et al., 2016) polymer matrices. Enforcement of polymer by graphene is governed by the polymer/filler interaction and dispersion of graphene. An increased polymer/filler interaction facilitates the load transfer, resulting in higher reinforcement. Additionally, better dispersion is essential to obtain a stronger composite.

Table 1.3 presents the influence of graphene on the mechanical properties of immiscible polymer blend composites, reported in literature. Typically, the addition of graphene resulted in improved tensile strength and stiffness of the composite, whereas reduced the toughness of the blend composite (Abbasi et al., 2019; Guo et al., 2020; Haghnegahdar et al., 2017; Khadri Diallo et al., 2022; Parameswaranpillai et al., 2019; Tu et al., 2017a). However, exceptions were also reported. For example, Pour et al. (Pour et al., 2016) and Anjos et al. (dos Anjos et al., 2022) showed that better dispersion of graphene and a strong graphene/matrix interaction improved the tensile toughness of the composite. Besides, an improvement of impact strength of the composite as a result of the addition of rigid fillers was reported too (Bijarimi et al., 2019; Parameswaranpillai et al., 2019). This effect of rigid filler is achievable in polymer composites when their crack-resisting (Juan, 2020) influence is more dominant than their influence as defect centers (Dikobe & Luyt, 2017).

Table 1.3 The influence of graphene, on the mechanical properties of immiscible polymer blend composites, in literature

Blend composition	Source of graphene	Graphene (wt. %)	Change in properties				Ref.
			EB[1] (%)	TS[2] (%)	TM[3] (%)	IS[4] (%)	
PC/PVDF - 70/30	XG Sciences,USA	1			20		(Chiu et al., 2021)
PC/ABS - 45/55	Avanzare Innovacion Tecnologica S.L., Spain	1			6	-84	(Lago et al., 2020)
PP/EPDM - 80/20	Angstron Materials, USA	1	-24	24	24	-4	(Haghneg ahdar et al., 2017)
PP/EPDM - 60/40	Angstron Materials, USA	1	-32	32	13	-4	(Haghneg ahdar et al., 2017)
Prime HDPE/recHDPE - 50/50	NanoXplore Inc., CA	1		4	10		(Khadri Diallo et al., 2022)
PP/PS - 80/20	XG Sciences, USA	1	-40		15		(Parames waranpill ai et al., 2015)
PC/ABS - 70/30	XG Sciences, USA	3	100	14	29		(Pour et al., 2016)
PP/PS - 80/20	XG Sciences, USA	3	-71	8	30		(Abbasi et al., 2019)
PC/ABS/ ABS-g-MAH - 85/10/5	Cheaptubes, USA	5	-33	2	3	-85	(dos Anjos et al., 2022)
PP/EPDM - 80/20	XG Sciences, USA	5	-71	42	19	-8	(Haghneg ahdar et al., 2017)

[1] EB – Elongation at break

[2] TS – Tensile strength

[3] TM – Tensile modulus

[4] IS – Impact strength.

Blend composition	Source of graphene	Graphene (wt. %)	Change in properties				Ref.
			EB[1] (%)	TS[2] (%)	TM[3] (%)	IS[4] (%)	
PP/EPDM - 60/40	XG Sciences, USA	5	-44	26	19		(Haghnegahdar et al., 2017)
PC/ABS - 85/15	Cheaptubes, USA	5	20	10	13	-86	(dos Anjos et al., 2022)
PS/LDPE/SEBS-1/1/1	XG Sciences, USA	5	-21	10	37	11	(Parameswaranpillai et al., 2019)
PS/LDPE - 50/50	XG Sciences, USA	5	-34	6	67	-82	(Parameswaranpillai et al., 2019)
ABS/EPDM - 70/30	Lab processed graphene	6		12		6	(Bijarimi et al., 2019)
PE/PP-60/40	Lab processed graphene	7		73	108	-14	(Tu et al., 2017a)
PBAT/PLA - 75/25	XG Sciences,USA	10	-89	5	200	-60	(Guo et al., 2020)

1.3.3.3 Resistance to photodegradation

Polymeric materials undergo photodegradation under UV exposure. Typically photodegradation of polymer chains involves the following steps (Karimi et al., 2021; Ranby, 1989):

Initiation step: Polymer chains (RH) are attacked by UV radiation and O_2 molecules. At this stage, polymer chains start to break into alkyl radicals (R^o) and hydroperoxy radicals (HO_2^o):

$$RH \xrightarrow{O_2,UV} R^0 + HO_2^0 \tag{1.2}$$

Propagation step: This step involves the following reactions. In this step, new polymer chains are attacked by previously formed free radicals:

- Formation of alkyl peroxyl radical (ROO^o):

$$R^0 + O_2 \rightarrow ROO^o \quad (1.3)$$

- Subsequent reaction between (ROO^o) and RH to form further alky radicals (R^o) and hydroperoxides (ROOH):

$$ROO^0 + RH \rightarrow R^o + ROOH \quad (1.4)$$

- Hydroperoxides (ROOH) are decomposed as below in the presence of heat and UV:

$$ROOH \xrightarrow{\text{heat,UV}} RO^o + OH^o \quad (1.5)$$

- Alkyl oxy (RO^o) and hydroxyl (OH^o) radicals further attack new polymer chains and continue further degradation, as represented by the following reactions:

$$RO^0 + RH \rightarrow R^o + ROH \quad (1.6)$$

$$OH^0 + RH \rightarrow R^o + H_2O \quad (1.7)$$

Finally, this degradation process comes to an end, when the formation of radicals is terminated. In this case, the presence of graphene in a polymer matrix can retard the photo-degradation process. It has been mentioned in the literature that the photo-stabilizing effect of graphene involves UV absorption and screening, radical scavenging, quenching, and physical barrier effect (Karimi et al., 2023).

UV absorption is considered as the first and most dominant UV stabilizing action of graphene (Hasani et al., 2018; Mistretta et al., 2019). Graphene absorbs UV radiation, with wavelength ranging from 100 nm to 280 nm. The absorption is attributed to $\pi \rightarrow \pi^*$ transitions of conjugated π electrons. UV absorption by graphene, prevents the initiation step of polymer photodegradation.

Besides, graphene can screen UV radiation due to its two-dimensional structure. At this stage, the action of graphene as free radical scavenger decelerates the photodegradation process of polymer chains. The radical scavenging effect of graphene refers to its ability to neutralize free radicals, which are highly reactive molecules or atoms with unpaired electrons. Graphene's radical scavenging properties are primarily attributed to the availability of ample active sites for interacting with free radicals. Graphene possesses a highly conductive π-electron system, which allows it to readily donate or accept electrons. When graphene encounters free radicals, it can transfer electrons to or from the radicals, stabilizing them within the system. By neutralizing free radicals through electron transfer, graphene prevents them from initiating chain reactions that lead to oxidative damage.

Moreover, the quenching effect is another photostabilizing mechanism of graphene (Ran et al., 2012). Quenching involves absorbing energy from the molecules in an excited state and rendering them non-reactive entities. In this case, graphene's π-conjugated structure allows it to efficiently receive the energy from the excited states of molecules and to release it as heat, afterwards.

In addition to the properties, graphene and its derivatives serve as effective physical barriers against the diffusion of low molecular compounds, such as oxygen, into polymers. This barrier effect is facilitated by graphene's 2D geometry, high specific surface area, and high aspect ratio (Cui et al., 2016; Yoo et al., 2014). Specifically, the incorporation of graphene into a polymer matrix creates convoluted pathways that impede the diffusion of oxygen and free radicals into the bulk of the polymer. Consequently, the rate of the initial reaction in the propagation step,

which is diffusion-controlled, decreases, resulting in a slowdown of the propagation of photodegradation.

1.3.3.4 Processing Aid

As discussed in this chapter, various fillers are incorporated into thermoplastics to enhance the properties of polymer composites mentioned above. However, numerous publications have demonstrated that adding nanofillers or fillers to molten polymers significantly increases their viscosity (Koodehi & Dadvand Koohi, 2018; Lago et al., 2020). This phenomenon poses challenges to the melt processing of rigid filler-filled polymer composites, as it requires more energy. In this context, graphene, as a 2-D filler, has been reported to assist in processing (Ferreira et al., 2019; Genoyer et al., 2023; Khadri Diallo et al., 2022) while incorporating the desired effects of the filler. These studies have indicated that graphene and its derivatives can serve as process-aiding additives. Specifically, these studies have observed a reduction or maintenance of viscosity, even after filler addition. These observations are attributed to the super lubricity effect extended by 2-D fillers. This super lubricity effect arises from the compatible contacts of filler agglomerates. These random contacts help to maintain or facilitate both the slippage and mobility of molten polymer chains within the composites (Ferreira et al., 2019). In principle, the agglomerates contain numerous flake–flake contacts, resulting in low slipping resistance and additional space between them. These effects contribute to faster polymer chain relaxation and enhanced flowability.

1.4 Approach of this Study

In addition to the challenges, associated with an immiscible polymer blend, mixed plastic waste stream is associated with other challenges; for example: rare information about composition, amount of impurities, type of plastic content and extent of degradation. These uncertainties deteriorate the properties of recycled plastics. A systematic study to upcycle the MPWS is interesting and desired. Considering the abovementioned potentials of graphene, we are highly motivated to analyze the ability of commercial graphene (less expensive than lab-grade

graphene) to upcycle MPWS. More precisely, this research was conducted to address the following points:

1. The influence of FLG on the following properties of a model PE/PP blend composites:
    - Morphology
    - Electrical conductivity
    - Mechanical properties
    - Photostability
2. The impact of FLG (solely or in combination with prime PE, PP, or copolymer) on the following properties of MPWS:
    - Morphology
    - Processability
    - Mechanical properties

3. Finally, the effect of different concentrations and localization of FLG on the photodegradation behavior of MPWS and a prime polyolefin blend.

1.4.1 Overview of Sample Preparation

The samples for this work were processed by using a HAAKE twin-screw extruder (Rheomex OS PTW16/40). The specific extrusion conditions for each sample are detailed in the respective chapters.

After extrusion, the pellets were injection molded using an Arburg Allrounder 221K-350-100 injection molding machine to produce dog-bone-shaped specimens for tensile testing and rectangular specimens for impact testing. Dog-bone-shaped specimens with dimensions of 160 mm in length, 12 mm in width, and 3.5 mm in thickness were used to characterize the tensile properties, while specimens with dimensions of 62 mm in length and 12 mm in width were used for Izod (notched) impact strength characterization. The

injection molding process followed a specific temperature profile: zone 1 at 175 °C, zones 2 to 4 at 180 °C, and zone 5 at 185 °C, with an injection speed of 0.3 in^3/sec and an injection pressure of 8500 psi. The injection duration was 30 seconds, with a 5 second pressing time, a clamping pressure of 1000 psi, and a cooling time of 25 seconds, while the mold temperature was maintained at 70 °C. Additionally, 1 mm thick and 25 mm diameter disks were prepared by compressing the composites at 200 °C and 10 MPa for 10 minutes in a compression mold to characterize the electrical properties of the samples.

For the investigation of mechanical properties (tensile, flexural, and impact), at least five replicas of each sample were tested. The average values are reported along with the standard deviation, represented as error bars. For melt flow index characterization, at least five cycles were conducted.

CHAPTER 2

THE INFLUENCE OF A COMMERCIAL FEW-LAYER GRAPHENE ON ELECTRICAL CONDUCTIVITY, MECHANICAL REINFORCEMENT AND PHOTODEGRADATION RESISTANCE OF POLYOLEFIN BLENDS

S. M. Nourin Sultana [a] , Emna Helal [a,b] , Giovanna Gutiérrez [b], Eric David [a], Nima Moghimian [b] and Nicole R. Demarquette [a]

[a] Mechanical Engineering Department, Ecole de Technologie Superieure, 1100 Notre-Dame Street West, Montreal, Quebec, Canada H3C 1K3
[b] NanoXplore Inc., 4500 Thimens Blvd, Saint-Laurent, QC H4R 2P2, Canada

Paper submitted for publication, June 2024

Chapter outline: Chapter 2 reports the impact of few-layer graphene on a controlled polyolefin blend system, focusing on electrical conductivity, mechanical properties, and photodegradation resistance. The chapter begins with an abstract summarizing the main findings of the study, followed by an introduction that cites and discusses relevant literature. A detailed description of the materials and methods is then provided, along with an outline of the characterization techniques employed. The results and discussions section covers the morphology of neat blends, the influence of FLG on blend morphology, electrical conductivity, the effects of deformation on conductivity, and mechanical properties before and after UV exposure, culminating in a comprehensive discussion. The chapter concludes with a summary of the findings. This study has been submitted to the journal Crystals for publication.

Abstract

This work demonstrates the potentials of a commercially available few-layer graphene (FLG) in enhancing the electro-dissipative properties, mechanical strength, and UV protection of polyolefin blend composites; interesting features of electronic packaging materials. Polyethylene (PE)/ polypropylene (PP)/ FLG blend composites were prepared following two steps. Firstly, different concentrations of FLG were mixed with either the PE or PP phases.

Subsequently, in the second step, this pre-mixture was melt-blended with the other phase of the blend. FLG-filled composites were characterized in terms of electrical conductivity, morphological evolution upon shear-induced de-formation, mechanical properties, and UV stability of polyolefin blend composites. Premixing of FLG with the PP phase has been observed to be a better mixing strategy to attain higher electrical conductivity in PE/PP/FLG blend composite. This observation is attributed to the influential effect of FLG migration from a thermodynamically less favourable PP phase to a favourable PE phase via the PE/PP interface. Interestingly, the addition of 4 wt.% (~2 vol.%) and 5 wt.% (~2.5 vol.%) of FLG increased an electrical conductivity of ~10 orders of magnitude in PE/PP—60/40 (1.87×10^{-5} S/cm) and PE/PP—20/80 (1.25×10^{-5} S/cm) blends, respectively. Furthermore, shear-induced deformation did not alter the electrical conductivity of the FLG-filled composite, indicating that the conductive FLG network within the composite is resilient to such deformation. In addition, 1 wt.% FLG was observed to be sufficient to retain the original mechanical properties in UV-exposed polyolefin composites. FLG exhibited pronounced UV stabilizing effects, particularly in PE-rich blends, mitigating surface cracking and preserving ductility.

Keywords: graphene; polyolefin; electrical conductivity; photoprotection; mechanical properties

2.1 Introduction

Currently, the incorporation of carbonaceous filler (dos Anjos et al. 2022; dos Anjos et al. 2022; Chaudhuri et al. 2017; Chiu et al. 2021; Cui et al., 2016; Dan et al., 2006; Lago et al. 2020; López-Martínez et al. 2022; Nunes et al. 2021) in the polymer matrix is a promising field of research, aiming at the improvement of the properties of polymers. Among these carbon-based fillers, carbon black is zero-dimensional, carbon nanotube is one-dimensional, and graphene is two-dimensional (Afzal et al., 2016). Due to the two-dimensional geometry of graphene, the extent of dermal effect, inhalation problem, and gene toxicity associated with graphene is much less than that of carbon black or carbon nanotube (Moghimian & Nazarpour, 2020). This ensures the safer handling of graphene. Moreover, graphene (Sun et al., 2021) stands out as a highly promising candidate. Theoretically, sp2-hybridized carbon atoms are arranged in a hexagonal lattice within atomic thickness to form pristine graphene (Choi et al.,

2010). This unique structure offers remarkable characteristics. A perfect single-layer graphene is not only the lightest (weighing merely 0.77 milligrams per square meter) but also the strongest (300 times stronger than Kevlar) nanofiller discovered to date (Chakraborty & Hashmi, 2018). Furthermore, graphene demonstrates exceptional electrical and thermal conductivity, along with remarkable flexibility, capable of stretching up to 25% of its original length without fracturing. These remarkable attributes refer to graphene as a wonder material with the capability of enhancing its properties (processability (Ferreira et al., 2019), photostability (Karimi et al., 2023), mechanical (Abbasi et al., 2019), and electrical (Haghnegahdar et al., 2017)) of polymer composites.

In general, graphene has been observed to enhance the tensile strength and stiffness of polymeric systems, often at the expense of ductility and impact strength (Abbasi et al., 2019; Haghnegahdar et al., 2017; Parameswaranpillai et al., 2015). Nevertheless, some exceptional observations can be found in the literature (Bijarimi et al., 2019; Pour et al., 2016). Due to graphene's intrinsic electrical conductivity, it can significantly improve the electrical conductivity of polymer composites (Rafeie et al., 2018; Sadeghi et al., 2019). Furthermore, polymer blend composites often exhibit an even higher electrical conductivity than single polymer/conductive filler composites. This is attributed to the double percolation effect (Al-Saleh et al., 2013; Jia et al., 2016; Otero-Navas et al., 2017; Pan et al., 2016; Strugova et al., 2021; M. Sumita et al., 1992), which is achievable in co-continuous polymer blend composites. Moreover, the migration of electrically conductive filler from one phase to another via the polymer phase interface (achievable via strategic mixing conditions) can also facilitate the improvement of electrical conductivity in polymer blend composites (Strugova et al., 2021).

Numerous studies (Bouhfid et al., 2016; Graziano et al., 2020; Graziano, Garcia et al., 2020; Wang et al., 2015) have investigated the influence of laboratory-processed graphene on the mechanical and electrical properties of various polymer composites. However, the large-scale production of very pure and fully exfoliated graphene is challenging (Zhong et al., 2015). In contrast, mass production of few-layer graphene (FLG) is obtainable following the cost-effective mechanochemical exfoliation of graphite (Moghimian et al., 2017), which involves a

lower carbon footprint in comparison to mass production of carbon black (Aprianti et al., 2023). Despite exhibiting a wider size distribution and increased defects compared to lab-grade graphene, particles produced through this process still retain many of graphene's notable properties. Accordingly, better electrical conductivity, improved mechanical strength, and improved photostability of commercial-grade few-layer graphene-filled (FLG) polymer composites have been reported in the literature (Batista et al., 2019; Karimi et al., 2023). Nevertheless, research aiming to achieve a combination of improved electrical conductivity, mechanical strength, and photoprotection in the same polymer blend composite remains limited in the literature.

In this connection, polyolefin systems were chosen due to their versatility in domestic and industrial applications. Moreover, approximately 50% of global plastic waste is composed of PE/PP mixtures (Singh et al. 2023). A significant portion of this plastic waste can be recovered as a PE/PP mixture from post-consumer waste using simple separation steps. However, further separating PE from PP is both complex and costly (Karlsson, 2004). This motivates research into enhancing the properties of controlled PE/PP blend systems to gain a deeper understanding. Such knowledge could be valuable in guiding the upcycling of polyolefin mixtures recovered from post-consumer waste. In this study, polyethylene (PE), polypropylene (PP), and PE/PP blend systems were selected to explore the potential of incorporating commercially available FLG. Different concentrations of FLG were melt-mixed with PE, PP, and PE/PP blend systems. For the PE/PP blend system, two different FLG mixing strategies were employed to investigate their influence on the electrical properties of the composite. However, if the filler fails to stabilize the morphology, subsequent morphological evolution during post-processing is a likely phenomenon for an immiscible polymer blend composite. Shear-induced deformation followed by small-amplitude oscillatory shear (SAOS), a rheological approach (Vandebril et al., 2010), was conducted to study the morphological stability/evolution of the PE/PP/FLG blend composite. After the deformation step, SAOS was performed to reach an equilibrium state of the deformed morphology. A similar approach has been extensively studied for droplet-dispersed type polymer blend systems (Thareja et al.,

2010). Furthermore, the influence of adding FLG on the mechanical properties of the composites before and after UV exposure was documented.

2.2 Materials and Methods

2.2.1 Materials

GrapheneBlack 3X, a few-layer (6 to 10) graphene powder, was received from NanoXplore Inc., Montreal, QC, Canada, to prepare the composites for this study.

Two homopolymers, high-density polyethylene (HDPE) and polypropylene (PP), were used as the thermoplastic components of the composites. Table 2.1 outlines the specifications of the polymers.

Table 2.1 Identification, MFI, and density of the polymers used in this work

Polymer	**Commercial Name**	**MFI (g/10 min)**	**Density (g/cm^3)**
HDPE	Alathon H5618	17 (190 °C, 2.16 kg)	0.955
PP	Polypropylene 3720 WZ	20 (230 °C, 2.16 kg)	0.905

2.2.2 Methods

To prepare the composites for this study, master batch (MB) pellets of either PE/FLG or PP/FLG were used for the preparation of composites. The MB pellets contained 30 wt.% FLG, provided by NanoXplore, Inc. The samples were produced by using a HAAKE twin-screw extruder (Rheomex OS PTW16/40).

PE and PP were separately blended at 200 °C and 150 rpm with their respective MB pellets to create the PE/FLG and PP/FLG composites. Each composite consisted of 1 and 5 wt.% of FLG, respectively.

In addition, PE/PP—20/80 and PE/PP—60/40 blend composites with the FLG concentration ranging from 1 to 5 wt.% were prepared in two steps. First step: PE/FLG or PP/FLG MB pellets were blended with PE or PP at 200 °C and 150 rpm, referred to as the premixing step. Second step: these premixtures were melt-blended with the other respective polymer blend at 190 °C and 115 rpm.

Finally, extruded pellets were injection molded in an Arburg Allrounder 221K-350-100 Injection molding machine to prepare dog-bone-shaped specimens and rectangular specimens for the characterization of tensile and impact properties, respectively. During injection molding, a certain temperature profile (zone 1: 175 °C, zone 2—180 °C, zone 3—180 °C, zone 4—180 °C, zone 5—185 °C) was followed at a 0.3 in3/sec injection speed and 8500 Psi injection pressure. It is worth mentioning that the injection duration was 30 s, pressing was continued for 5 s, clamping pressure was maintained at 1000 psi, and the injected samples were cooled for 25 s while the mold temperature was maintained at 70 °C.

Moreover, disks of 1 mm thickness and 25 mm diameter were prepared by compressing the composites at 200 °C and 10 MPa for 10 min in a compression mold.

2.2.3 Photodegradation process

The injection-molded composites were weathered in a QUV chamber. The samples were treated under UV radiation for a total of 2 weeks and 4 weeks by following the alternating two steps mentioned in Table 2.2:

Table 2.2 Weathering condition of the specimens in QUV chamber

Step	**Function**	**Irradiance (W/m^2)**	**Temperature (°C)**	**Time (h:m)**
1	Exposure to UV radiation	0.89	60	8:00
2	No UV radiation	n/a	50	4:00

2.3 Characterizations

Scanning electron microscope (SEM) images were captured by using a Hitachi SEM S3600-N (Model: MEB-3600-N, manufactured by Hitachi Science Systems, Ltd., Japan). Prior to SEM imaging, the surface (cryo-fracture or UV exposed) of the samples was gold coated by employing a Gold Sputter Coater (Model: K550X, manufactured by Quorum Technologies Ltd, East Sussex, UK).

The electrical conductivity of the composites was assessed using a broadband dielectric spectrometer (BDS) from Novocontrol Technologies GmbH & Co. KG, Montabaur, Germany. The investigation was conducted under an excitation voltage of 3 VRMS across a frequency range from 1×10^{-2} to 3×10^{5} Hz. Gold-coated disk-shaped composites of 1 mm thickness were sandwiched between two brass disks (electrodes) of 25 mm diameter in order to create a plane capacitor structure for the analysis of the electrical properties. The real part of the complex electrical conductivity at the lowest frequency (1×10^{-2} Hz) has been reported as the electrical conductivity of the composite in the subsequent section of this study.

Shear-induced coalescence followed by SAOS was conducted on the rheometer, MCR 501. Compression-molded neat and FLG-filled PE/PP—20/80 composites were sheared at 0.05 s^{-1} rate for 500 s, 2000 s, and 5000 s, respectively. In other words, the samples were deformed at 25, 100 and 250 strains (shear rate × duration), respectively. After each extent of deformation, the sample was subjected to SAOS for stabilization of the deformed morphology, and the sample was saved for further investigation. A schematic representation of the rheological approach has been provided in Figure 2.1. The shear rate (0.05 s^{-1}) was chosen low enough to favor coalescence. This shear rate was selected based on the critical capillary number (a function of the viscosity ratio of the dispersed matrix phase, the viscosity of the matrix phase, the interfacial tension and the average droplet size). Relevant theory (Grace 1982; Tucker III and Moldenaers 2002), the calculation of the critical capillary number, and the selection of the shear rate to investigate the morphological evolution are provided in the Annex-I of this work.

It is worth mentioning that the deformed samples were saved and cryo-fractured, followed by a gold coating to investigate the resultant morphology using SEM images.

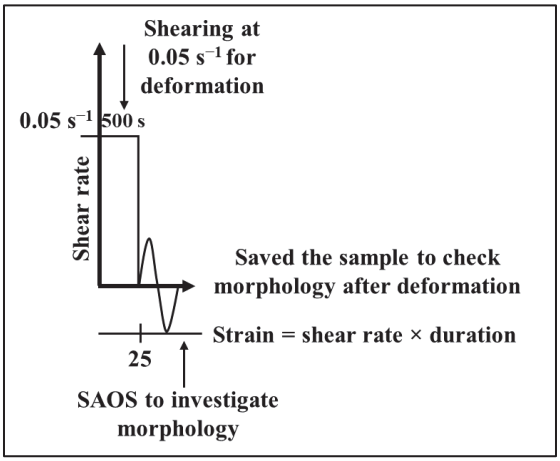

Figure 2.1 A schematic representation of the shear deformation followed by SAOS, a rheological approach, to study the morphological evolution of neat and FLG-filled PE/PP blends. A similar approach was followed for 2000 s and 5000 s, respectively.

The tensile properties were characterized according to ASTM D638 at room temperature with a 10 kN load cell and a crosshead speed of 50 mm/min. The MTS Alliance RF/200 tensile test apparatus was used for the investigation of tensile property. Dog-bone-shaped samples with 160 mm length, 12 mm width, and 3.5 mm thickness were used to characterize the tensile properties of the samples.

The Izod (notched) impact strength was investigated according to ASTM D256 by using the impact strength tester device (manufactured by International Equipments, India). Prior to the test, a notch was created on each sample (62 mm × 12 mm) by using a motorized notch cutter, manufactured by International Equipments, India.

At least five replicas were considered for each sample to investigate mechanical properties, and the average value has been reported along with the standard deviation (SD) as an error bar.

A Perkin-Elmer FTIR spectrometer (manufactured by PerkinElmer, Llantrisant, UK), specifically the Spectrum Two™ model equipped with a diamond crystal, was utilized for

capturing the Attenuated total reflectance-Fourier transform infrared spectroscopy (ATR-FTIR) spectrum. Thin films collected from the surface of both neat and FLG-filled composites (both pre- and post-UV exposure) were analyzed to obtain their respective FTIR spectra. Each spectrum comprised 10 scans and was collected at a resolution of 4 cm^{-1} across the wave number range of 400–4000 cm^{-1}.

FTIR spectra were utilized to investigate the relative carbonyl content of each sample, employing Equation 2.1.

$$\text{Relative carbonyl content} = \frac{A_{C=O} \text{ after UV exposure}}{A_{C=O} \text{ before exposure}} \tag{2.1}$$

In this context, A(C=O) denotes the area under the peak (within the wave number range of 1680–1800 cm^{-1}), indicative of the C=O functional group (Karimi et al., 2023). FTIR spectra of samples before and after UV exposure can be found in the supplementary section (see Figure A-I-1(a-e)). Evaluating the relative carbonyl content is of interest as it serves as an indicator of polymer degradation over time. To ensure accuracy, a minimum of three spectra from distinct regions of the samples were analyzed to compute and present the average carbonyl content values.

2.4 Results and Discussions

2.4.1 Morphology of Neat Blends

Figure 2.2(a-c) illustrate the microstructure of neat PE/PP blends with ratios of 20/80, 60/40, and 80/20, respectively. All the blends presented a droplet-dispersed morphology. However, droplet phase and size are governed by the blend composition. For instance, the PE/PP—20/80 blend represents PE droplets in the PP matrix. In contrary, PE/PP—60/40 and PE/PP—80/20 blends show PP droplets dispersed in the PE matrix. However, PP droplet size is bigger in PE/PP—60/40 than that of PE/PP—80/20. This size difference is attributed to the higher proportion of the PP phase (minor phase) in the PE/PP 60/40 blend system. The presence of a comparatively higher portion of the minor phase in an immiscible polymer blend increases the

probability of droplet coalescence. This phenomenon may result in bigger droplets in the matrix phase.

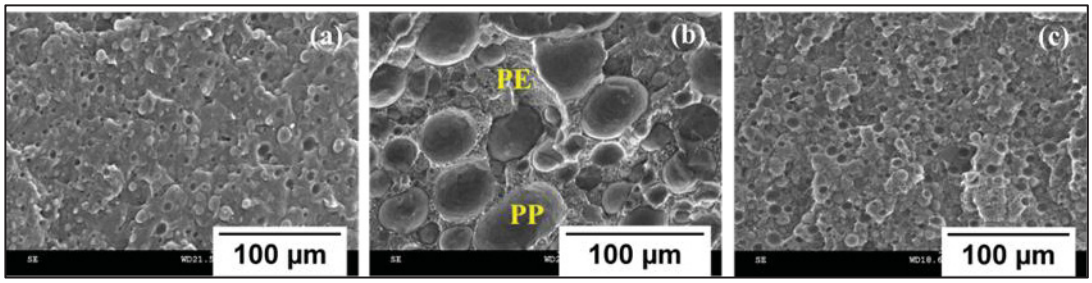

Figure 2.2 SEM images of PE/PP blends: (a) PE/PP—20/80, droplets representing PE phase; (b) PE/PP—60/40, droplets representing PP phase; (c) PE/PP—80/20, droplets representing PP phase

2.4.2 Influence of FLG on Morphology of Blend Composite

Figure 2.3 illustrates the distribution of PP droplet size (number average droplet radius, R_N) in a neat and FLG-filled PE/PP—20/80 blend composite. The addition of FLG results in a reduced and narrower distribution of PE droplet size. The addition of 2 wt.% and 5 wt.% of FLG results in a notable reduction in droplet size. The formation of finer morphology is attributed to the inhibition effect of rigid filler against the coalescence of droplets to grow bigger. A similar effect of rigid fillers was reported in the literature (Graziano et al., 2020).

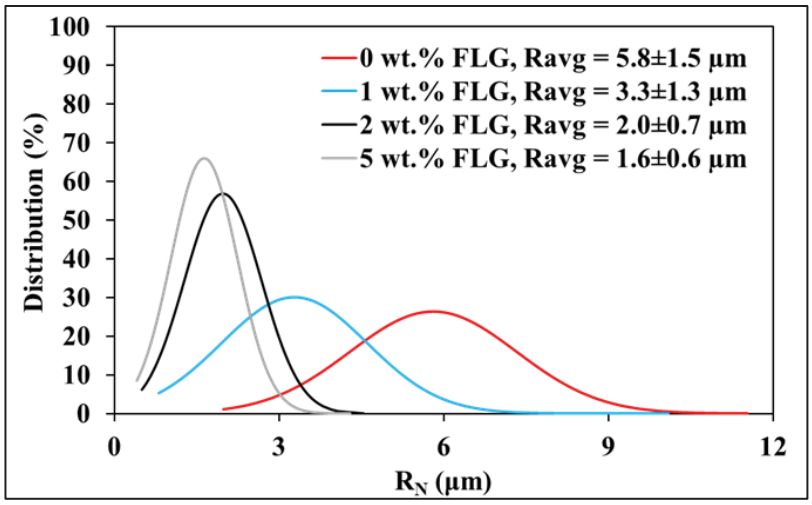

Figure 2.3 Distribution of PE droplet size in neat and FLG-filled PE/PP—20/80 blend composite with 1,2 and 5 wt.% of FLG, respectively

The SEM micrographs in Figure 2.4(a-c) depict the influence of the addition of 5 wt.% of FLG on the microstructure of PE/PP blend composites. The introduction of FLG causes de-formation of PE droplets in PE/PP—20/80 and PP droplets in PE/PP—60/40 and PE/PP—80/20 blends, respectively. Particularly in the PE/PP—60/40 blend, the deformation of relatively larger PP droplets enhances the likelihood of continuity in the minor PP phase. This phenomenon, in turn, can facilitate the creation of an uninterrupted network of electrically conductive fillers in the polymer blend composite.

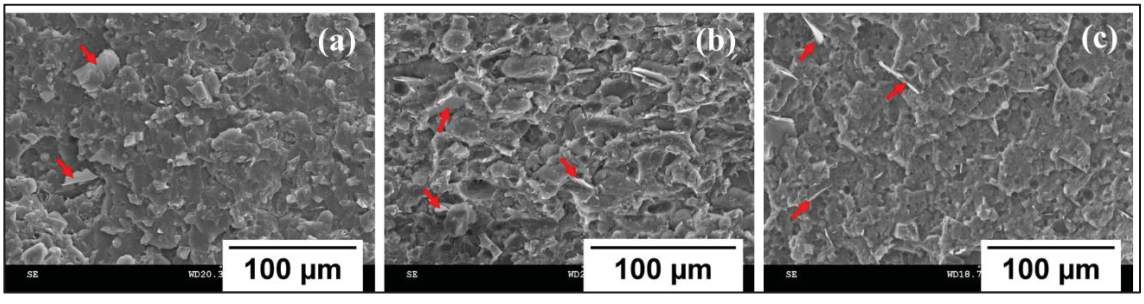

Figure 2.4 SEM images of the phase morphology of 5 wt.% FLG-filled composites; (a) PE/PP—20/80; (b) PE/PP—60/40 and (c)PE/PP—80/20. The red arrows are used to indicate the presence of FLG in the composites.

2.4.3 Influence of FLG on Electrical Conductivity of Composites

The impact of different FLG mixing strategies has been studied (see Figure A-I-2 in the Annex -I)) on the electrical conductivity of a PE/PP—60/40 blend composite. Notably, the composite exhibits significantly higher electrical conductivity when FLG is pre-mixed with the PP phase compared to when it is pre-mixed with the PE phase. This observation motivated us to carry on the rest of the study with composites, where FLG was pre-mixed with the PP phase. Figure 2.5 reports the change in electrical conductivity in FLG-filled composites with different concentrations of FLG in the composites. The graph displays that the electrical conductivity of PE/PP—60/40 blend composite is higher than that of PE/PP—20/80 blend composite, specifically up to 4 wt.% of FLG. However, when the FLG concentration reaches 5 wt.%, both blend composites demonstrate similar electrical conductivity. This suggests that the electrical properties are significantly influenced by the morphology, governed by blend compositions. In contrast, FLG-filled PE, PP, and PE/PP—80/20 remain insulative, even at a dosage of 5 wt.% FLG. Notably, the PP/FLG composite exhibits higher electrical conductivity than that of PE/FLG at 9 wt.% concentration of FLG. This observation implies that a relatively lower concentration of FLG is required in the PP matrix compared to the PE matrix to establish a continuous FLG network.

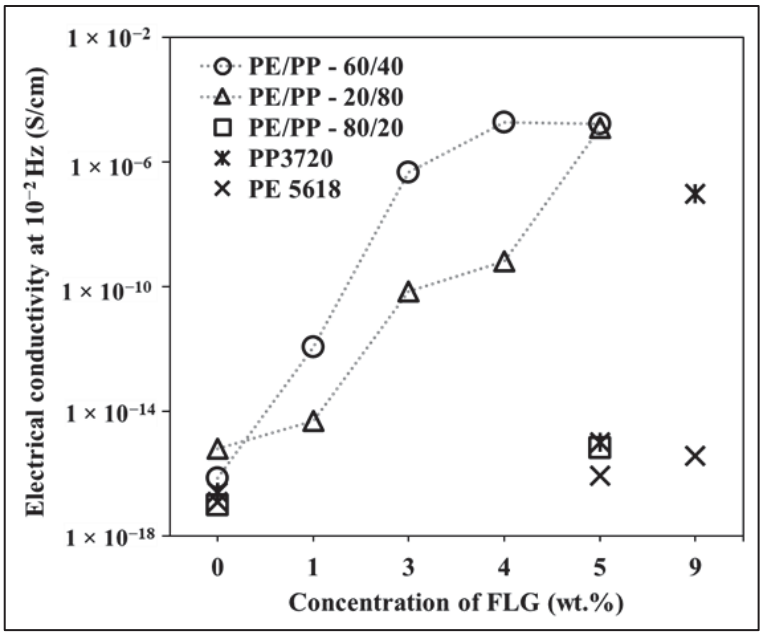

Figure 2.5 Real part of the conductivity of the compounds at 10−2 Hz (the lowest frequency) for different concentrations of FLG. Dotted lines are used to guide the reader's eye

2.4.4 Influence of Deformation on Electrical Conductivity of Blend Composite

Figure 2.6 presents the electrical conductivity of the deformed PE/PP—20/80 blend composite, containing 5 wt.% FLG, as a function of the frequency of the applied electric field. After deforming the composite in molten condition in the Rheometer, the samples were preserved to investigate the electrical conductivity. Intriguingly, despite the deformation in morphology (discussed using Figure A-I-3, in the Annex I) and a change in filler localization (A-I-4, in the Annex I), the electrical conductivity of the composite remained unchanged. This underscores the robustness of the FLG network in withstanding mechanical deformation in molten conditions. This observation is in agreement with the observation reported in the literature (Strugova et al., 2023).

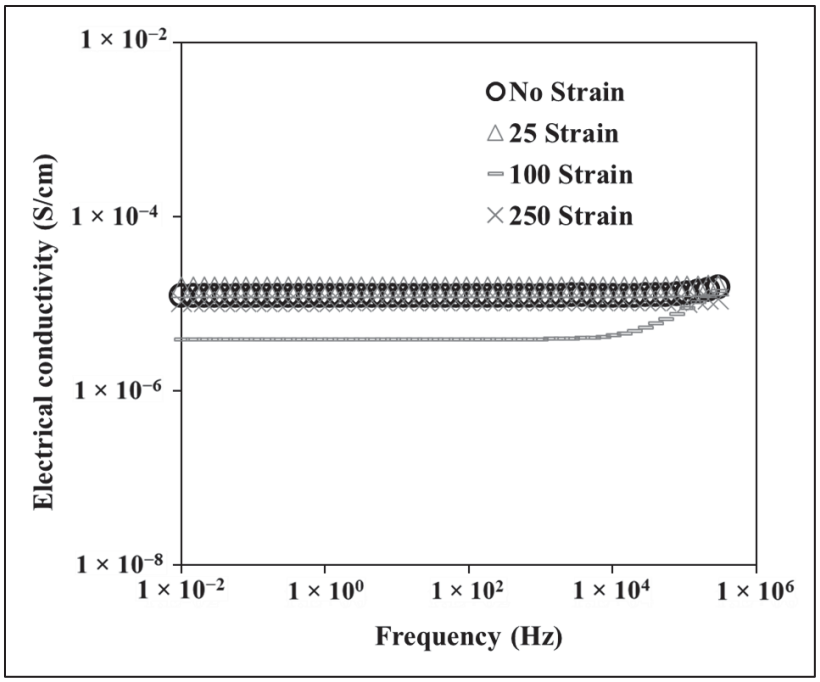

Figure 2.6 Electrical conductivity of PE/PP -20/80 blend composite (containing 5 wt.% FLG) after deformation by different strains, as a function of frequency.

2.4.5 Influence of FLG on Mechanical Properties Polyolefin Composites

In Figure 2.7a–c, the mechanical properties of the samples are plotted as a function of FLG concentration. Since the ductility of PE is around 10 times higher than that of neat PP, the ductility of PE has been plotted on the secondary axis of Figure 2.7c with different concentration of FLG. Figure 2.7a illustrates that the tensile modulus of neat PP is higher than that of neat PE. In addition, the tensile moduli of PE, PP, and PE/PP blends are increased by the additions of FLG. It is worth mentioning that the tensile strength of the samples as a function of the concentration of FLG has been provided in Figure A-I-5 in the Annex I. The stiffness of polymeric materials can be increased due to the reinforcement effect of rigid fillers. Analogous findings can be observed in the literature (Guo et al., 2020; Parameswaranpillai et al., 2019). Figure 2.7b shows that the impact strength of PE, PP, and PE/PP blend composites was not significantly affected by the presence of FLG. A similar effect of rigid filler on the impact strength of polymer material was reported earlier (Juan, 2020). However, Figure 2.7c shows that the addition of FLG decreased the ductility of the composites. The reduction in

elongation at break of PE and PE/PP—60/40 (PE- rich blend) composites is statistically more significant than that of PP and PE/PP—20/80 (PP- rich blend) composites. The presence of rigid filler hinders the polymer chain mobility, which ultimately affects the ductility of the composite. Several works in the literature have reported similar findings (Abbasi et al., 2019; dos Anjos et al., 2022; Parameswaranpillai et al., 2015).

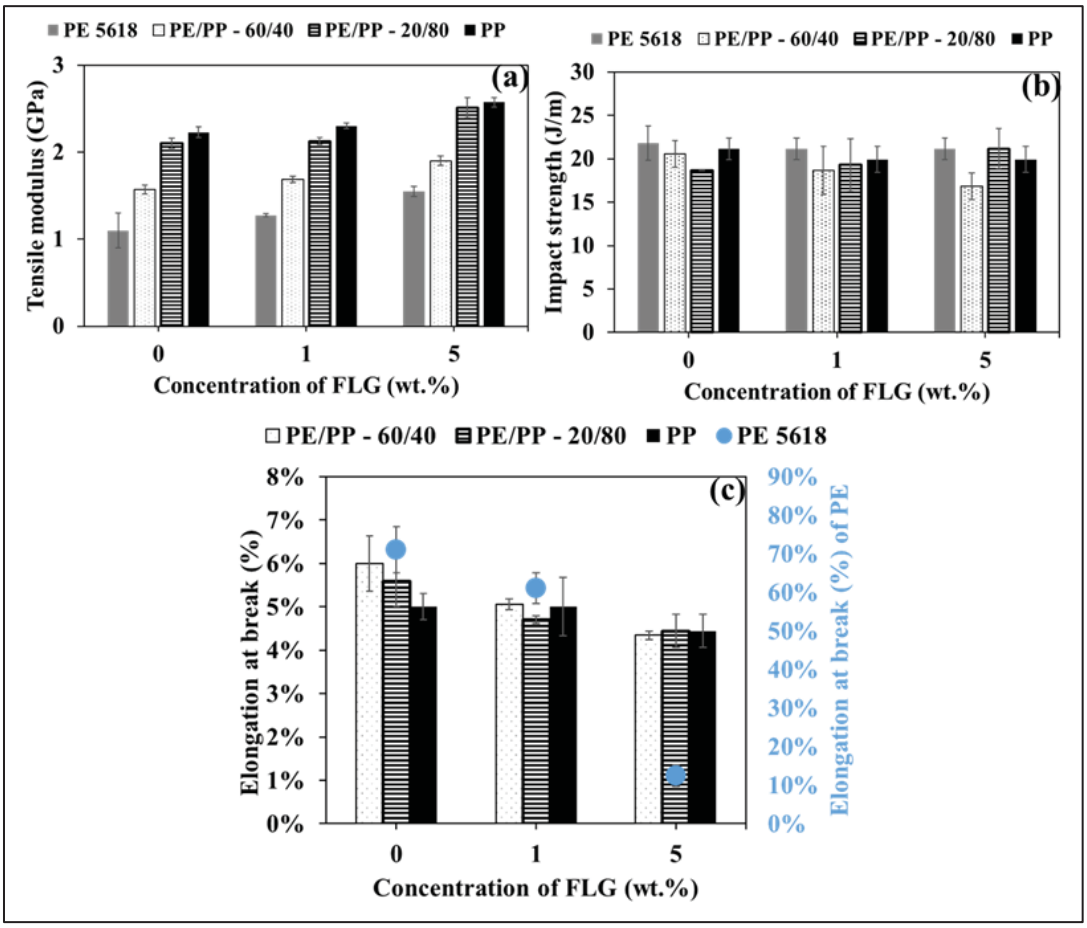

Figure 2.7 Mechanical properties of: (a) tensile modulus, (b) impact strength, and (c) elongation at break of PE, PE/PP blends, and PP composites with different concentration of FLG

2.4.6 Effect of Adding FLG on UV-Exposed Composites

2.4.6.1 Property Retention of UV-degraded Composites

In Figure 2.8, the retention of elongation at break (a sensitive property to UV degradation) after 4 weeks of UV exposure for neat and FLG-filled PE, PE/PP—60/40, PE/PP—20/80, and PP is plotted as the FLG concentration was varied in the composites. The figure illustrates that UV-exposed unfilled PE, PP, and PE/PP blends become too brittle to capture the correct elongation at break under the testing condition. This indicates a substantial UV degradation of the pure polyolefins. Conversely, FLG-filled polyolefin composites exhibit enhanced retention of ductility under UV radiation, owing to the photoprotective properties of FLG. Nevertheless, this photoprotective effect of FLG is more pronounced in polymeric systems where PE is the predominant phase compared to those where PP is the major component. Further analyses have been carried out in terms of sample surface imaging and FTIR investigation.

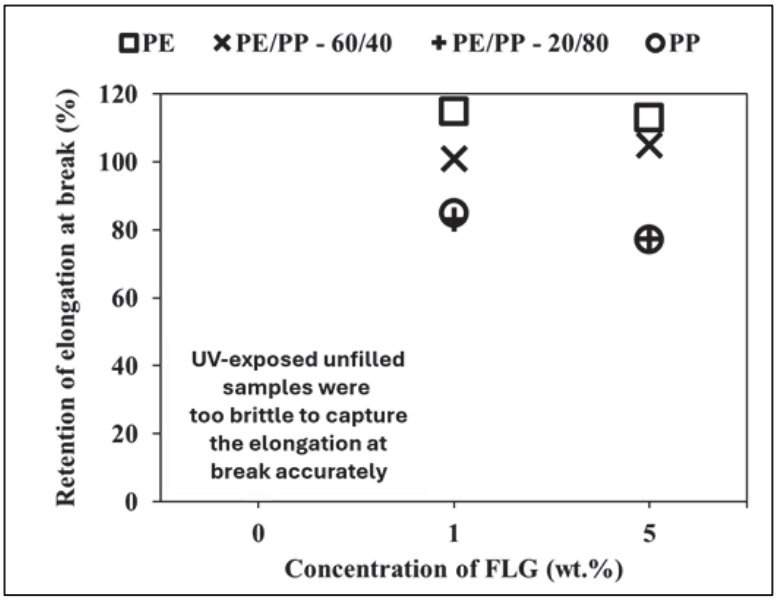

Figure 2.8 Retention of elongation at break of UV-exposed PE, PE/PP blends, and PP as the FLG concentration increased in the specimens

2.4.6.2 Appearance of the Compounds after UV Exposure

The SEM images in Figure 2.9a–c illustrate the surfaces of neat PE, PE/PP—60/40 blend, and PP samples, which were exposed for 4 weeks under UV radiation. Figure A-I-6 been provided in the Annex I to extend the idea of the appearance of a polyolefin sample before UV exposure. Additionally, Figure 2.9d–f display the UV-degraded surfaces of PE, PE/PP—60/40 blend, and PP composites, containing 1 wt.% FLG, respectively. Apparently, the presence of FLG lessens the occurrence of UV degradation-driven cracks in the samples' surface compared to their neat counterparts. This suggests that FLG can mit-igate the UV degradation process in polyolefins.degradation-driven cracks in the samples' surface compared to their neat counterparts. This suggests that FLG can mitigate the UV degradation process in polyolefins.

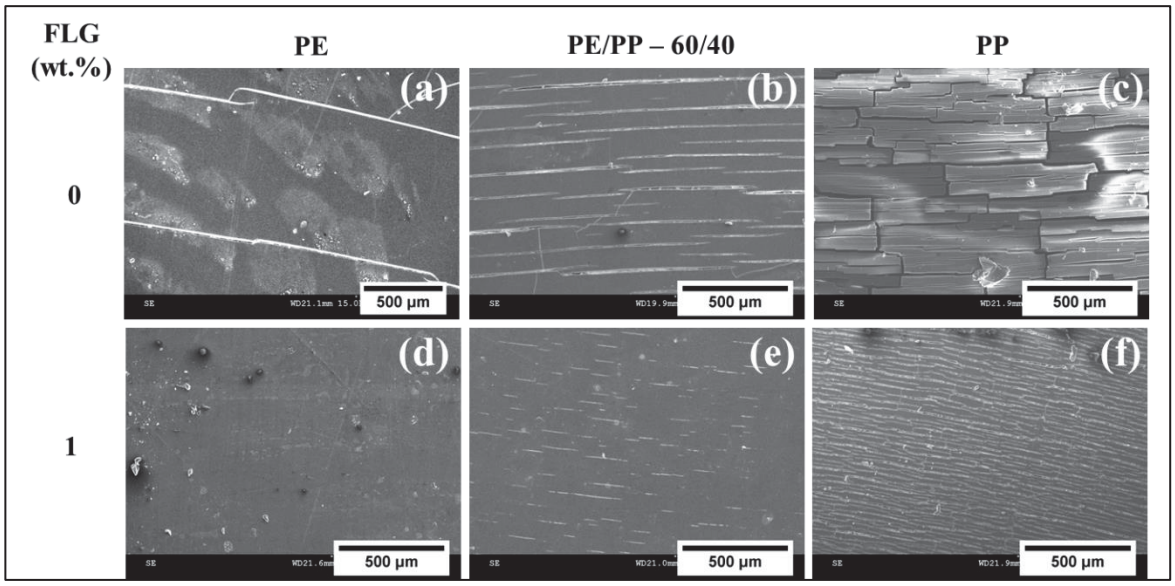

Figure 2.9 SEM micrographs of the UV-exposed unfilled (**a**) PE, (**b**) PE/PP—60/40, and (**c**) PP along with 1 wt.% FLG-filled (**d**) PE, (**e**) PE/PP—60/40 and (**f**) PP composites.

2.4.6.3 Chemical Analysis

In Figure 2.10, the relative carbonyl content of UV-exposed samples of PE, PE/PP—60/40, PE/PP—20/80 blends, and pure PP, both without and with FLG, is plotted against exposure time. The relative carbonyl content is determined by analyzing the FTIR absorption spectra of each UV-exposed sample and normalizing them against the carbonyl content of the corresponding sample prior to UV exposure. The incorporation of FLG reduces the formation of carbonyl content in UV-exposed composites, indicating the UV-stabilizing effect of FLG in polyolefin systems.

Furthermore, it is evident that the relative carbonyl content in UV-exposed PP is significantly higher compared to that in PE, suggesting that PP is more susceptible to UV degradation than PE. This tendency towards UV degradation is also observed in PE/PP blends; blends with a higher proportion of PP exhibit greater susceptibility to UV degradation compared to those with more PE. An explanation has been extended in the discussion part. Figure 2.10 illustrates the order of UV degradation tendency in the PE/PP polymer system as follows: PP > PE/PP—20/80 > PE/PP—60/40 > PE. A similar order of UV degradation tendency is noted in FLG-filled PE/PP composites, but the degradation rate is slower, attributed to the UV-stabilizing effect of FLG.

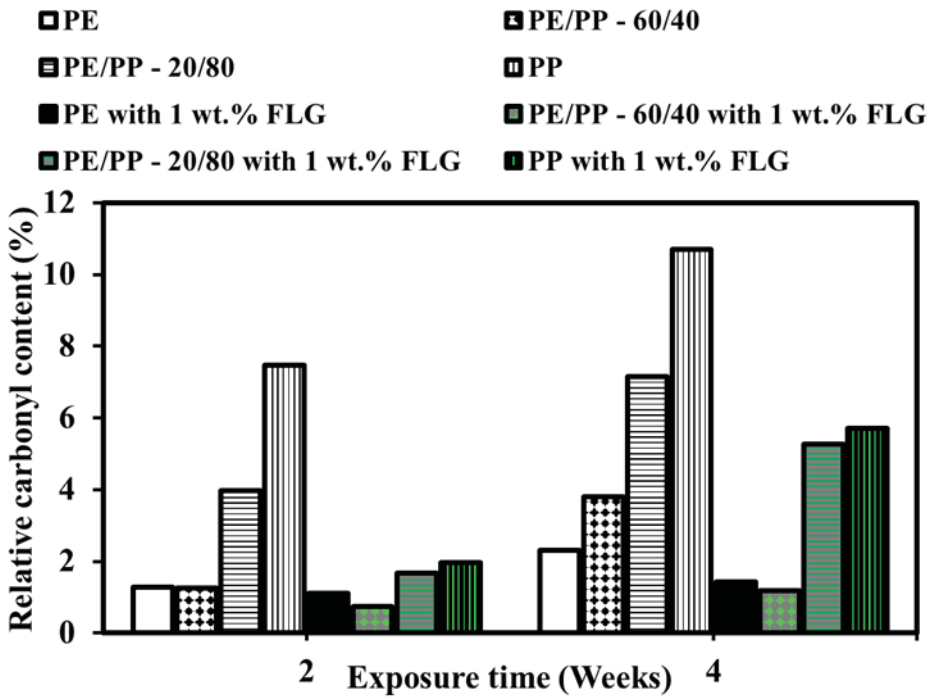

Figure 2.10 Change in the relative carbonyl content of UV-exposed PE, PE/PP blends, and PP samples with the duration of the UV exposure.

2.4.7 Discussion

The comprehensive analysis of the morphology, electrical properties, mechanical properties, and UV degradation behavior of FLG-filled PE/PP blend systems provide valuable insights into the multifaceted effects of FLG on polyolefin blend systems.

In a filler-filled, immiscible polymer blend system, double percolation (Al-Saleh et al. 2013; Jia et al. 2016; Otero-Navas et al. 2017; Pan et al. 2016; Strugova et al. 2021; Sumita et al. 1992) is an interesting phenomenon. This phenomenon refers to the percolation of one phase through another phase with the concomitant formation of a filler network through one of the percolating phases. In the case of a conductive filler, the double percolation effect increases the electrical conductivity of the composite by a significant order of magnitude. In this work, Figure 2.4b shows that the PP phase was not percolated through the PE matrix in the 5 wt.% FLG-filled PE/PP—60/40 blend composite. Despite lacking the double percolation effect, this

composite presents higher electrical conductivity. In fact, the predominant presence of FLG in the PP phase of the PE/PP blend composite is likely due to the premixing of FLG with the PP phase. Moreover, FLG migration from the PP to PE phase via PE/PP interface is also realized according to thermodynamic prediction (Tu et al., 2017a). Therefore, thermodynamic preference-induced FLG migration from the PP to PE phase via the PE/PP interface and volume exclusion effect of the PE phase in PE/PP—60/40 and 20/80 blend are two dominant factors in tailoring the conductive FLG network in PE/PP—60/40 and 20/80 blend composites. It has been reported in the literature (Arjmand et al., 2012) that once the conductive filler network is fully developed, further addition of filler does not reflect any significant effect on the conductivity of the composite. This phenomenon can be referred to as the saturated effect of the filler network. Moreover, blends with ratios of 60/40 and 20/80 exhibit superior conductivity compared to PE/FLG or PP/FLG composites, even when FLG concentration is higher (9 wt.%). This difference can be attributed to the poor dispersion of FLG in the PE phase compared to the PP phase under the same processing conditions. Moreover, superior electrical conductivity in the PE/PP—60/40 blend composite is not observed when FLG is pre-mixed with PE (see Figure A-I-2 in the Annex I). This could be attributed to the possible wrapping of FLG by insulating PE due to a stronger affinity between FLG and PE. Consequently, an interrupted FLG network results in reduced electrical conductivity in PE, even at higher concentrations of FLG. Additionally, during composite cooling, small PE crystals may form on FLG surfaces, impeding FLG contact and resulting in lower electrical conductivity in FLG-filled PE/PP—60/40 blend composites, prepared by FLG premixing with PE phase. These findings underscore the critical role of FLG dispersion and localization in attaining optimal electrical properties in polyolefin blend composites.

Furthermore, the shear-induced deformation applied in the molten condition of the compound does not affect the electrical conductivity of the composite in its solid state. This indicates that the conductive network established by FLG remains unaffected even under applied shear deformation. This highlights the resilience of FLG-filled composites to mechanical deformation while maintaining electrical performance.

FLG addition enhances the tensile modulus of both PE and PP, indicating improved stiffness attributed to the reinforcement effect of FLG. When mechanically strong, rigid fillers are present in polymer-like materials, the fillers act like stress concentrators, facilitating load transfer. In turn, the stiffness of filler-filled composite increases. Furthermore, better filler-matrix adhesion results in higher strength in the composite. Moreover, FLG incorporation does not adversely affect the impact resistance of the polyolefin blend composites. In general, rigid fillers have two opposing effects on the impact strength of a filler-filled composite. One effect is its role as a defect center, responsible for reducing the impact strength of the composite. Another role is to resist the crack, which is responsible for increasing the im-pact strength of the composite. When these two effects counterbalance each other, the impact strength of the filler-filled composite may remain unchanged. However, the impact strength of a filler-filled composite can also be influenced by filler-matrix adhesion, filler loading, and the interfacial properties of the composite. The preservation of mechanical properties coupled with the enhancement of stiffness underscores the potential of FLG as a multifunctional filler in polyolefin blend systems. However, the presence of graphene reduced the ductility of the composite, irrespective of the composition of the sample. In general, the presence of rigid particles like few-layer graphene restrains the mobility of polymer chains, which results in a reduction in the ductility of the filler-filled polymer composite.

Furthermore, FLG demonstrates a UV stabilizing effect on polyolefin composites, reducing the formation of carbonyl content, indicative of UV degradation of polymers. Usually, light-absorbing groups (chromophores), as internal or external components in polymer materials, initiate photodegradation (Karimi et al., 2021). Initially, chromophores absorb photons from UV radiation and become excited. These excited chromophores then break down into free radicals due to further UV exposure in the presence of oxygen. These free radicals attack the polymer chains and propagate the photodegradation process. The presence of graphene in the polymer matrix can decelerate the photodegradation process by absorbing photons. Additionally, graphene can interact with excited chromophores, absorbing their energy and releasing it as heat, which is known as the quenching effect. Moreover, the π-conjugated electrons in graphene can react with free radicals, neutralizing them and thereby slowing down

the photodegradation of the polymer material via the free radical scavenging effect of graphene. Apart from these chemical effects of graphene, it can also act as a physical barrier against oxygen diffusion through the polymer matrix due to its two-dimensional geometry. It has been noticed that the UV stabilizing effect of FLG is more pronounced in PE-rich blends compared to PP-rich blends, highlighting the differential susceptibility of PE and PP to UV degradation. PP exhibits a comparatively higher sensitivity to UV degradation, potentially attributed to the presence of tertiary carbon atoms within the polymer chain (Gijsman et al., 1999). The tertiary carbon atom can be readily attacked by UV radiation, which makes PP more susceptible to UV degradation than PE. The presence of FLG mitigates UV-induced surface cracking and preserves the ductility of the composite materials, further emphasizing its role in enhancing the durability and performance of polyolefin blend composites under UV exposure.

2.5 Conclusions

This study underscores the notable influence of FLG inclusion on the electrical con-ductivity, mechanical properties, and UV protection of polyolefin blend composites, as follows:

- The addition of FLG results in electrically conductive, mechanically strong, and more durable PE/PP blend composites.
- The application of shear-induced deformation in molten conditions can change the phase morphology of the blend composite, yet the electrical conductivity remains unaffected, highlighting the resilience of the conductive network within the FLG-filled composites.
- Only 4 wt.% (~2 vol.%) of commercial-grade and low-cost FLG could induce an electrical conductivity of the order of 1.87×10^{-5} S/cm (elector dissipative material) in PE/PP—60/40.
- As little as 1 wt.% FLG is adequate to retard the UV degradation of polyolefin composite.

- FLG demonstrates a UV stabilizing effect, more pronounced in PE-rich blends, mitigating UV-induced surface cracking and preserving ductility.

In conclusion, FLG offers a versatile solution for designing a reinforced electrostatic dissipative polyolefin composite with improved UV resistance. By understanding the interplay between FLG dispersion, morphology, and filler-polymer interactions, it is possible to tailor the properties of these composites for a variety of applications, from electric applications (semi-conductive separators in power cables, electro-dissipating packaging materials, etc.) to outdoor structural components.

Supplementary Materials

The supporting information can be fonuded in Annex I.

Funding

This research was funded by NanoXplore Inc.; Natural Sciences and Engineering Research Council (grant number CRDPJ 538482—18); PRIMA Quebec (grant number R18-46-001); Fonds de Recherche du Québec-Nature et Technologies (grant number 318813). The APC was funded by discounts from Editorial Office, MDPI and IOAP of Ecole de Technologie Superieure (ETS) Montreal.

CHAPTER 3

EFFECT OF FEW-LAYER GRAPHENE ON THE PROPERTIES OF MIXED POLYOLEFIN WASTE STREAM

S. M. Nourin Sultana [a] , Emna Helal [a,b] , Giovanna Gutiérrez [b], Eric David [a], Nima Moghimian [b] and Nicole R. Demarquette [a]

[a] Mechanical Engineering Department, Ecole de Technologie Superieure, 1100 Notre-Dame Street West, Montreal, Quebec, Canada H3C 1K3
[b] NanoXplore Inc., 4500 Thimens Blvd, Saint-Laurent, QC H4R 2P2, Canada

Paper published in *Crystals*, February 2023
DOI: 10.3390/cryst13020358

Chapter outline: Chapter 3 investigates the effect of few-layer graphene on the properties of mixed polyolefin waste streams. This chapter starts with an abstract summarizing the main findings of the study, followed by an introduction that sets the context. It then provides a detailed description of the materials and methods used, including specific materials and processing techniques. The chapter outlines the characterization methods employed, such as melt flow index (MFI), rheological properties, mechanical properties, and morphological characterization. The results and discussions section presents and analyzes the findings, supported by relevant figures. The chapter concludes with a summary of the findings.

Abstract: This work demonstrates how the addition of few-layer graphene (FLG) influences the processability and mechanical properties of the mixed polyolefin waste stream (R-(PE/PP)). Three different types of compounds were investigated: (1) R-(PE/PP) with FLG; (2) blends of R-(PE/PP) with prime polyethylene (PE) or polypropylene (PP) or PP copolymer; and (3) R-(PE/PP) with both the prime polymer and FLG. The processability was assessed by measuring the torque during melt extrusion, the melt flow index (MFI), and viscosity of the compounds. Investigations of the processability and mechanical properties of the composites indicate that the presence of FLG can reinforce the composites without hindering the

processability, an unusual but desired feature of rigid fillers. A maximum increase in tensile strength by 9%, flexural strength by 23%, but a reduction in impact strength were observed for the compounds containing R-(PE/PP), 4 wt.% FLG, and 9 wt.% prime PP. The addition of FLG concentrations higher than 4 wt.% in R-(PE/PP), however, resulted in higher tensile and flexural properties while preserving the impact strength. Remarkably, the addition of 10 wt.% FLG increased the impact strength of the composite by 9%. This increase in impact strength is attributed to the dominant resistance of the rigid FLG particles to crack propagation.
Keywords: graphene; mixed polyolefin; waste stream; processability; mechanical properties.

3.1 Introduction

Over the recent years, polymer materials have demonstrated a promising role in household as well as industrial applications. Consequently, plastic waste accumulation is soaring. According to a survey by Deloitte (Petigny et al., 2019), over 11 Mt of plastics were wasted in Canada during 2016 only, and only 9% was recycled; around 4% was incinerated for energy recovery and 87% was dumped into the environment. The estimated loss was CAD 7.8 billion for Canada.

Polyolefins (different types of polyethylene (PE) and polypropylene (PP)) are widely used in packaging materials (Jubinville et al., 2020) and are heavily present in post-consumer plastic residues. However, because they have comparable densities, they cannot be easily separated using standard techniques available in most sorting facilities. The most straightforward solution to recycle them consists of blending them and using them as it is. However, this is quite problematic as PE and PP are thermodynamically immiscible with each other, resulting in a material with weak mechanical properties. Hence, this type of mixed plastic waste is often directed to incineration and landfills (Maris et al., 2018). Therefore, improving the properties of mixed polyolefin waste streams is highly desired to enable the recycling of a huge portion of polymer waste.

In general, the mechanical recycling of plastic waste involves mixing with a rigid filler, prime polymer, or both (Khadri Diallo et al., 2022). In this regard, several investigations have been reported on the influence of adding different copolymers (Blom et al., 1996; Parameswaranpillai et al., 2019; Vranjes & Rek, 2007; Yang et al., 2003), solid particles (Ashenai Ghasemi et al., 2017; Hsieh et al., 2017; Qiu et al., 2002; Ramos & Belmontes, 1991), and combinations of copolymers and solid particles (Ashenai Ghasemi et al., 2017; Mofokeng et al., 2018; Parameswaranpillai et al., 2019; Parameswaranpillai et al., 2019) on the mechanical properties of prime polyolefin mixtures. However, these studies cannot be necessarily applied to mixed polyolefin waste due to many uncertainties such as polymer aging, presence of impurities, varied molecular structure, and molecular weight. Hence, more research work on the improvement of the mechanical properties of a mixed polyolefin waste stream is needed. A few studies are available on the upgrade of mixed polyolefin waste streams (Fang et al., 2013; Karaagac et al., 2021; Kazemi et al., 2015; Najafi et al., 2006) involving a copolymer and a few rigid fillers. These additives in PE/PP blends mostly increase the impact strength (impact toughness) and elongation at break (tensile toughness or ductility), but deteriorate the strength and modulus (stiffness) compared to the unfilled blends. Generally, impact modifying copolymers increase toughness but hinder the strength of the original material. Unlike copolymers, inorganic rigid fillers act as stress concentrators and mostly increase the stiffness and strength but reduce toughness. Therefore, different dosages of mechanically strong fillers and/or impact modifying copolymers need to be explored to obtain a better balance of stiffness, strength, and toughness in the composite.

Concomitantly, graphene is a 2D carbonaceous filler with lightweight and excellent mechanical strength. Moreover, commercially available few-layer graphene (FLG), mass-produced from natural graphite by a mechanochemical exfoliation process, allows for an economically viable use of graphene at an industrial scale. Although there have been several reports on the effect of adding modified and unmodified graphene on electrical properties (Al-Saleh, 2016; Du et al., 2018; Mun et al., 2019; Tu et al., 2017b, 2022; Wei et al., 2019), only a few have focused on the mechanical properties (Al-Saleh, 2016; Graziano et al., 2020) of prime PE/PP blends. Furthermore, the effect of the addition of FLG to improve the properties

of a mixed polyolefin waste stream, to our knowledge, has not been investigated. Therefore, this study was conducted to analyze the potential of commercially available FLG, which is less expensive than lab-grade graphene, to improve the properties of a mixed polyolefin waste stream.

In this work, a mixed polyolefin waste stream (designated as R-(PE/PP) mixture was melt blended with either FLG alone, a prime polymer alone (PE, PP homopolymer, or PP copolymer), or FLG in combination with a prime polymer. To prepare the composites containing R-(PE/PP) and FLG, the FLG concentration was varied from 1 to 10 wt.%. To prepare the blends of R-(PE/PP), FLG, and each of the three prime polymers, only a 4 wt.% loading was selected. Torque during extrusion, melt flow index (MFI), and viscosity of the samples were measured to evaluate the influence of adding FLG on the processability of the composites. In addition, the tensile, flexural, and impact properties of the composites of R-(PE/PP) containing FLG and/or the prime polymers were evaluated. Finally, the influence of adding FLG on the microstructure, and subsequently, the mechanical properties of the composites were investigated by scanning electron microscopy (SEM).

3.2 Materials and Methods

3.2.1 Materials

FLG powder (GrapheneBlack 3X) from NanoXplore Inc., Montreal, Canada, produced through a water-based environmentally friendly mechano-chemical exfoliation process was used in this work. The average thickness of FLG is 6–10 atomic layers and the lateral primary particle size is 1 to 2 μm. Loose clusters of primary particles form secondary particles. The average lateral size of secondary particles is around 30 μm.

A R-(PE/PP) mixture sourced from a local recycler in Quebec was selected for this work. According to the supplier's information, the mixture contains around 30 to 40 wt.% PP with less than 5 wt.% contamination (dye, ink, or pigment, etc.). Differential scanning calorimetry

(DSC) analysis of the R-(PE/PP) samples (Figure A-II-1, provided in the Annex II) indirectly confirmed the composition to be about PE/PP-60/40.

Masterbatches loaded with 30 wt.% FLG in three different prime polymers (PE homopolymer, PP homopolymer, and PP copolymer), provided by NanoXplore Inc., Montreal, Canada, were used in this work. In addition, a masterbatch obtained by adding 20 wt.% FLG to the R-(PE/PP) was also prepared and used. The specifications of the masterbatch polymers used in the present work are summarized in Table 3.1.

Table 3.1 Identification, MFI, and density of the polymers used in this work

Masterbatch Polymer	**Commercial Name**	**MFI (g/10 min)**	**Density (g/cm^3)**
R-(PE/PP)	N/A	≥4 (230 °C, 2.16 kg)	N/A
PE homopolymer	Alathon H5618	17 (190 °C, 2.16 kg)	0.955
PP homopolymer	Polypropylene 3720 WZ	20 (230 °C, 2.16 kg)	0.905
PP copolymer	Formolene 2620 A	20 (230 °C, 2.16 kg)	0.900

3.2.2 Processing

Three types of composites were obtained:

Type 1: R-(PE/PP)/FLG composites by blending the R-(PE/PP) with the R-(PE/PP)/FLG masterbatch to analyze the individual effect of adding FLG.

Type 2: R-(PE/PP)/prime polymer compounds by mixing the R-(PE/PP) with the prime polymer (PE, PP homopolymer, and PP copolymer) to analyze the effect of adding only the prime polymer.

Type 3: R-(PE/PP)/prime polymer/FLG composites by mixing the R-(PE/PP) with the prime polymer /FLG masterbatch to investigate the combined effect of adding the prime polymer and FLG.

All of the samples were processed in a HAAKE twin-screw extruder, (Rheomex OS PTW16/40) at 150 rpm, and 200 °C in all zones. Table 3.2 summarizes the nomenclature and corresponding compositions of the samples.

Table 3.2 Sample nomenclature and respective composition of the samples

Type of Compounds	Samples Nomenclature	R-(PE/PP) Concentration (wt.%)	Prime Polymer Concentration (wt.%)	FLG Concentration (wt.%)
As received mixed polyolefin waste stream	R-(PE/PP)	100	0	0
Type 1	R-(PE/PP)/FLG= 99/1	99	0	1
	R-(PE/PP)/FLG= 96/4	96	0	4
	R-(PE/PP)/FLG= 93/7	93	0	7
	R-(PE/PP)/FLG= 90/10	90	0	10
Type 2	R-(PE/PP)/PE/FLG = 87/13	87	13	0
	R-(PE/PP)/PP/FLG = 87/13	87	13	0
	R-(PE/PP)/PPcop/FLG = 87/13	87	13	0
Type 3	R-(PE/PP)/PE/FLG = 87/9/4	87	9	4
	R-(PE/PP)/PP/FLG = 87/9/4	87	9	4
	R-(PE/PP)/PPcop/FLG = 87/9/4	87	9	4

In the case of the Type 3 composites, 4 wt.% concentration of FLG was selected for further investigation. This choice was based on the performance of Type 1 composites, which, after the addition of 4 wt.% FLG, started to exhibit observable differences in the mechanical properties of the composites. Therefore, 87 wt.% R-(PE/PP) was blended with the 13 wt.% prime polymer/FLG masterbatch, resulting in Type 3 composites with 4 wt.% FLG. The final composition resulted in the R-(PE/PP)/prime polymer/FLG = 87/9/4.

3.3 Characterizations

3.3.1 Melt Flow Index (MFI)

A melt flow index (MFI) tester (manufactured by International Equipments, India) was used to estimate the MFI of the samples according to ASTM D1238.

3.3.2 Rheological Properties

A capillary rheometer (model: Instron SR20) was used to measure the viscosity of the samples at 200 °C at a shear rate varying from 50 s^{-1} to 1000 s^{-1}. This range was selected because it includes the shear rate that the polymer may undergo during the extrusion or injection processes. The length and diameter of the capillary were 40 mm and 1 mm, respectively, resulting in an L/D ratio of 40.

3.3.3 Mechanical Properties

An MTS Alliance RF/200 tensile test device was used to study the tensile and flexural properties of the samples. Tensile properties were studied according to ASTM D638 at a crosshead speed of 50 mm/min to measure the tensile strength, tensile modulus, and elongation at break at room temperature. Flexural strength and modulus were analyzed according to

ASTM D790 with a 0.1 (mm/mm)/min outer fiber strain rate (Z). For each case, a 10 kN load cell was used.

An impact strength tester device (manufactured by International Equipments, India) was used to measure the notched impact strength of the samples. The impact strength was evaluated according to ASTM D256. A motorized notch cutter (manufactured by International Equipments, India) was used to make notches in the samples.

At least five specimens of each composite were tested at room temperature to report the tensile, flexural, and impact properties. The average value is reported along with the standard deviation.

3.3.4 Morphological Characterization

A SEM S3600-N Hitachi (Model: MEB-3600-N) was used to obtain scanning electron microscope (SEM) images of the samples' fractured surface. The FLG powder was attached to the double-sided carbon tape without any gold coating to obtain the SEM image. To obtain the SEM images of the composites, the samples were cryo-fractured to analyze the morphology. In addition, a few samples were fractured by applying an impact load. A Gold Sputter Coater (Model: K550X) was used to coat the surface of the compounds before taking the SEM images.

3.4 Results and Discussions

3.4.1 Rheological Properties

The MFI values (Figure A-II-2, provided in Annex II) of the neat R-(PE/PP) and FLG-filled composites (Type 1 and Type 3) were found to be independent of the studied additive concentrations and types. Similarly, the applied torque during extrusion remained at 48 ± 1 Nm, irrespective of the FLG concentration in the composites. Both observations indicate that

unlike other solid particles (Koodehi & Dadvand Koohi, 2018; Lago et al., 2020), which adversely affect the processability and flow properties of the polymeric materials, FLG had very little or no effect on the flow behavior of the R-(PE/PP) when added up to 10 wt.%.

Furthermore, Figure 3.1 shows the viscosity as a function of shear rate at 200 °C (processing temperature) for a few of the studied compounds. It can be seen that the viscosity of the materials was not affected by the addition of graphene. This can be attributed to the lubrication effect of FLG (Ferreira et al., 2019). Similar findings were reported by the co-authors in a previous study regarding prime high density polyethylene (HDPE)/recycled HDPE/FLG blend composites (Khadri Diallo et al., 2022). Another study (Ferreira et al., 2019) reported similar results for HDPE/graphite composites.

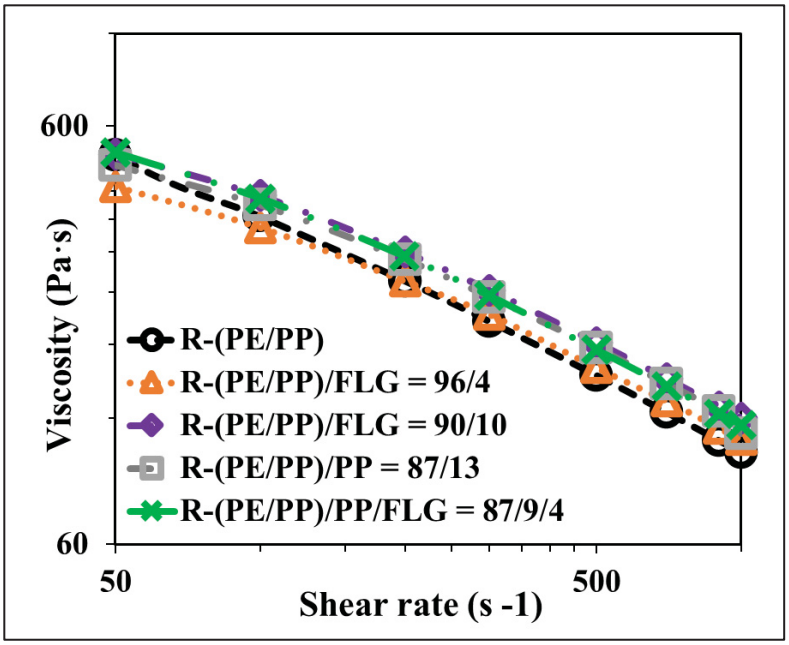

Figure 3.1 Apparent viscosity of the neat R-(PE/PP) and the additive (FLG, prime polymer) filled R-(PE/PP) samples at 200 °C as a function of shear rate

3.4.2 Mechanical Properties

The tensile and flexural properties of the R-(PE/PP)/FLG composites (Type 1) as a function of FLG concentration were investigated. Figure 3.2 (a) shows the tensile and flexural strengths, and Figure 3.2 (b) shows the tensile and flexural moduli of the studied compounds. Figure 3.2 (c) displays their impact strength, and Figure 3.2 (d) indicates their tensile toughness and elongation at break.

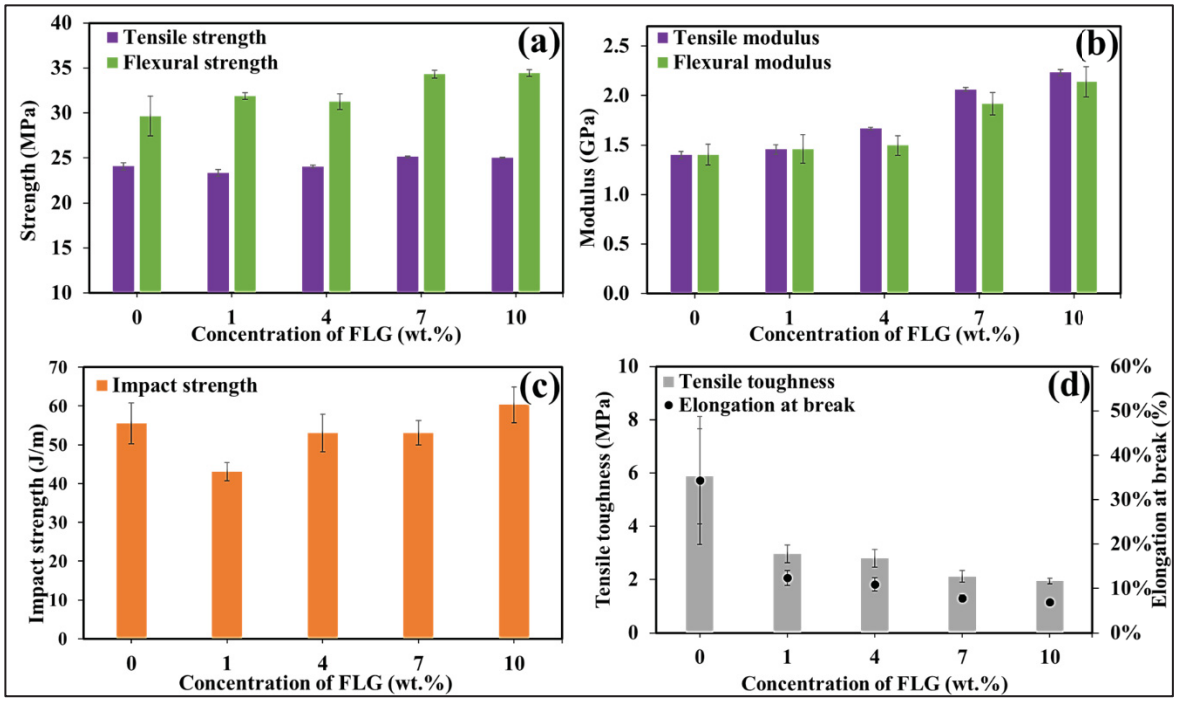

Figure 3.2 Tensile strength and flexural strength, (b) tensile modulus and flexural modulus and (c) impact strength, and (d) tensile toughness and elongation at break of the R-(PE/PP)/FLG composites as a function of FLG concentration

From Figure 3.2 (a) and Figure 3.2 (b), it can be observed that the presence of FLG resulted in an increase in the strength and modulus (stiffness) of the composites when compared to the one of the unfilled R-(PE/PP). The most significant increases in the tensile, flexural, and impact properties were observed for the R-(PE/PP)/FLG = 90/10 composite. These increases in strength and stiffness can be attributed to the reinforcement effect of the FLG particles in the R-(PE/PP). Previously, a similar reinforcing behavior of carbon fiber (Hsieh et al., 2017), glass

beads (Qiu et al., 2002), short glass fiber (Ramos & Belmontes, 1991), and wood flour (Feng et al., 2020) in a controlled PE/PP blend system has been reported in the literature.

As illustrated in Figure 3.2 (c), the addition of 1 wt.% FLG resulted in a reduced impact strength while 4 and 7 wt.% FLG did not reduce the impact strength of the composites. However, an increase in the impact strength was observed in the R-(PE/PP)/FLG = 90/10 composite. This unusual trend in the impact strength by the addition of rigid fillers has only been reported in a few studies, and was attributed to the resistance of the rigid filler particles to crack propagation throughout the composite (Juan, 2020).

Both elongation at break and tensile toughness of the FLG-filled composites decreased as the FLG concentration increased, as can be seen in Figure 3.2 (d). This is a common effect of the addition of rigid fillers and has been reported in the literature (Ashenai Ghasemi et al., 2017; Batista et al., 2019).

It is worth noting that the increase in the FLG loading yielded the opposite effect on the tensile toughness and impact resistance of the Type 1 composites. Possible reasons explaining this difference are presented in the Discussion section.

Mechanical properties of the Type 2 (R-(PE/PP)/prime polymer = 87/13) and Type 3 (R-(PE/PP)/prime polymer/FLG = 87/9/4) composites are summarized in Figure 3.3. The tensile strength, flexural strength, tensile modulus, flexural modulus, elongation at break, tensile toughness (estimated by the calculating the area underneath the stress–strain curve), and impact strength are, respectively, presented in Figure 3.3 (a–g), as a function of the type of prime polymer present in the Type 2 and Type 3 composites.

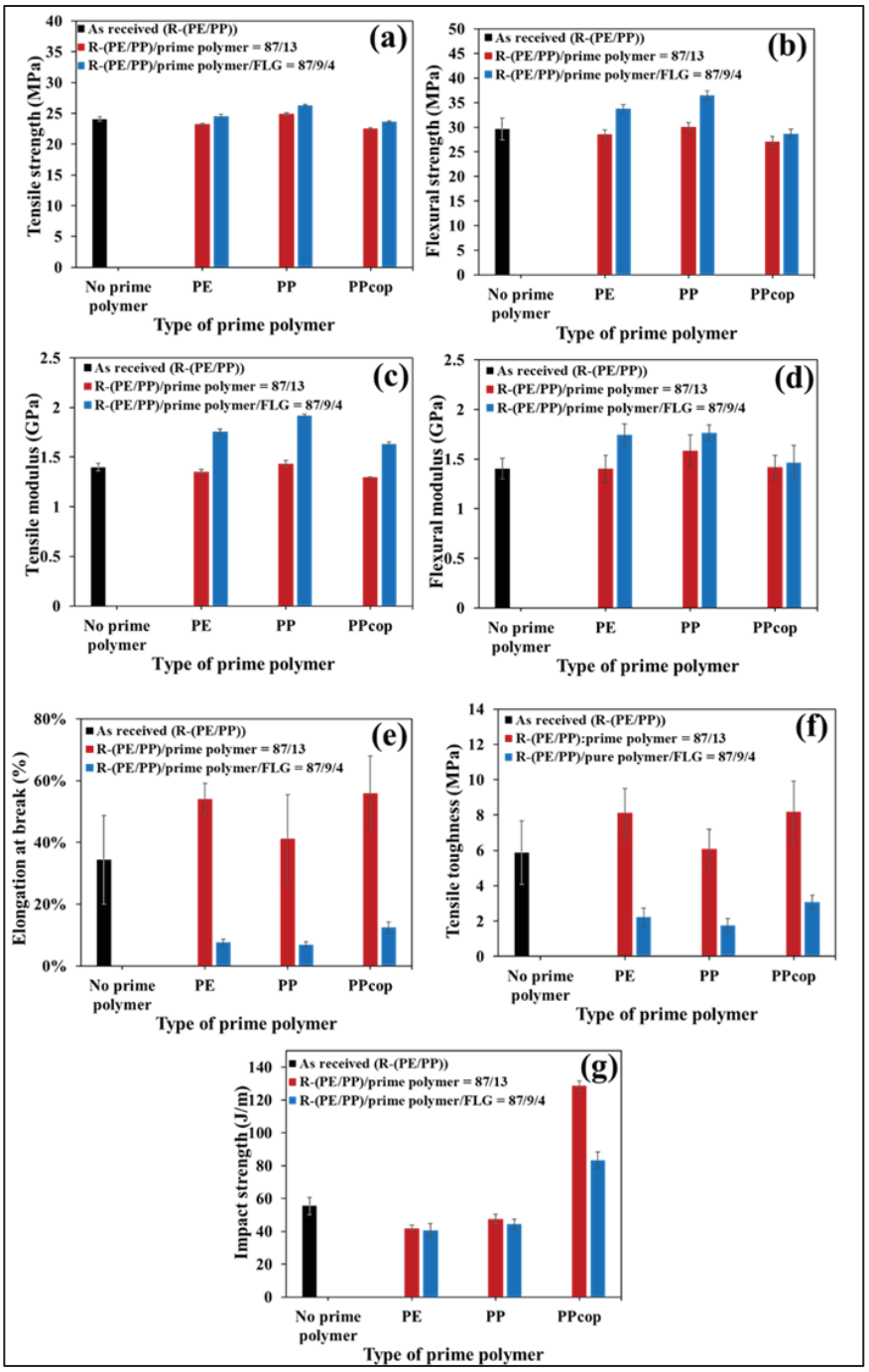

Figure 3.3 (**a**)Tensile strength, (**b**) flexural strength, (**c**) tensile modulus, (**d**) flexural modulus, (**e**) elongation at break, (**f**) tensile toughness, and (**g**) impact strength of the Type 2 and Type 3 samples as a function of the type of the used prime polymer. The properties of the as received R-(PE/PP) are presented by the black bars as a baseline

As observed in Figure 3.3(a–d), the Type 3 composite containing both the prime polymer (PE or PP) and FLG presented higher tensile and flexural properties than that of the neat R-(PE/PP) and respective Type 2 samples. For example, with 4 wt.% FLG and 9 wt.% PP, the flexural strength of Type 3 was 21% higher than the corresponding one of the Type 2 composite with 13 wt.% PP.

However, the Type 2 composites showed a higher elongation at break, tensile toughness, and impact strength than the corresponding ones of Type 3. A substantial increase in the impact strength and ductility was observed in the Type 2 composite containing the PP copolymer.

Precisely, the addition of the impact-modifying PP copolymer resulted in a sharp increase in the fracture toughness by 132% for Type 2 and by 50% for Type 3 when compared to the neat R-(PE/PP). A similar effect resulting from the addition of copolymers has been reported (Blom et al., 1996; Parameswaranpillai et al., 2019; Vranjes & Rek, 2007; Yang et al., 2003).

3.4.3 Morphology

Figure 3.4 shows the SEM images of the cryo-fractured surface of (a) R-(PE/PP), (b) and (c) R-(PE/PP)/FLG = 96/4 and (d) FLG powder.

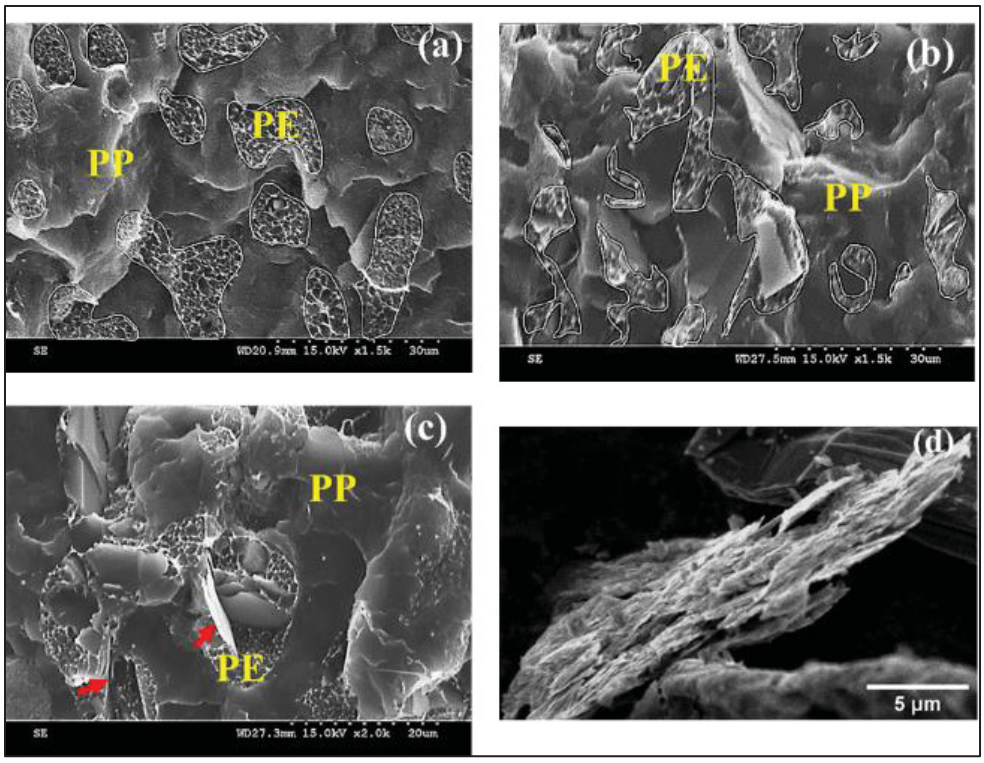

Figure 3.4 SEM images of (**a**) neat R-(PE/PP), (**b**) and (**c**) R-(PE/PP)/ FLG = 96/4, and (**d**) FLG powder; in (a) and (**b**), the domain of the PE phase is marked by a white outline and in (**c**), the localization of FLG in the PE phase is marked by the red arrow to guide the readers' eyes

In Figure 3.4 (a) and 3.4 (b), two different phases are visible. The rough phase corresponds to PE and the smooth phase to PP. PP has a much higher glass transition temperature than PE. During cryo-fracturing, PP dips below its glass transition temperature much easier than the case for PE. Consequently, the PE undergoes ductile fracture while the PP undergoes brittle fracture (Kazemi et al., 2015). Although PE was the major component of the mixed polyolefin waste stream of this work, the area of the PE phase domain was smaller than that of the PP phase. In the case of an immiscible polymer blend, the morphology is directly dependent on the viscosity ratio of the constituting polymer components at the processing conditions. In the PE/PP immiscible blend systems, PP can form the matrix of the blend morphology with minor weight contribution, if the viscosity of PP is less than that of PE. A similar observation of creating a matrix by the minor component of the blend has been reported in the literature

(Kazemi et al., 2015). The authors showed this observation in the case of a PE/PP-65/35 blend where the viscosity of PE was 500 Pa·s and the viscosity of PP was 300 Pa·s.

Moreover, Figure 3.4 (c) indicates the localization of FLG in the PE phase, which was similar to the observations by other authors (Tu et al., 2017b). The SEM image of the FLG powder on carbon tape is provided in Figure 3.4 (d) as a reference and for the purpose of comparison. The preferential localization of FLG in the PE phase is attributed to lower interfacial tension between PE and graphene than that of PP and graphene (Tu et al., 2017a). Moreover, it is observed that the addition of FLG resulted in a finer or elongated domain size of the PE phase in the R-(PE/PP)/FLG = 96/4 composite compared to that of the neat R-(PE/PP). A similar refinement of morphology in the presence of FLG has been reported by other authors (Khadri Diallo et al., 2022).

3.4.4 Discussion

As shown in Figure 3.1, the viscosity of the FLG-filled composites remained independent of the loading of FLG. The observed torque during extrusion and the MFI values (provided in Figure A-I-2 of Annex II) also support this finding. Therefore, it can be stated that FLG loadings up to 10 wt.% do not affect the processability of the composites. This may be the outcome of commensurable contacts of filler agglomerates, which maintain both the slippage and mobility of the molten polymer chain in the filled composites, similar to the unfilled compound (i.e., lubricant effect) (Ferreira et al., 2019).

It was observed that in the Type 1 composites, higher loadings of FLG increased both the tensile and flexural strength and modulus of the composites. This is attributed to the reinforcing effect of strong solid particles (Feng et al., 2020; Hsieh et al., 2017; Ramos & Belmontes, 1991) such as FLG. Furthermore, decreasing trends of both elongation at break and tensile toughness were observed at increasing concentrations of FLG. In contrast, the impact strength (fracture toughness) behavior as a function of FLG loading showed a different trend. Low (1 wt.%), medium (4 and 7 wt.%), and high loadings (10 wt.%) of FLG resulted in reduced,

similar, and increased impact strength, respectively, compared to the one of neat R-(PE/PP). In particular, the R-(PE/PP)/FLG = 90/10 composites showed an increase in the fracture toughness but a decrease in elongation at break and tensile toughness. In homogeneous or single-phased materials, both impact toughness and tensile toughness follow a similar trend of variation. More complicated trends might be at play in heterogeneous or multiphase composite systems. In fact, the elongation at break of a polymer composite depends mostly on the extent of the polymer chains' mobility while the impact strength depends on the rate of crack propagation throughout the compound. Solid particles reinforcing the polymer composites may have a positive or negative effect on the impact strength by acting either as defect centers (Dikobe & Luyt, 2017) or crack resisting points (Juan, 2020), depending on their strength and stiffness. In other words, the overall impact strength of the solid particle filled blend composites is the outcome of the competition between the negative effect of a filler as a defect center and the positive effect of the crack resistance of the filler. A higher impact strength of the composite can be achieved if the loading of the rigid filler is within an optimum concentration range where the crack propagation resistance of the filler is the dominant factor. In this work, the reduction in the impact strength of the R-(PE/PP)/FLG = 99/1 composite indicates that 1 wt.% FLG was not within the desired optimum concentration range to overcome the negative effect of fillers as defect centers in the composite. On the other hand, the increased impact strength of the R-(PE/PP)/FLG = 90/10 composite suggests that 10 wt.% FLG was adequate and within the optimum concentration range to increase the resistance to crack propagation, and to overcome the negative effect of FLG as a defect center, on the impact toughness of the composite. For reference, the SEM images of the fractured surfaces of the neat R-(PE/PP), R-(PE/PP)/ FLG = 96/4, and R-(PE/PP)/FLG = 90/10 composites are shown in Figure 3.5 (a–c), respectively.

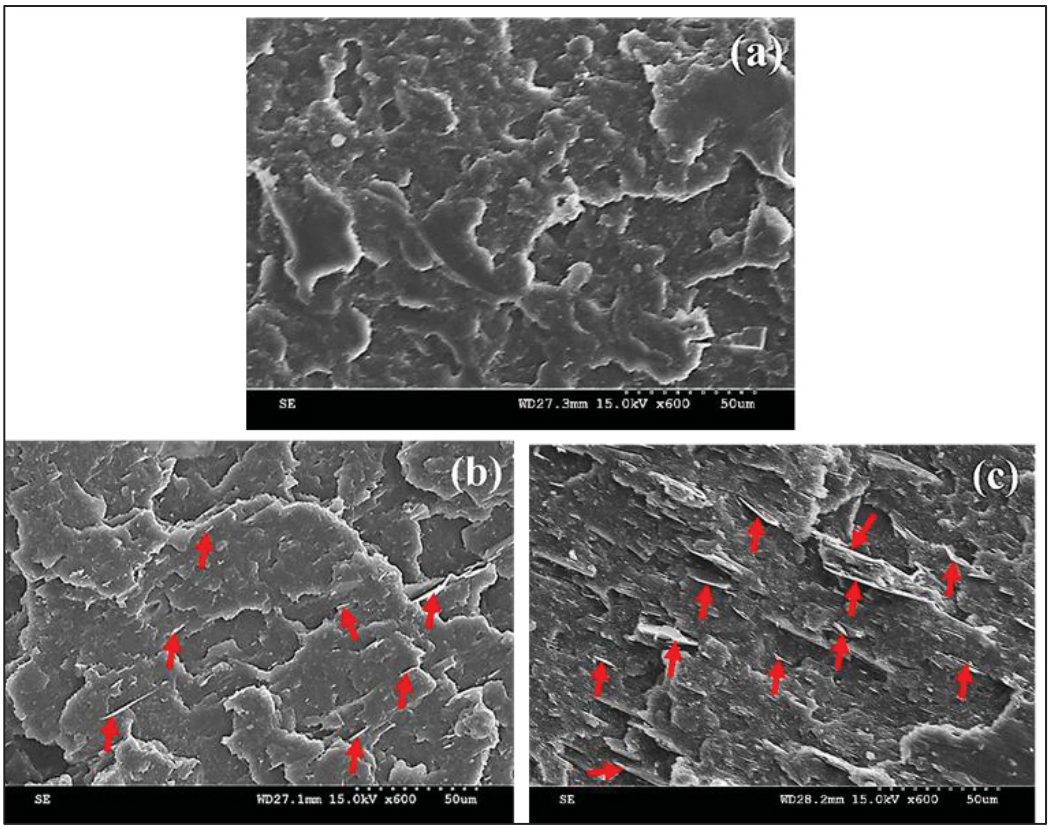

Figure 3.5 SEM images of the fractured surface of the (**a**) neat R-(PE/PP), (**b**) R-(PE/PP)/FLG = 96/4, and (**c**) R-(PE/PP)/FLG = 90/10. The arrows indicate a few of the FLGs, visible on the fractured surface of the R-(PE/PP)/FLG composites

It can be seen in Figure 3.5 (b) and Figure 3.5 (c) that more FLG was visible in the R-(PE/PP)/FLG = 90/10 composite than in the R-(PE/PP)/FLG = 96/4 composite. In other words, R-(PE/PP)/FLG-90/10 (shown in Figure 3.5 (c)) had more impact crack resisting sites than the neat R-(PE/PP) and R-(PE/PP)/FLG = 96/4 (as can be seen in Figure 3.5 (b)). This phenomenon resulted in a higher impact strength for the R-(PE/PP)/FLG = 90/10 composite. However, the polymer chain mobility or slippage of the polymer chains in the solid state was restricted by strong and rigid FLG, which reduced the elongation at break of R-(PE/PP)/FLG = 90/10. Simultaneous increment in the impact toughness and reduction in the tensile toughness in the same composite was also observed by Antimo et al. (Graziano et al., 2020) in a PE/PP-90/10 composite with 4 wt.% graphene derivatives.

Based on the analysis of the plots in Figures 3.2 and 3.3, it can be concluded that R-(PE/PP)/FLG = 90/10, R-(PE/PP)/PP/FLG = 87/9/4, and R-(PE/PP)/PPcopolymer = 87/13 compounds have shown significant improvement in different properties compared to that of the unmodified R-(PE/PP). Table 3.3 shows the variation in the mechanical properties of the best performing samples in this work.

Table 3.3 Mechanical property variation (%) in compounds showing a significant change in properties compared to the neat R-(PE/PP)

		Property Variation (%)		
Properties	**As Received R-(PE/PP)**	**Type 1 with 10 wt.% FLG**	**Type 2 with 13 wt.% PPcopolymer**	**Type 3 with 9 wt.% PP and 4 wt.% FLG**
Tensile strength	24 MPa	+4%	−6%	+9%
Tensile modulus	1.4 GPa	+60%	−7%	+37%
Flexural strength	30 MPa	+16%	−9%	+23%
Flexural modulus	0.9 GPa	+46%	+1%	+34%
Elongation at break	34%	−80%	+63%	−80%
Tensile toughness	6 MPa	−67%	+39%	−70%
Impact strength	55.5 J/m	+9%	+132%	−20%

Further analysis of the data presented in Table 3.3 suggests that, if the target application requires an overall increase in the strength, stiffness, and fracture toughness in the mixed polyolefin waste stream, then the addition of a higher loading of FLG is recommended. Since any reprocessing step or inclusion of any additive (fillers or nanofillers) will increase the cost of R-(PE/PP), the addition of a higher loading of FLG will increase the price of the R-(PE/PP)/FLG composite. However, it is worth mentioning that an industrial grade FLG was used in this work, which is more cost effective than other grades of carbon based nanofillers such as carbon nanotubes (CNT). In addition, FLG has the potential to reduce the

photodegradation of polymer composites (Karimi et al., 2021). Therefore, it is expected that FLG-filled composites feature a higher strength and durability compared to those of the unmodified mixed polyolefin waste stream, at a cost of the added FLG. Finally, the presented approach is intended to recover mixed plastic waste streams that have little or no value at the base and are otherwise landfilled. For superior impact and tensile toughness, the strategy of the mixing of R-(PE/PP) with a copolymer would be more useful. For applications requiring higher strength and stiffness and less sensitivity to toughness, compounds containing both prime PP and FLG would be interesting.

3.5 Conclusions

We investigated the influence of adding FLG on the processability and mechanical properties of mixed polyolefin waste streams. FLG alone, the prime polymer (PE, PP, or PP copolymer) alone, and FLG in combination with different prime polymers were melt blended with the R-(PE/PP). MFI, effective torque during extrusion, and viscosity of the FLG-filled composites remained unchanged for concentrations of FLG up to 10 wt.%. Moreover, it was shown that the addition of 4 wt.% FLG in combination with prime PP increased the tensile strength by 9%, the tensile modulus by 37%, the flexural strength by 23%, and the flexural modulus by 34%, but reduced the impact strength by 20% compared to the respective properties of the neat R-(PE/PP). However, the addition of 10 wt.% of FLG increased the tensile strength by 4%, tensile modulus by 60%, flexural strength by 16%, flexural modulus by 46%, and the impact strength by 9% compared to that of the neat R-(PE/PP). This desired increase in the tensile and flexural properties is attributed to the reinforcing effect of FLG. The increase in the impact strength of R-(PE/PP)/FLG with a higher loading (10 wt.%) of FLG was attributed to the resistance effect of strong FLG particles to impact crack propagation.

Based on the experimental and morphological observations, this work reports that FLG enables the processability of R-(PE/PP) while improving the mechanical properties of FLG-filled R-(PE/PP) composites. This work outlines the possibility of channeling a mixed polyolefin waste stream back to various regular applications with more strength, without altering the

processability. FLG-reinforced R-(PE/PP) composites can be used in outdoor furniture and in the construction industry. As a result, the demand for virgin polymers could be reduced, which would be a big step toward the protection of biodiversity and a reduction in harmful gas emissions. Moreover, this study suggests a useful application of commercially produced FLG.

Supplementary Materials

The supporting information can be fonuded in Annex II, Figure A-I-1: DSC analysis of unfilled R-(PE/PP), Figure A-I-2: MFI of (a) R-(PE/PP)/FLG composites as a function of the concentration of FLG and (b) R-(PE/PP)/prime polymer/FLG composites as a function of the type of prime polymer.

Funding

This research was funded by NanoXplore Inc.; Natural Sciences and Engineering Research Council (grant number CRDPJ 538482—18); PRIMA Quebec (grant number R18-46-001); Fonds de Recherche du Québec-Nature et Technologies (grant number 318813). The APC was funded by discounts from Editorial Office, MDPI and IOAP of Ecole de Technologie Superieure (ETS) Montreal.

CHAPTER 4

THE INFLUENCE OF A COMMERCIAL FEW-LAYER GRAPHENE ON THE PHOTODEGRADATION RESISTANCE OF A WASTE POLYOLEFINS STREAM AND PRIME POLYOLEFIN BLENDS

S. M. Nourin Sultana [a] , Emna Helal [a,b] , Giovanna Gutiérrez [b], Eric David [a], Nima Moghimian [b] and Nicole R. Demarquette [a]

[a] Mechanical Engineering Department, Ecole de Technologie Superieure, 1100 Notre-Dame Street West, Montreal, Quebec, Canada H3C 1K3
[b] NanoXplore Inc., 4500 Thimens Blvd, Saint-Laurent, QC H4R 2P2, Canada

Paper published in *Recycling*, April 2024
DOI: 10.3390/recycling9020029

Chapter outline: This chapter begins with an abstract, followed by an introduction that provides background and sets the context for the study. The results and discussions section then presents the morphology of the composites, the dispersion of FLG within the composites, and the effect of adding FLG on UV-exposed composites, culminating in a comprehensive discussion. The materials and methods section outlines the specific materials used, the methods employed, the photodegradation process in a QUV chamber, and the characterization techniques. Finally, the main findings are summarized in the conclusion section. This work was published in Recycling.

Abstract: : This work investigated the photostabilizing role of a commercially available few-layer graphene (FLG) in mixed polyolefins waste stream (MPWS), ensuring extended lifespan for outdoor applications. The investigation was conducted by analyzing carbonyl content increase, surface appearance, and the retention of mechanical properties of UV-exposed MPWSs/FLG composites. Despite the likely predegraded condition of MPWS, approximately 60%, 70%, 80%, and 90% of the original ductility was retained in composites containing 1, 4, 7, and 10 wt.% FLG, respectively. Conversely, just 20% of the original ductility was retained

in unfilled MPWS. Additionally, less crack density and lower carbonyl concentrations of the composites also highlighted the photoprotection effect of FLG. For prime polyolefin blends, only 0.5 wt.% or 1 wt.% FLG was sufficient to preserve the original surface finishing and protect the mechanical properties from photodegradation. Hence, it was observed that MPWS require more FLG than prime polyolefin blends to get to comparable property retention. This could be attributed to the poor dispersion of FLG in MPWS and inevitable uncertainties such as the presence of impurities, pre-degradation, and polydispersity associated with MPWS. This study outlines a potential approach to revalorize MPWS that possess a minimal intrinsic value and would otherwise be destined for landfill disposal.

Keywords: graphene; polyolefin; waste; photodegradation; photoprotection; mechanical properties

4.1 Introduction

Worldwide, approximately 350 million metric tons (Mt) of plastic waste are generated each year, and a substantial part, approximately 50%, is composed of polyolefin mixture (Singh et al., 2023). Therefore, the development of effective strategies to revalorize mixed polyolefins waste stream (MPWS) would pave the way to utilize a significant portion (Jubinville et al., 2020) of plastic waste with a small or no base commercial value that would otherwise be disposed of in landfills. Consequently, the scientific research on reusing post-consumer waste-recovered polyolefin blends is getting more attention. Several studies have been developed targeting the modification of mechanical properties of MPWS (Fang et al., 2013; Karaagac et al., 2021; Kazemi et al., 2015; Najafi et al., 2006; Sultana et al., 2023) through, for instance, the addition of copolymers or rigid fillers. However, the photodegradation (Gutiérrez-Villarreal & Zavala-Betancourt, 2017; Karimi et al., 2023; Ojeda et al., 2011; Peng et al., 2017) of polyolefins is a key challenge that should be successfully resolved to attain an extended lifespan in outdoor applications, such as containers, bumpers, dashboards, garden furniture, playground equipment, bottle crates, etc.

Photodegradation is initiated when internal or external light-absorbing groups (chromophore groups) of a polymer absorb photons from the UV radiation (wavelength ≤400 nm) of sunlight. This irreversible phenomenon may alter the chain length, mechanical properties, and appearance (color and surface finish) (Yousif & Haddad, 2013) of materials. In turn, the performance of the materials is compromised. The photodegradation of polymeric materials is governed by two influential steps (Rabek, 1995; Ranby, 1989):

Initiation: The production of primary radicals due to the absorption of photons by chromophore groups.

Propagation: The production of successive polymer radicals due to the attack of primary radicals on the polymer chains, followed by consequential crosslinking or chain scission.

These things considered, photodegradation of polymers is mainly governed by the presence of chromophore groups (Karimi et al., 2021). Chromophores can be both internal and external (catalyst, solvents, additives, in-chain or end-chain unsaturated double bonds, etc.). For example, the photodegradation of polyolefins is caused by the presence of external impurities (Rabek, 1995; Ranby, 1989), which might have been produced during polymerization and post-polymerization processing steps. Additionally, chromophores can be an integrated group into the polymer chains. For instance, photodegradation of poly(styrene) (PS) is mainly caused by the presence of UV-absorbing aromatic groups (Waldman & De Paoli, 2008). Traditionally, rigid filler (carbon black (Karimi et al., 2021)) or different chemicals (phenolic/nonphenolic UV absorbers (Karimi et al., 2021), hindered amines (Gijsman et al., 1993), and phenolic antioxidants) are used as photostabilizing additives to protect thermoplastics from photodegradation. However, some of these additives are associated with health concerns (Chaudhuri et al., 2017; Tipton & Lewis, 2008), toxicity (Alotaibi et al., 2015), and the migration of small molecules over time.

Concomitantly, graphene, a carbon-based material, is gaining attention as a prospective photostabilizer due to the presence of π bonds and two-dimensional (2D) geometry (Karimi et

al., 2023). The chemical structure enables graphene to absorb light in the UV region, through $\pi \rightarrow \pi^*$transitions (Dash et al., 2014; Johra et al., 2014), while the 2D structure allows it to act as a physical barrier to small molecules (Cui et al., 2016; Ferreira Junior et al., 2022; Yoo et al., 2014). Additionally, a recent study has confirmed that few-layer (6 to 10 layers) graphene (FLG) does not have the same adverse dermal, inhalation, and gene toxicity effects that are well-known for other nanocarbons (Moghimian & Nazarpour, 2020). Therefore, FLG is expected to be a safer option over some traditionally used photostabilizers. Consequently, different graphene derivatives (graphene, graphene oxide, and reduced graphene oxide) have been investigated to photostabilize several polymers (Goodwin et al., 2020; Hasani et al., 2018; Mistretta et al., 2019; Moon et al., 2011; Nuraje et al., 2013; Oliveira et al., 2019).

In the case of polymer blends, the photostability depends on the blend composition and chemical structure of individual phases, as well as the interaction between the respective blend components. Several studies on the photostability of blends have been summarized by Manita et al. (Mantia et al., 2017). Some results, as reported in the literature, are listed in Table 4.1, along with key findings of the present work.

Table 4.1 Photooxidation behavior of several polymer blends compared to that of their component polymers, cited in the literature

Polymer blend system	**Findings of the authors on photostability**	**Ref.**
Polycaprolactone (PCL)/Poly vinyl chloride(PVC)	A positive interaction effect of the components resulted in an increased photostability of the blend compared to that of the homopolymers.	(Christensen et al., 2008)
PP/high impact polystyrene (HIPS)	The blend was found to be more photostable than pure PP as a result of the opacity of the blend and the larger scattering effect by the phase interface.	(Fernandes et al., 2010)
Polystyrene (PS)/ poly(viny1 acetate) (PVAc)	An accelerated photodegradation tendency of the blend was reported. The degradation behavior	(Halina, 1995)

Polymer blend system	**Findings of the authors on photostability**	**Ref.**
	was found to be significantly influenced by the composition and morphology of the blend.	
Polyvinyl methyl ether (PVME)/PS	The photodegradation of the blend was deemed to be governed by the photooxidation trend of PVME.	(Mailhot et al., 2000)
PP/poly(butylene terephthalate) (PBT)	The photodegradation of the blend was considered to involve both photolytic degradation and photooxidation of PBT sequence.	(Rivaton et al., 1998)
Low-density polyethylene (LDPE)/cellulose	The blend was reported to be less photostable and more biodegradable than the pure components.	(Ołdak et al., 2005)
Liner low-density polyethylene (LLDPE)/plastic waste (46 wt.% LLDPE, 51 wt.% LDPE, 1 wt.% HDPE, and 2 wt.% PP)	The presence of plastic waste was found to affect the photostability of pure LLDPE.	(Al-Salem et al., 2016)
LLDPE/LDPE	The addition of carbonaceous fillers (carbon black, carbon nanotube and graphene) was found to improve the photostability of the blend composite.	(López-Martínez et al., 2022)
1) MPWS 2) prime PE/PP	The addition of commercial-grade few layer-graphene resulted in the retardation of photodegradation of the blend systems.	This work

A range of comprehensive studies on the photodegradation process of different polymer blends is available in the literature (Fang et al., 2013; Jubinville et al., 2020; Karaagac et al., 2021; Karimi et al., 2023; Kazemi et al., 2015; Najafi et al., 2006; Singh et al., 2023; Sultana et al., 2023) Photoprotection of polymer blends, however, has rarely been addressed. In particular, no study has been found to report the photostabilizing influence of commercial grade few layer-graphene in PE/PP blend systems. Therefore, this work aims to explore the photo-stabilizing potential of a commercial few-layer graphene to extend the lifetime of polyolefin blends, for both a mixed waste stream , as well as, a prime PE/PP control blend. It is worth mentioning that the used graphene is produced by an environment-friendly mechanochemical exfoliation process. The collaborating research group of this study has previously reported that the addition of such commercial-grade FLG can improve mechanical properties of a polyolefin waste stream (Khadri Diallo et al., 2022; Sultana et al., 2023). The potential of this FLG to enhance UV protection would eliminate or significantly reduce the use of traditional photo-stabilizers and also increase the lifetime of post-consumer waste recovered polymer, intending for outdoor application.

4.2 Results and Discussion

4.2.1 Morphology

Figure 4.1 shows the morphology of the waste polyolefin mixture and neat prime PE/PP – 60/40 blend. Here, the rough phase corresponds to PE phase and the smoother phase represents the PP phase of the blend, as indicated in the Figure 4.1. The morphology of control polyolefin blend mimics the microstructure of MPWS.

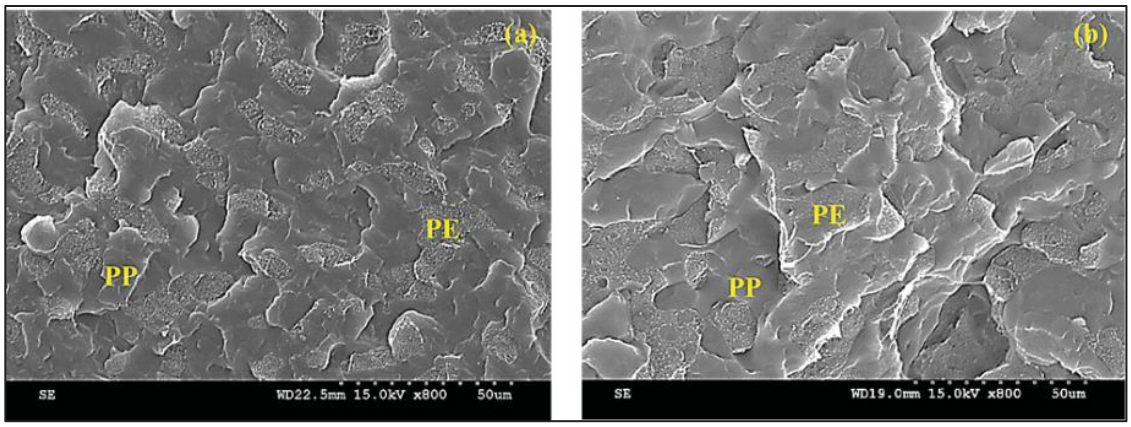

Figure 4.1 SEM image of (a) MPWS and (b) neat prime PE/PP – 60/40 blend

Figure 4.2 (a,b,c1,c2) illustrate the microstructure of the compression molded MPWS composite and prime PE/PP – 60/40 blend composite, containing 1 wt.% FLG. Figure 4.2 (a) shows that preferentially, FLG locates to PE phase which was also reported in our previous work (Sultana et al., 2023) for the composite containing 4 wt.% FLG. Similarly, Figure 4.2 (b), representing the composite where FLG was premixed with PE, shows that FLG is selectively localized in PE phase without any indication of FLG migration to PP phase. In contrast, Figure 4.2 (c1) and 4.2 (c2), representing the composite where FLG was premixed with PP, indicates that FLG is located in both PP phase and PE/PP interface. This localization of FLG in PE/PP interface is an indication of the preference of FLG towards PE over PP. A similar observation was reported in literature (Tu et al., 2017a).

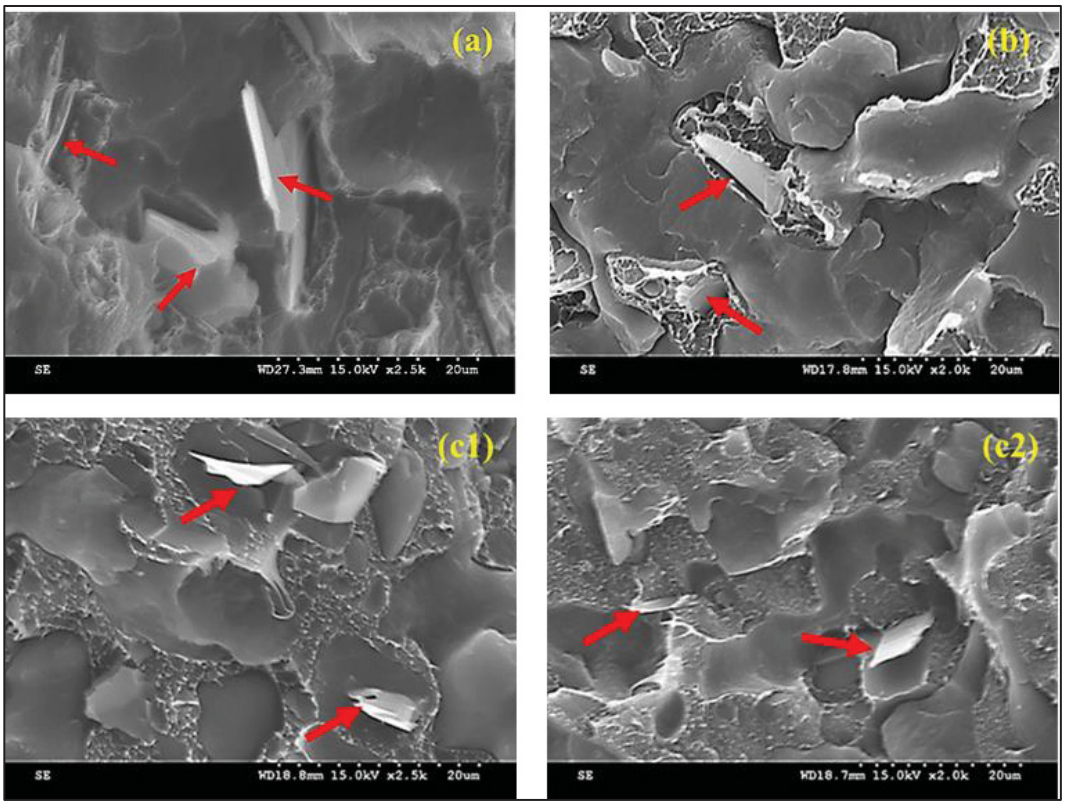

Figure 4.2 SEM images of 1 wt.%-FLG filled (a) MPWS composite, prime PE/PP blend composite; (b) FLG premixed with PE phase, (c1, c2) FLG premixed with PP phase and the localization of FLG has been marked by the red arrow to guide the readers' eyes

4.2.2 Dispersion of FLG

Figure 4.3 (a) and 4.3 (b) display the processed optical microscope images of thin film of MPWS and prime PE/PP composites, respectively, each containing 1 wt.% of FLG. Dark regions represent FLG particles and white background represents the polymeric phases of the composites. Additionally, Figure 4.3 (c) illustrates the frequency of FLG agglomerates as a function of agglomerate area in the composites to quantify the dispersion of FLG in MPWS and prime PE/PP blend. The grey bars represent the agglomerate size distribution in the prime blend composite, while the black bars represent the distribution in MPWS composite.

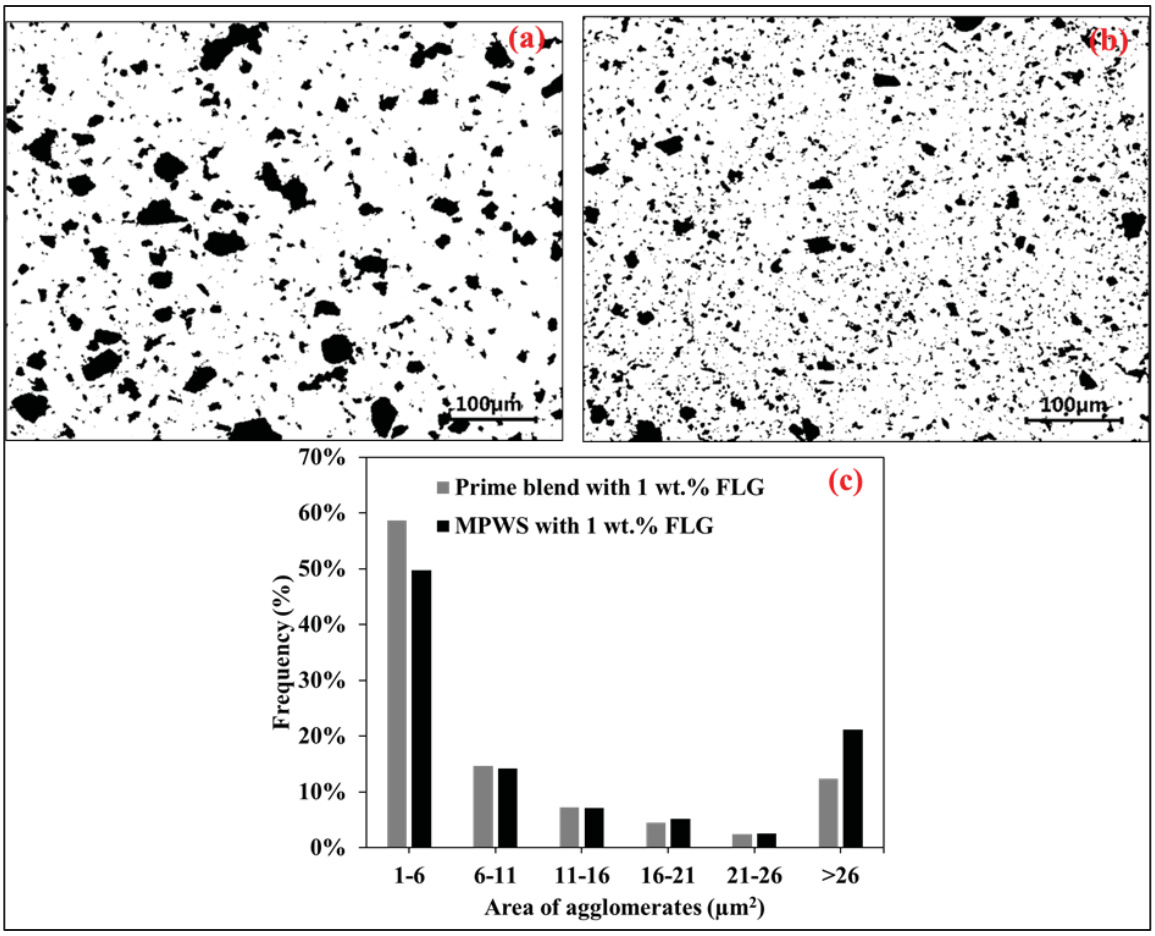

Figure 4.3 The representation of FLG dispersion in (a) MPWS and (b) prime polyolefin blend along with (c) the frequency of FLG agglomerates in 1 wt.% FLG-filled MPWS and prime PE/PP blend as a function of FLG agglomerate area

Remarkably larger agglomerates can be seen in Figure 4.3(a), indicating poor dispersion of FLG in MPWS composite. Conversely, the prime PE/PP composite exhibits better dispersion with smaller FLG agglomerates. This difference in dispersion of FLG could be attributed to dissimilar rheological property of the polymer content of the composites. Notable differences can be observed at the two extremes of the X-axis, representing the size ranges of the agglomerates. It is observed that prime blend composite possesses higher percentage (~ 60%) of smaller FLG agglomerates than that (~ 50%) of MPWS composite or vice versa. Despite following similar processing condition, different FLG dispersion is observed in two different matrices. To investigate the root cause, the MFI value of MPWS and prime PE/PP blend was

measured. The MFI of MPWS and prime blend was found to be 12±2 g/10 min and 3±0.5 g/10 min, respectively. Hence, prime PE/PP blend of this work is much more viscous than MPWS. During melt mixing, higher viscosity driven shear stress would have facilitated better dispersion of FLG in viscous prime PE/PP blend than in comparatively less viscous MPWS of this work. It is worth mentioning that better dispersion in more viscous matrices was also observed by other authors (Kasaliwal et al., 2011).

4.2.3 Effect of Adding FLG on UV-Exposed Composites

4.2.3.1 Chemical Analysis

In Figure 4.4, calculated carbonyl index of prime PE/PP blend and MPWS have been plotted along with error bars (standard deviation for the replicas of each sample) as a function of exposure time. The carbonyl index (CI) was calculated by analyzing the FTIR absorption spectra of the respective polyolefin blend. It can be noticed that carbonyl index of MPWS is significantly higher (almost 2 times) than that of prime blend, both before exposure and after 4 weeks of exposure. This observation suggests that MPWS is more susceptible to photo degradation compared to the prime blend. In other words, polyolefin waste may require more additive to prevent photo degradation. However, up to first two weeks, the growth of carbonyl formation in MPWS is lower than that of neat prime blend. This could be attributed to the photo protection effect of the black pigment, already present in the as received MPWS. Nevertheless, the protection effect of black pigment in MPWS is inadequate and ineffective for long-term, as evidenced by almost two times higher CI of MPWS than that of neat prime blend, exposed to UV radiation for 4 weeks.

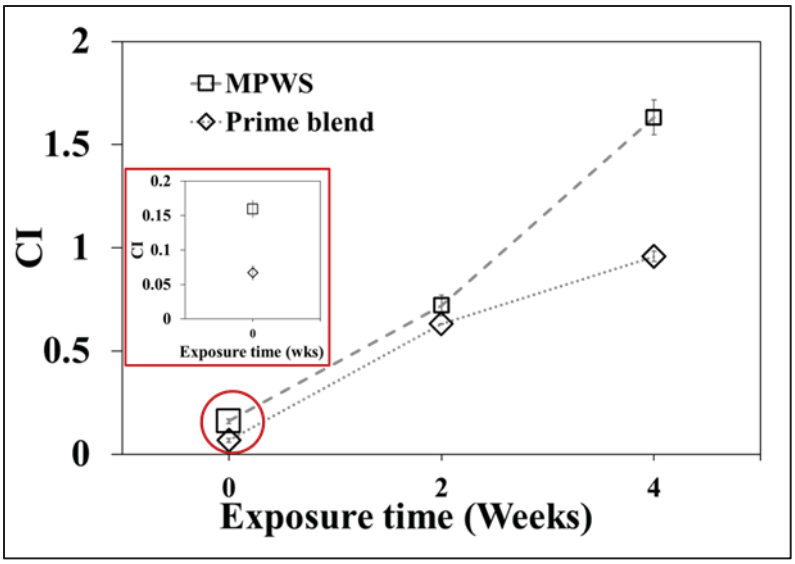

Figure 4.4 CI of prime polyolefin blend and MPWS as function of exposure time. Dotted lines are used to guide reader's eyes

Figure 4.5 (a) and 4.5 (b) represent the CI of FLG-filled MPWS and prime polyolefin composites as a function of UV exposure time. It can be seen that carbonyl formation rate in unfilled polyolefin blend (both waste and control) is much higher than FLG filled composites. In case of MPWS composites, containing higher concentration of FLG (> 1 wt.%), CI starts to increase only after 2 weeks of exposure. A higher value of CI is observed after 4 weeks of exposure in the MPWS composites, irrespective of the concentration of FLG. Interestingly, a decelerated growth of CI in MPWS composites is observed with higher concentration of FLG. In contrast, based on CI value, carbonyl formation is not evident in FLG-filled prime blend composite over the entire UV exposure period. This holds true for both 0.5 and 1 wt.% FLG dosage in the control blend. Eventual retardation and termination of carbonyl formation in UV-exposed MPWS and prime polyolefin blend composites, respectively, indicate the photo stabilizing potential of FLG. Moreover, this finding also suggests that the addition and mixing of a small amount of FLG in polyolefins prior to real-life applications, would extend the lifespan of the commodities, made of polyolefins. It is worth mentioning that in an earlier publication by the co-authors (Karimi et al., 2023), an Electron Paramagnetic Resonance (EPR) analysis was conducted to investigate the performance of FLG as a photo-stabilizer. The study

reported that FLG effectively attenuates the characteristic EPR signal intensity, indicating both UV absorption/reflection and the scavenging of free radicals by FLG.

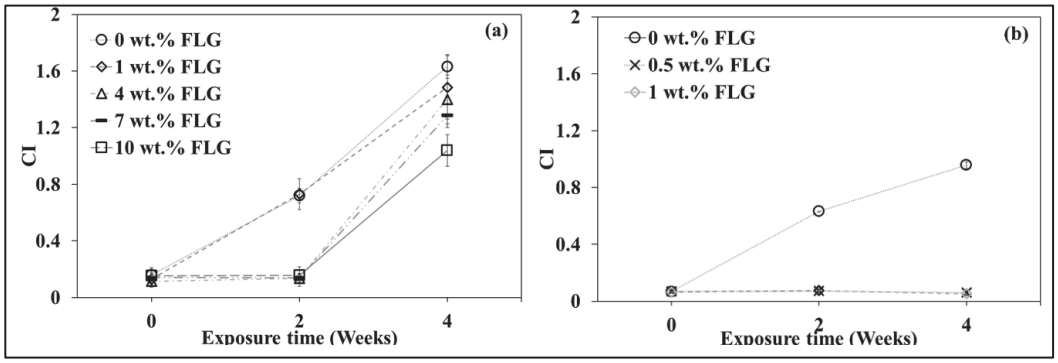

Figure 4.5 CI of (a) MPWS/FLG and (b) FLG-filled prime polyolefin composite as function of UV exposure time. Dotted lines are used to guide reader's eyes

4.2.3.2 Surface Appearance

Figure 4.6 (a) and 4.6 (b) show the surface finish of unfilled MPWS and 1 wt.% FLG-filled MPWS composite, after 4 weeks of exposure to UV radiation. In addition, Figure 4.6 (c) and 4.6 (d) showcase the surface finish of both the neat PE/PP blend and the PE/PP blend composites with 0.5 wt.% FLG, after a 4 weeks exposure to UV light. As a result of photodegradation, numerous longitudinal and transverse cracks appeared on the surface of neat MPWS sample. Although several cracks are observed after UV exposure on the MPWS/FLG composite with 1 wt.% FLG, the quantity is considerably reduced when compared to that of unfilled-MPWS. Similar to the case of MPWS, many longitudinal and transverse cracks are evident on the unfilled and UV exposed prime PE/PP blend surface. However, in contrast to the FLG-filled MPWS composite, there are no visible cracks on the surface of FLG-filled prime PE/PP blend composite. These observations suggest that even a FLG concentration as low as 0.5 wt.% is adequate to provide satisfactory UV protection to prime PE/PP, although not to mixed polyolefin waste-based compounds. The likely reasons for this are discussed in the subsequent section of this work.

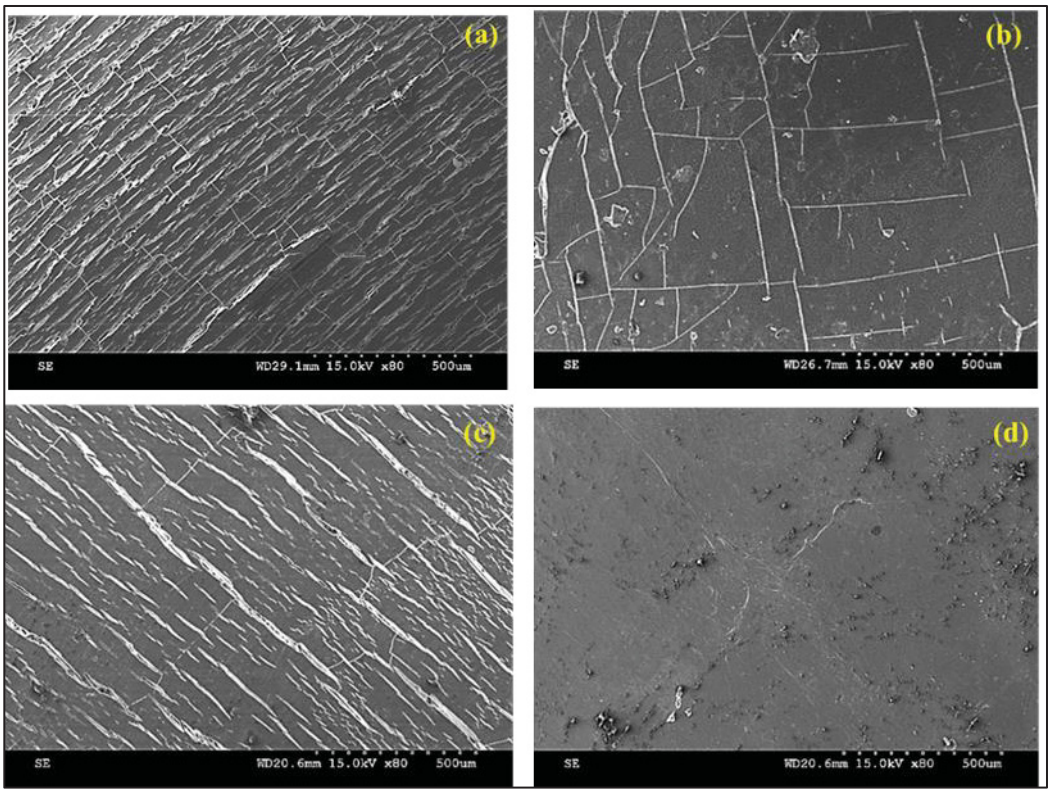

Figure 4.6 SEM images of the surfaces of (a) MPWS without FLG, (b) MPWS with 1 wt.% FLG, (c) Prime blend without FLG, and (d) Prime blend with 1 wt.% FLG; after 4 weeks of UV exposure

To have an overview of crack formation, the crack density on the surface of UV-exposed samples has been calculated. Figure 4.7 shows crack density of FLG-filled MPWS and prime blend composites, after 4 weeks of UV exposure, as a function of FLG concentration. Photodegradation driven crack density on the surface of UV-exposed MPWS compounds decreases as the concentration of FLG is increased in the composite. A concentration of FLG > 4 wt.% can effectively prevent crack formation (SEM images of the corresponding samples, Figure A-III-1(a,b), are provided in the supplementary information section). On the other hand, 1wt.% FLG is observed sufficient to prevent crack formation on the composite surface during UV exposure. These observations indicate that the presence of FLG slows down the UV degradation of polyolefin blend.

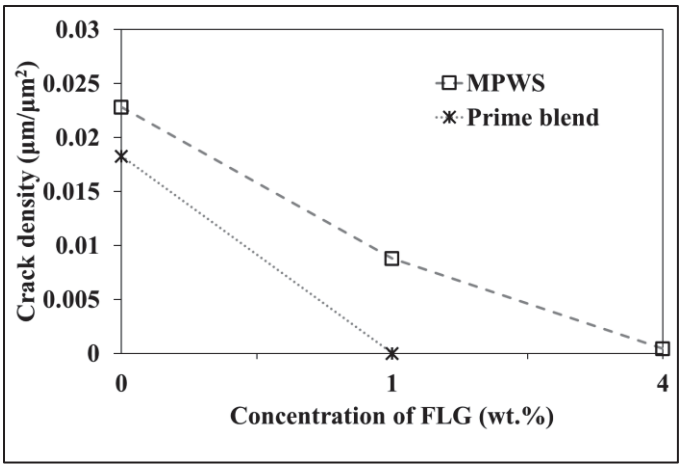

Figure 4.7 Crack density of MPWS/FLG composites, after 4 weeks of UV exposure, as a function of concentration of FLG

4.2.3.3 Mechanical Properties

Figure 4.8 (a) and 4.8 (b) present the elongation at break and the impact strength of FLG-filled MPWS composites, respectively, plotted along primary Y-axis as a function of the concentration of FLG. The retention of the respective properties after 4 weeks of UV exposure are plotted along the secondary Y-axis. Worth mentioning, the error bars (indicating standard deviation) for the ductility of unprocessed and unfilled MPWS are considerably wider as compared to the performance of any of the other composites depicted in the Figure 4.8 (a). Experimental results suggest that the mixed polyolefin waste stream possesses a higher polydispersity or inhomogeneity. Conversely, the error bars associated with the ductility of the FLG-filled composites exhibit relatively smaller variations. This can be ascribed to the homogenizing influence of FLG, a phenomenon previously noted by the coauthors in a blend of recycled and prime PE in a prior study [42]. In addition, Figures 4.8 (c) and 4.8 (d) represent the retention of elongation at break and impact strength, respectively, of prime PE/PP blend composites after 4 weeks of UV exposure as a function of the concentration of FLG. In these figures, the unfilled bars correspond to the performance of neat (unfilled) blend, black bars represent the composites where FLG was premixed with PE and grey bars stand for the samples where FLG was premixed with PP.

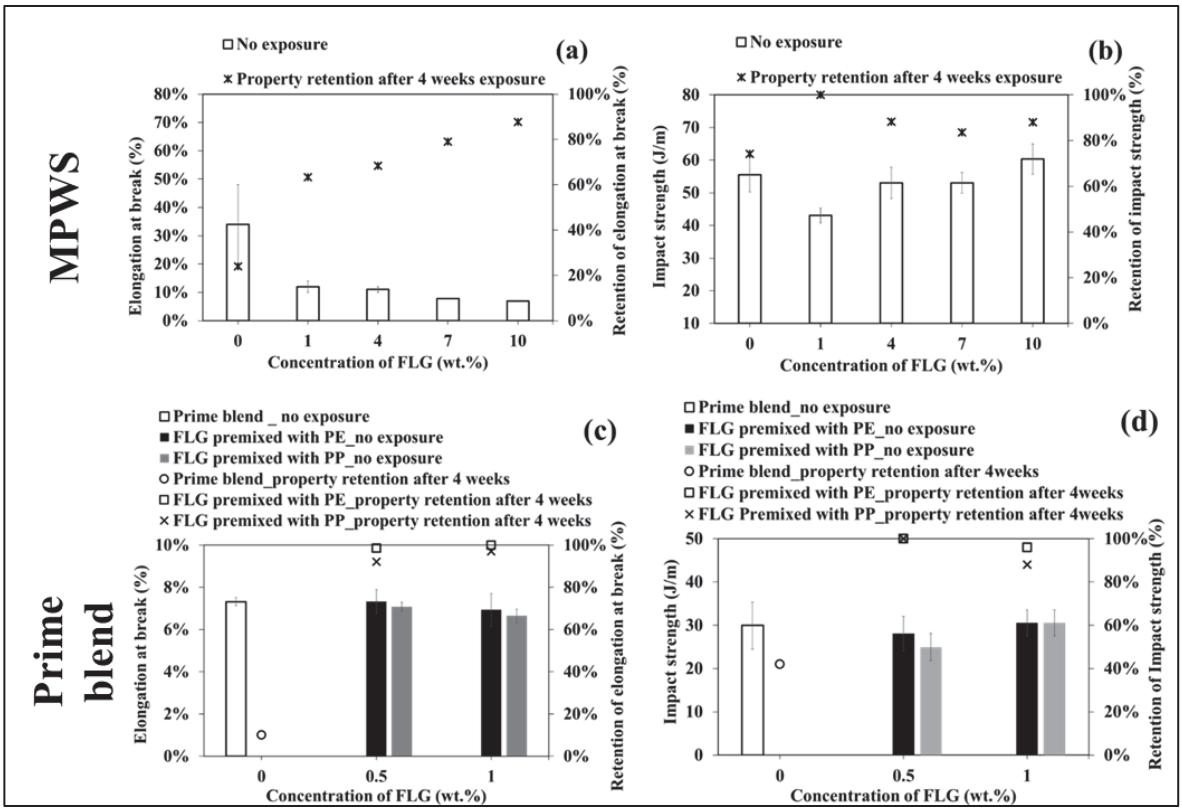

Figure 4.8 (a) Elongation at break along with retention of elongation at break (after UV exposure) and (b) impact strength along with retention of impact strength (after UV exposure) of MPWS/FLG composites as a function of FLG concentration; (c) elongation at break along with retention of elongation at break (after UV exposure) and (d) impact strength along with retention of impact strength (after UV exposure) of prime PE/PP blend composites as a function of FLG concentration, present in the composites

As noticed in Figure 4.8 (a), the presence of FLG resulted in a reduction in the ductility of the MPWS composites compared to that of neat MPWS as reported previously (Sultana et al., 2023). Notably, a 65 % reduction of ductility is observed with the addition of 1 wt.% FLG. Further addition of 4, 7 and 10 wt.% FLG resulted in 68%, 77% and 80% reduction of original ductility, respectively. This reduction in ductility of polymer blend composite is attributed to the compromised mobility of polymer chains, due to the presence of rigid fillers. Similar observation was reported earlier by other authors (Abbasi et al., 2019; Haghnegahdar et al., 2017; Parameswaranpillai et al., 2015). In contrast, an increment in the ductility of rigid filler-filled polymer blend composite, facilitated by the positive effect of good dispersion of filler and a strong matrix/filler interaction was also reported in literature (Bijarimi et al., 2019; Pour

et al., 2016). After 4 weeks of UV exposure, around 20% of the original ductility is preserved in neat MPWS. Contrary to neat MPWS, around 60% of the original ductility is preserved in MPWS composites containing 1 and 4 wt.% FLG. Remarkably, an even higher (∼ 90%) ductility retention is observed in MPWS composites, containing 10 wt.% FLG. This finding suggests that the presence of FLG slows down the photodegradation of mixed polyolefin waste stream. Similar photostabilization effect of this commercially available FLG has also been reported in high density polyethylene by the co-authors of this work (Karimi et al., 2023). In line with the observation from Figure 4.8 (a), it is evident in Figure 4.8 (b) that the impact strength retention of UV-exposed MPWS is significantly lower as compared to that of FLG-filled MPWS composites. Conversely, the tensile modulus and tensile strength retention for each of the exposed samples are well above 90% (see Figure A-III-2(a, b) in the Annex III), indicating that these properties of the polymeric materials have been less sensitive to UV exposure, at least for the irradiation duration, adopted in this study. Similar observation was reported by other authors in unfilled-polyolefin blends (Al-Salem et al., 2016). Polymers undergo simultaneous chain scission and crosslinking during photo degradation (Hocker et al., 2018; Karimi et al., 2023). Chain scission (negative effect) and crosslinking (positive effect) have two opposing effects on both strength and stiffness of polymeric material. Therefore, changes in tensile strength and modulus are not clearly evident in the initial stage of UV exposure. However, after a certain period of irradiation, the negative effect of chain scission on tensile strength and modulus becomes predominant, resulting in reduction of the respective properties.

Similar to aforementioned observations, Figure 4.8 (c) and 4.8 (d) show that the property retention of neat-prime PE/PP after 4 weeks of UV exposure is much less than those of FLG-filled prime PE/PP blend composites. Besides, a higher property retention is noted in FLG-filled prime blend composites after UV exposure, irrespective of the FLG mixing strategy. As opposing to the case of MPWS/FLG composites, a higher percentage of ductility and impact toughness is preserved in UV exposed prime PE/PP composite at a very low concentration of FLG (0.5 or 1 wt.%). This can be explained by the poor dispersion of FLG in MPWS as compared to that of prime polyolefin blend, as presented in Figure 4.3 (a,b,c). The associated

findings reinforce the notion that the same FLG concentration has a more pronounced influence on the prime polyolefin blend as compared to MPWS. Moreover, the presence of higher carbonyl content in the MPWS (being a mix of recycled polymers), than in the prime blend (shown in Figure 4.4) indicates that a higher dosage of FLG would be required to slow down the photodegradation process of pre-degraded polyolefin waste like the MPWS used in this work.

4.2.4 Discussions

The results show that the addition of FLG is an efficient strategy to slow down the photo-degradation processes in polyolefin blends, both recovered post-consumer waste mixtures and prime polyolefin blends. Photodegradation of the samples has been investigated in terms of the carbonyl concentration increase, crack density and mechanical property retention of the compounds after 4 weeks of UV exposure. Table 4.3 highlights the photoprotection effect of FLG in a waste and prime polyolefin mixture.

Table 4.2 Change in carbonyl index (CI), crack density and retention of ductility after 4 weeks of UV exposure in MPWS and prime blend composites as a function of concentration of FLG

Parameters	**MPWS**					**Prime blend (FLG premixed with PE)**		
Concentration of FLG (wt.%)	0	1	4	7	10	0	0.5	1
Change in CI (%)	1069	964	903	821	645	1325	No significant change	
Crack density (μm/μm^2)	0.0228	0.0088	0.0004	No visible cracks but surface delamination		0.0182		
Retention of ductility (%)	20	60	70	80	90	10		

Based on the information presented in Table 4.3, the efficiency of FLG as a photostabilizer is more evident in prime polyolefin blend than in mixed plastic waste. The findings of Figure 4.3 (c) help to explain this observation. The plot outlines that FLG was poorly dispersed in MPWS compared to prime PE/PP blend composites, prepared under the same processing conditions. It has been reported in literature (Karimi et al., 2023) that FLG mostly slows down the photo-degradation of polymer material via UV absorption/reflection and free radical scavenging. Moreover, FLG also acts as a physical barrier to oxygen which limits the oxygen penetration through the polymer which also minimize photo-oxidative degradation of respective plastic material. Therefore, poor dispersion of FLG in polymeric material leads to less efficient utilization of FLG.

Besides, polyolefins are ideally expected to be resistant to photodegradation as they do not have any unsaturated chromophores or carbon bonds in their backbone. However, external impurities or structural defects can initiate the photodegradation process, resulting in chain scission and eventual formation and accumulation of carbonyl groups. These initial unsaturated double bonds of carbonyl groups turn polyolefins to be more susceptible to photodegradation. Therefore, comparatively less photoprotection attained in FLG filled waste polyolefins than that of controlled composites could be attributed to the inherent uncertainties associated to plastic waste such as the presence of impurities, presence of pre-degraded polymer chains and, polydispersity. Larger standard deviations of ductility and comparatively higher carbonyl index of waste polyolefin mixture (compared to prime polyolefin blend of this work) present experimental evidence that support the fact that more inhomogeneity and predegraded plastic are present in MPWS. Hence, the combination of comparatively poor dispersion of FLG with the presence of impurities and predegraded elements in MPWS makes this mixture more susceptible to photodegradation, requiring more dosage of FLG to attain a satisfactory level of photoprotection.

In this context, it is noteworthy to highlight the findings of Figure 4.5(b). The plot indicates no carbonyl growth in UV-exposed primary polyolefin composites after a 4-week UV exposure period. In other words, the photodegradation of prime polyolefin was significantly decelerated

due to the presence of FLG. This insight implies the recommendation of adding FLG into polyolefins as a pretreatment step. It is expected that post-consumer polyolefin waste generated from FLG-filled polyolefin will experience reduced photodegradation, resulting in both extended lifespan and requiring a smaller quantity of FLG for the photo protection of the subsequent MPWS for reuses.

Concurrently, this study has investigated the impact of selectively localized FLG in different phases of the blend on the retardation of photodegradation. By employing a premixing approach, FLG was predominantly located within either PP or PE phase of the prime polyolefin blend. The results indicate that the efficiency of FLG as a photostabilizer remains unaffected by its preference within a specific phase. This could be attributed to the inherent qualities of FLG as a photostabilizer, which are not significantly influenced by or contingent upon its selective localization in the blend. It is worth noting that this finding underscores the application of FLG as a suitable photostabilizing additive for mixed polyolefin waste streams, especially in scenarios where achieving predominant selective localization of unfunctionalized FLG is unattainable.

4.3 Materials and Methods

4.3.1 Materials

FLG powder (GrapheneBlack 3X) from NanoXplore Inc., Montreal, Canada, was used in this work. This grade of FLG typically consists of 6 to 10 atomic layers. The primary particles exhibit a lateral size ranging from 1 to 2 μm. These primary particles in dry powder state, form loose clusters also known as secondary particles. The average lateral size of these secondary particles is approximately 30 μm.

For this study, a mixed polyolefin waste mixture was obtained from a local recycler in Quebec. The information provided by the supplier indicates that the mixture comprises polyethylene (PE) along with approximately 30 to 40 wt.% polypropylene (PP) and ≤5 wt.% contamination

(such as dye, ink, or pigment). Differential scanning calorimetry (DSC) analysis were used to assess that the composition of the mixture (PE/PP-60/40), as reported in our previous work (Sultana et al., 2023).

A prime PE/PP - 60/40 blend was prepared, replicating the morphology of MPWS blends. To maintain controlled and simplified conditions, the prime blend was investigated both without FLG and with FLG, excluding other impurities or uncertainties likely associated with MPWS. Table 4.2 outlines the identification and MFI of the polymers, used in this work:

Table 4.3 Identification and MFI of the polymers used in this work

Polymer	**Commercial Name**	**MFI (g/10 min)**
MPWS	N/A	≥ 4 (230 °C, 2.16 kg)
PE	Formolene HB5502B	0.35 (190 °C/2.16 kg)
PP	Polypropylene 3720 WZ	20 (230 °C, 2.16 kg)

4.3.2 Methods

In this study, master batch (MB) pellets composed of FLG and polymers (PE, PP, or MPWS) were utilized to prepare the composites.

In case of MPWS/FLG composites, the MPWS/FLG MB was further diluted with MPWS to prepare composites with 1, 4, 7 and, 10 wt.%. of FLG, respectively.

In addition, FLG-filled prime PE/PP blend composites were prepared through a two-step process. In the initial step, PE/FLG or PP/FLG MB was diluted with PE or PP, respectively, which can be referred as a premixing step. In the subsequent step, these pre-mixed composites were melt-blended with the other corresponding polymer of the PE/PP blend. Prime PE/PP blend composites containing 0.5 and 1 wt.% FLG were also prepared in this work, via FLG pre-mixing with PE or PP. All the samples were processed in a HAAKE twin-screw extruder,

(Rheomex OS PTW16/40, manufactured by Thermo Fisher Scientific, Germany) at 150 rpm, and 200 °C in all zones.

Extruded pellets were injection molded to prepare specimens for tensile and impact property analysis. Injection molding was done by using the Arburg Allrounder 221K-350-100 Injection molding machine (manufactured by Arburg GmbH + Co KG, Germany).

4.3.3 Photodegradation Process

The injected specimens were subjected to an accelerated weathering condition by using a QUV chamber, equipped with UVA-340 type lamps. According to the guidelines of cycle A outlined in ASTM G154 (ASTM International, 2023), the samples were exposed to an irradiation of 0.89 W/m^2 at 60°C for 8 hours, followed by 4 hours of water condensation at 50°C. The specimens were taken out of the QUV chamber after exposure durations of 2 weeks (336 hours) and 4 weeks (672 hours).

4.3.4 Characterizations

Scanning Electron Microscope (SEM) images of the UV exposed surfaces of the samples were obtained using a Hitachi SEM S3600-N (Model: MEB-3600-N, manufactured by Hitachi Science Systems, Ltd., Japan). Before imaging, the surface of the compounds was coated with a thin layer of gold using a Gold Sputter Coater (Model: K550X, manufactured by Quorum Technologies Ltd, East Sussex, UK). This gold coating enhances the conductivity of the samples and provides better imaging results in the SEM. To investigate the microstructure, the compression molded samples were cryo-fractured, prior to gold coating.

The optical microscope images of compression molded thin films of 1 wt.% FLG filled MPWS and prime PE/PP blend composites were observed by using an optical microscope (Model: Olympus BX51, manufactured by Olympus Corporation, Tokyo, Japan) in transmission mode. A minimum of 10 images were taken from different areas of the films. Subsequently, ImageJ

software (version number: 1.52a) was utilized to evaluate the FLG dispersion within the various matrices. Before the quantitative assessment of filler dispersion, image preprocessing steps involving noise reduction and removal of the polymeric matrix background were executed by using the imageJ software. Moreover, length of the surface crack of UV exposed samples were determined by using imageJ software to determine crack density by following Equation 4.1:

$$\text{Crack density } = \frac{\sum Crack\ length\ \ (\mu m)}{Area\ under\ consideration\ (\mu m^2)} \tag{4.1}$$

Melt flow index (MFI) of mixed polyolefin waste and prime polyolefin blend was investigated by using an MFI tester (manufactured by International Equipments, Mumbai, India). ASTM D1238 (ASTM International, 2010) was followed to measure MFI.

ATR-FTIR spectra of thin films of neat and FLG-filled composites were captured by using a FTIR spectrometer (manufactured by PerkinElmer, Llantrisant, UK) Spectrum two™, equipped with a diamond crystal. A number of 10 scans were acquired with a resolution of 4 cm^{-1} within the wave numbers range of 400–4000 cm^{-1}. These spectra were used to assess the carbonyl index (CI) of each of the samples by using the following Equation 4.2:

$$\text{CI} = \frac{A_{C=O}}{A_{CH_2}} \tag{4.2}$$

Here, $A_{C=O}$ is the peak area within 1680–1800 cm^{-1} wave number range and A_{CH_2} is the peak areas within 680–760 cm^{-1} wave number range, representing C=O and CH_2 functional groups, respectively. The assessment of CI is interesting because it is an indicator of the degradation of polymer during its lifespan. At least three spectra from different parts of each sample were considered to calculate and report the average CI values with standard deviation as error bars. The tensile properties of the samples were investigated using an MTS Alliance RF/200 tensile test apparatus (manufactured by MTS Systems Corporation, USA), following the guidelines

outlined in the ASTM D638(ASTM D638, Standard Test Method for Tensile Properties of Plastics, 2015). The tests were conducted at room temperature with a 10 kN load, and a crosshead speed of 50 mm/min. The key parameters analyzed include tensile strength, tensile modulus, and elongation at break.

The notched impact strength of the samples was determined using an impact strength tester device (manufactured by International Equipments, India). The measurement was carried out in accordance with the ASTM D256 (ASTM D256, Standard Test Methods for Determining the Izod Pendulum Impact Resistance of Plastics, 2023). To create notches in the samples, a motorized notch cutter (manufactured by International Equipments, India) was utilized. For each composite, at least five specimens were tested to investigate tensile and impact properties. In the subsequent sections of this report, we have graphically depicted the property (elongation at break, impact strength, tensile strength, and modulus) retention (%) of the composites after UV exposure as a function of FLG concentration within the composite. The graphical representation of property retention (%) has been adopted to portray the precise influence of adding FLG on the retardation of photodegradation of polyolefin blend. Property retention (%) has been calculated according to the following Equation 4.3:

$$\text{Property retention (\%)} = \frac{\text{Property after UV}}{\text{Property before UV}} \text{ x } 100\% \tag{4.3}$$

4.4 Conclusions

This work presents that FLG can successfully slow down the photodegradation processes in polyolefin blends. This observation is valid for both a plastic waste recovered polyolefin blend and a control prime polyolefin blend, ensuring longer lifespan of polyolefin blends used for outdoor applications. The main findings of this work can be concluded with the following points:

- The addition of FLG can effectively slow down the photodegradation of polyolefin blends.

- Although FLG exhibits a thermodynamic preference for PE over PP, the photostabilization of PE/PP blend is not significantly affected by the selective distribution of FLG in either phase.
- A mere 0.5 wt.% or 1 wt.% of FLG is found sufficient to ensure the photostability of a prime PE/PP blend.
- To ensure better photoprotection in recycled polymer blends, a higher concentration of FLG is required, attributed partly to the predegraded condition of MPWS
- Furthermore, pretreatment of prime polyolefins with FLG could be a recommended step, which in turn, would extend the lifespan and generate a less degraded MPWS for potential reuse.

This work underscores the potential to extend the lifespan of polyolefins, thereby decreasing the generation of plastic waste, through the addition of commercially available and low-cost FLG, produced in compliance with Canadian environmental regulations. By extending the use of plastic products, their entry into waste streams is delayed. Moreover, extending the lifespan of products is anticipated to decrease the demand for new ones. Thus, this study presents a promising method to elevate the value of MPWS, intrinsically with minimum worth, and which would otherwise be relegated to landfill disposal.

Supplementary Materials

The following supporting information can be found at Annex III: Figure A-III-1 SEM images of the surfaces of MPWS blend compounds with (a) 7 wt.% FLG and, (b) 10 wt.% of FLG; after 4 weeks of UV exposure; Figure A-III-2: (a) tensile strength and retention of tensile strength, and (b) tensile modulus and retention of tensile modulus of UV-exposed MPWS/FLG composites as a function of FLG concentration, present in the composites.

Funding

This research was funded by NanoXplore Inc.; Natural Sciences and Engineering Research Council (grant number CRDPJ 538482—18); PRIMA Quebec (grant number R18-46-001); Fonds de Recherche du Québec-Nature et Technologies (grant number 318813) and Quebec

Circular Economy Research Network . The APC was funded by discounts from Editorial Office, MDPI and IOAP of Ecole de Technologie Superieure (ETS) Montréal.

CONCLUSION

This section outlines the primary findings based on the objectives of the study. These findings are presented in the order they appear in the thesis. Subsequently, a general conclusion of this thesis work is provided at the end of this section.

Objective 1 : To examine the impact of a commercial FLG on the properties of prime polyolefin blends

The initial phase of this doctoral research involved the investigation of the influence of addition of few-layer graphene (FLG) on the properties of pristine polyolefin blends, polyethylene (PE)/ polypropylene (PP) – 20/80, 60/40 and 80/20, respectively. This purpose of this part was to understand, how the addition of FLG affect the morphology, electrical conductivity, mechanical strength, and UV resistance of control polyolefin blend systems. According to this objective, PE/ PP/ FLG blend composites were prepared. The composites were processed through a two-step process. In the first step, FLG (1 to 5 wt.%) was melt-blended with either the PE or PP phase. In the second step, this premixed material was melt-blended with the other phase of the blend. The key findings are outlined below:

- An electrically conductive, mechanically strong and more UV resistant polyolefin composite could be designed by incorporation of a commercially available FLG into polyolefins.
- Only 4 wt.% and 5 wt.% of FLG were sufficient to induce an electrical conductivity of the order of 10^{-5} S/cm (electrically dissipative) in PE/PP – 60/40 and PE/PP – 20/80, respectively.
- The FLG network in the electrically conductive composite was observed to maintain a stable electrical conductivity, even after shear-induced deformation.
- An enhanced resistance against photodegradation was attained in the polyolefin composites by incorporating FLG.

- A notably stronger UV-stabilizing effect of FLG was observed in polyethylene-rich polyolefin blends than in polypropylene-rich blends.

Objective 2 : To determine the influence of FLG on the properties of MPWS

The second phase of this work involved studying the influence of FLG on the processability and mechanical properties of mixed polyolefin waste stream (MPWS). For this investigation, three different types of compounds: (1) MPWS/FLG (2) MPWS/prime polymer (PE, PP or PP copolymer); and (3) MPWS/prime polymer/FLG, were melt-extruded. The processability of the compounds was investigated by measuring the torque during melt extrusion, the melt flow index (MFI), and viscosity of the compounds. The major findings are outlined below:

- The addition of FLG could effectively reinforce the MPWS composites as compared to the original material.
- The addition of 4 wt.% FLG in combination with prime PP significantly strengthened MPWS, by increasing its tensile strength by 9%, tensile modulus by 37%, flexural strength by 23%, and flexural modulus by 34%.
- An increase in the impact strength of MPWS/FLG composite, with a higher loading (10 wt.%) of FLG was observed. This is an unusual feature of a rigid filler in an immiscible polymer blend composite. This observation attributes to the dominant resistance effect of FLG particles against impact crack propagation.
- The inclusion of FLG had minimal to no impact on the processability of MPWS, emerged due to the lubricating effect of FLG agglomerates.

Objective 3 : To assess the photostabilizing effectiveness of FLG in both MPWS and prime PE/PP blends

The third phase of this work investigated the photo stabilizing role of FLG in polyolefins; a waste-recovered polyolefin mixture and a control polyolefin blend. The control polyolefin blend was compounded, replicating the PE/PP composition and phase morphology of MPWS. The photo stabilizing role of FLG was assessed by analyzing carbonyl content increase, surface appearance, and the retention of mechanical properties of UV-exposed and FLG-filled polyolefin composite.

- The addition of FLG effectively improved the resistance of polyolefin blends against photodegradation.
- The selective distribution of FLG was not identified as a critical factor in enhancing the UV resistance of FLG-filled polyolefin composite.
- A minimal concentration of 0.5 wt.% of FLG was adequate to ensure the improved photoresistance of a prime PE/PP blend.
- Achieving enhanced photoprotection in recycled polymer blends required a higher concentration of FLG, partly due to the predegraded condition of MPWS.
- Additionally, pretreating prime polyolefins with FLG would be a recommended step to extend their lifespan and produce less degraded MPWS for potential reuse.

General conclusion

In this study, we explored the mechanical upcycling of MPWS through the addition of commercially available FLG. MPWS was chosen due to its significant presence in plastic waste streams and its easy separation by using a simple water-based float-sink process. FLG was selected as it serves as an excellent reinforcing carbonaceous additive. Furthermore, the FLG used in this study was produced through a mechanochemical exfoliation process, adhering to Canadian environmental regulations.

Our investigation highlights that incorporating FLG is a promising approach to reinforce and enhance the photo-resistance of polyolefins, recovered from waste. Upcycling MPWS in this manner opens avenues for their diverse applications, thereby reducing the burden of plastic waste in landfills and lessening the demand for new polymers. Consequently, our study presents a promising and economically viable method for upcycling MPWS.

RECOMMENDATIONS

While this study has provided valuable insights into the valorization of waste-recovered polyolefin mixture by addition of FLG, it is important to acknowledge its limitations and consider avenues for further exploration. Considering the findings presented in this thesis, following points are recommended for future investigations:

- To explore copolymer/FLG composites as a medium to capture FLG at the PE/PP interface of the blend. This approach can be adopted in order to compatibilize as well as reinforce PE/PP blend. EPDM or PP copolymer may be chosen as the copolymer for this study.
- To investigate the influence of shear-induced deformation on the electrical conductivity of composites with lower FLG loading. This step would be interesting to investigate if deformation-driven filler movement, from one phase to a thermodynamically favorable phase, facilitates the formation of a conductive network.
- To study the reasons behind the lower electrical conductivity observed in PE/FLG composites compared to PP/FLG composites, despite equal FLG loading. This may involve examining factors such as poor FLG dispersion in PE, the ease of surface coverage of FLG by PE polymer chains, or the barrier effect of PE crystals between neighboring FLG in the composite.
- To investigate the electromagnetic interference (EMI) shielding effectiveness and thermal conductivity of FLG-filled and electrically conductive immiscible polyolefin composites can be another important research direction.
- To design and artificially age a simulated neat and FLG-filled polyolefin waste to assess the influence of FLG on preventing UV degradation and other degradation processes in different segments of artificial aging. This type of analysis can provide deeper understandings of the potential of FLG as a UV stabilizer.
- To study, if any potential synergistic effects of FLG/carbon black or FLG/CNT combinations can be gained towards strengthening and stabilizing polyolefin mixtures against UV degradation.

- To identify the methods to achieve improved dispersion of FLG in mixed plastic waste, as employed in this work, and studying the influence of better FLG dispersion on UV resistance compared to poor dispersion would be a promising avenue for future research.

Perspective

Table 0.1 shows the density of FLG, HDPE, PP, and FLG-filled composites, calculated based on the mixing rule and by using the densities of the components. The green color highlights FLG-filled composites that remain lighter than water (density < 1 g/cm³), even after incorporating FLG. These composites can be separated in a water-based float-sink tank for further recovery.

Table 0.1 The density of FLG, PE, PP and FLG-filled composites (calculated based on the components' density)

Blend components	**HDPE (gm/cm^3)**	**PP (gm/cm^3)**	**FLG (gm/cm^3)**
	0.955	0.905	2.267
	Density of FLG-filled composites (gm/cm^3)		
FLG concntration (%)	**PE/FLG**	**PP/FLG**	**MPWS/FLG**
1	0.968	0.919	0.948
2	0.981	0.932	0.962
3	0.994	0.946	0.975
4	1.007	0.959	0.988
5	1.021	0.973	1.002
6	1.034	0.987	1.015
7	1.047	1.000	1.028
8	1.060	1.014	1.042
9	1.073	1.028	1.055
10	1.086	1.041	1.068

Since PE is denser than PP, a higher concentration of FLG can be incorporated into PP without exceeding a density of 1 g/cm³. It is important to note that the composition of MPWS has been considered as PE/PP – 60/40 (composition of MPWS of this work) for calculating the MPWS/FLG density. The density of MPWS/FLG depends on both the PE/PP composition and the concentration of FLG. If the proportion of PP in MPWS is higher, the maximum concentration of FLG that keeps the MPWS/FLG density below 1 g/cm³ will be greater or, vice versa.

It is always advisable to upcycle MPWS by adding the minimum concentration of FLG. In this scenario, achieving better dispersion of FLG within MPWS is crucial for maximizing its utilization.

ANNEX I
SUPPORTING ELECTRONIC INFORMATION OF ARTICLE 1

THE INFLUENCE OF A COMMERCIAL FEW-LAYER GRAPHENE ON THE ELECTRICAL CONDUCTIVITY, MECHANICAL PROPERTIES AND PHOTODEGRADATION RESISTANCE OF POLYOLEFIN BLENDS

S. M. Nourin Sultana [a] , Emna Helal [a,b] , Giovanna Gutiérrez [b], Eric David [a], Nima Moghimian [b] and Nicole R. Demarquette [a]

[a] Mechanical Engineering Department, Ecole de Technologie Superieure, 1100 Notre-Dame Street West, Montreal, Quebec, Canada H3C 1K3
[b] NanoXplore Inc., 4500 Thimens Blvd, Saint-Laurent, QC H4R 2P2, Canada

Paper submitted for publication, June 2024

Background theory and the calculation of critical shear rate to ensure coalescence during deformation

The morphology of an immiscible polymer blend is governed by polymer composition and polymer processing conditions. During processing, polymer blends undergo breakup and coalescence phenomena. If processed under low stress and steady uniform shear flow, the deformation of droplets, in a droplet-dispersed morphology, is directly related to capillary number and viscosity ratio.

$$\text{Capillary number, } C_a = \frac{\eta_m R_v \dot{\gamma}}{\alpha} \quad \text{(A I-1)}$$

$$\text{Viscosity ratio, } \rho = \frac{\eta_d}{\eta_m} \quad \text{(A I-2)}$$

Here, η_m is the viscosity of matrix phase, η_d is the viscosity of dispersed phase, R_v is the volume average radius of droplets, $\dot{\gamma}$ is the applied shear rate, and α is the interfacial tension between matrix and dispersed phase.

As mentioned before, coalescence and droplet break up phenomenon take place during processing. However, break up is dominant when capillary number is above a critical value, C_{ac}. Below C_{ac} , coalescence takes place. Grace (Grace, 1982) outlined a relation between critical capillary number and viscosity ratio. The experimental fit of Grace's curve was modeled by Tucker and Moldenaers (Tucker III & Moldenaers, 2002) by following equation:

$$\log C_{ac} = -0.506 - 0.0994\log\rho + 0.124\,(\log\rho)^2 - \frac{0.115}{\log\rho - \log 4.08} \qquad \text{(A I-3)}$$

In this work, following parameter (shown in Table-A I-1) was used to calculate the shear rate to ensure droplet coalescence during the coalescence test, using the rheometer, MCR 501.

Table-A I-1 The parameters and corresponding values to calculate the shear rate to ensure droplet coalescence during the coalescence test

Parameter	Value
η_m	880 Pa.s
η_d	374 Pa.s
ρ	0.43
R_v	4.94 μm
α	1.21N/m (Tu et al., 2017a)

Calculated shear rate was 0.13 s^{-1} and 0.05 s^{-1} shear rate was used during coalescence test to ensure the occurrence of coalescence during the deformation.

FTIR spectrum of the samples before UV exposure

In Figure-A I-1, the absorbance by neat PE, PE/PP -20/80, PE/PP – 60/40 and PP has been plotted against wave number.

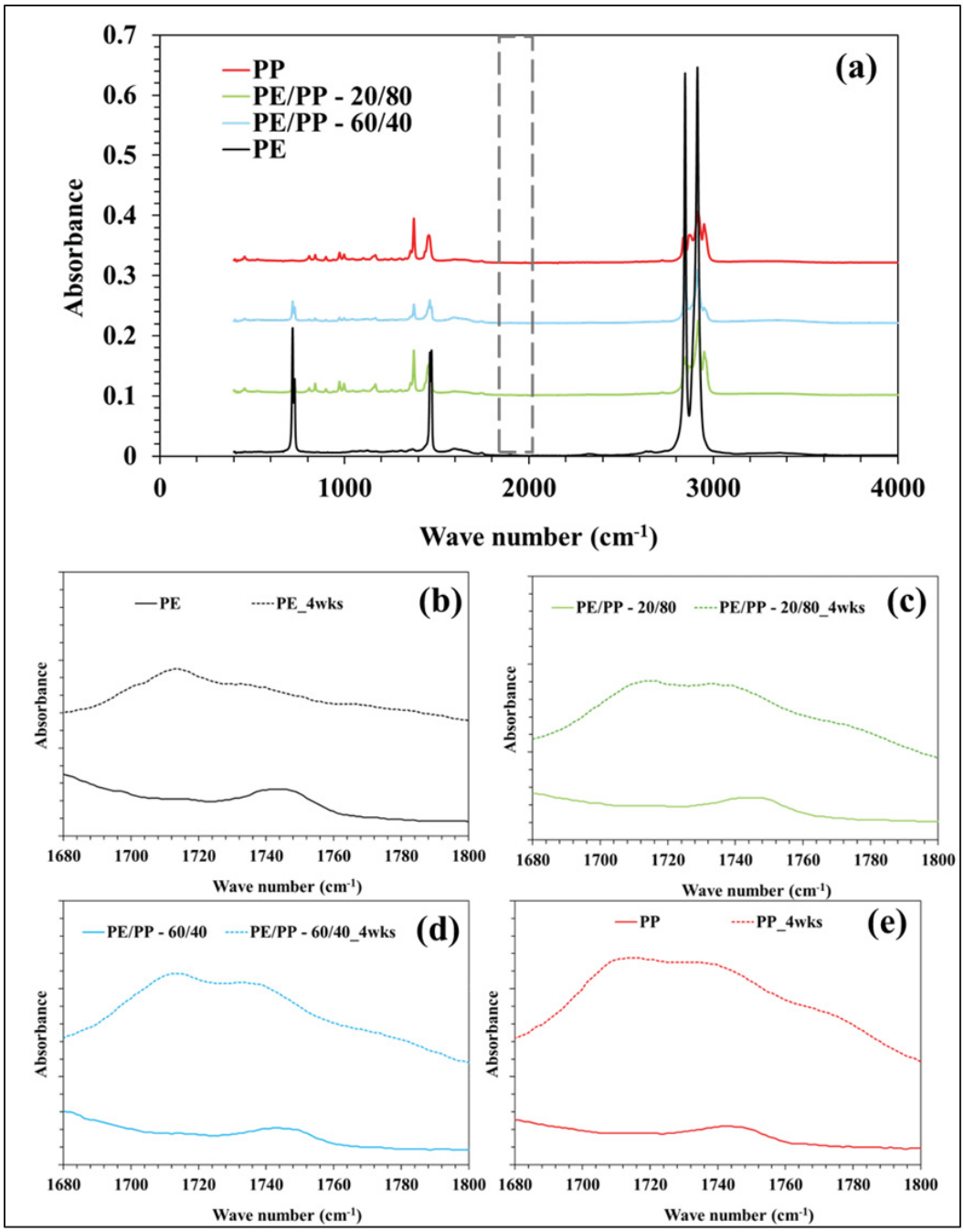

Figure-A I-1 FTIR spectra of neat (a) PE, PE/PP – 20/8, PE/PP – 60/40 and PP samples, and FTIR spectra of neat (b) PE, (c) PE/PP – 20/8, (d) PE/PP – 60/40 and (e) PP samples indicating the carbonyl growth after UV exposure within the wave number range of 1680 to 1800 cm^{-1}

Figure-A I-1 (a) shows that the peak intensity and area under the significant peaks vary based on the composition of the samples.

Effect of different order of mixing of FLG on the electrical conductivity

Figure-A I-2 illustrates the impact of different FLG mixing strategies on the electrical conductivity of a PE/PP – 60/40 blend composite containing 5 wt.% of FLG. Notably, the composite exhibits significantly higher electrical conductivity when FLG is pre-mixed with the PP phase compared to when it is pre-mixed with the PE phase. It is worth mentioning that FLG has a thermodynamic preference for PE over PP. Consequently, by pre-mixing FLG with the thermodynamically less favorable PP phase, there is a possibility of capturing FLG at the PE/PP interface as it tends to travel from the PP to the preferred PE phase. This, in turn, has a positive effect on the electrical conductivity of the composite. Similar findings have been reported by other researchers (Tu et al., 2017a). This observation motivated us to carry on the rest of the study with composites, where FLG was pre-mixed with the PP phase.

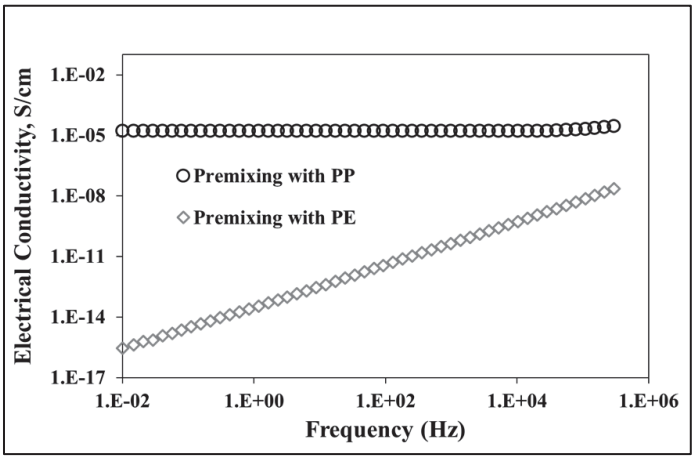

Figure-A I-2 Electrical conductivity of PE/PP – 60/40 blend composite with 5 wt.% FLG; premixed with PP phase and premixed with PE phase

Influence of deformation on the morphology of blend composite

Figure-A I-3 illustrates the distribution of PP droplet size (number average droplet radius, R_N) in neat and FLG-filled PE/PP – 20/80 blend composite after deformation test. The shear-induced deformation results in the coalesced of the droplets, resulting is bigger droplets. It is worth noting that addition of FLG initially inhibit the coalescence of the PE droplets during

processing which result in to smaller droplets of PE in FLG-filled PE/PP – 20/80 composite. However, this coalescence inhibition effect of FLG does not withstand during intense deformation by applied shear.

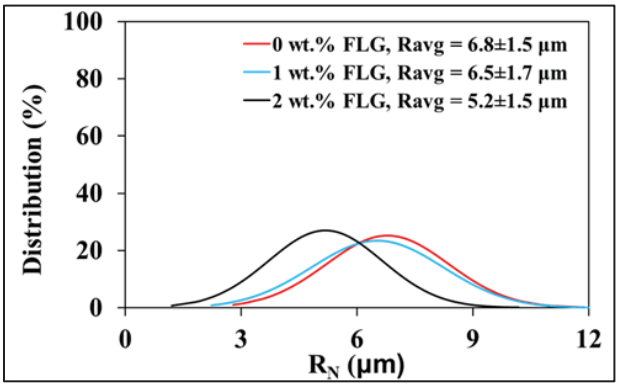

Figure-A I-3 Distribution of PE droplet size in neat and FLG-filled PE/PP – 20/80 blend composite with 1 and 2 wt.% of FLG, respectively, after deformation by 250 strain

Notably, the filler was initially premixed in the predominant PP phase. Due to thermodynamic affinity, FLG migrated from the PP phase to the PE phase during blend preparation, a phenomenon well-documented by other authors. Since extrusion is a rapid mixing process, a complete shifting of FLG from PP to PE during blend preparation is not possible. During the application of deformation in the rheometer via applied shear/strain, further transfer of FLG to thermodynamically favorable PE droplets from the PP matrix phase took place. In Figure-A I-4, the SEM image of the fractured surface of the PE/PP – 20/80 blend, display a remarkable presence of FLG on the PE phase, corroborating above-mentioned observation.

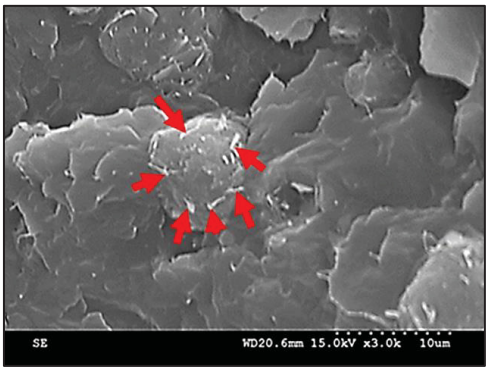

Figure-A I-4 SEM image of 2 wt.% FLG-filled PE/PP – 20/80 blend composite after deformation, red arrows indicate the deformation-driven migration of FLG from PP phase to PE droplet surface

Tensile strength of the samples as a function of FLG concentration

In Figure-A I-5, the tensile strength of the PE, PE/PP -20/80, PE/PP – 60/40 and PP compounds has been plotted as a function of the concentration of FLG.

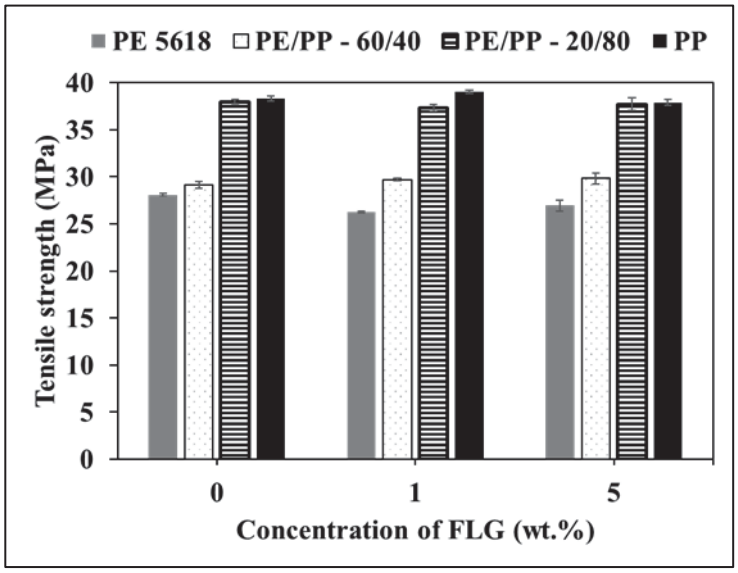

Figure-A I-5 Tensile strength of PE, PE/PP blends and PP composites as a function of FLG concentration

SEM images of the surface appearance of a polyolefin sample before UV exposure.

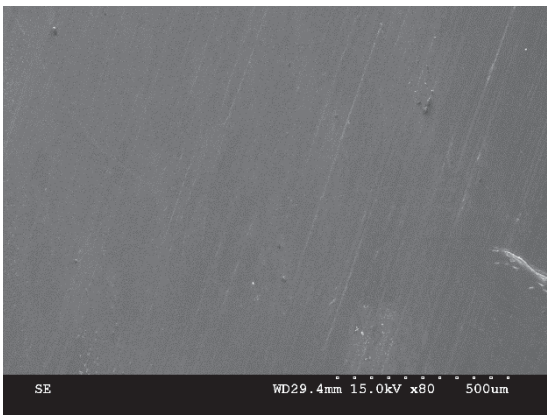

Figure S6: SEM images of the surface appearance of a polyolefin sample before UV exposure.

ANNEX II
SUPPORTING ELECTRONIC INFORMATION OF ARTICLE 2

EFFECT OF FEW-LAYER GRAPHENE OF THE PROPERTIES OF MIXED POLYOLEFIN WASTE STREAM

S. M. Nourin Sultana [a] , Emna Helal [a,b] , Giovanna Gutiérrez [b], Eric David [a], Nima Moghimian [b] and Nicole R. Demarquette [a]

[a] Mechanical Engineering Department, Ecole de Technologie Superieure, 1100 Notre-Dame Street West, Montreal, Quebec, Canada H3C 1K3
[b] NanoXplore Inc., 4500 Thimens Blvd, Saint-Laurent, QC H4R 2P2, Canada

Paper published in *Crystals*, February 2023
DOI: 10.3390/cryst13020358

Differential scanning calorimetry (DSC) analysis

Figure-A II-1 shows the differential scanning calorimetry (DSC) analysis of the mixed polyolefin waste stream (R-PE/PP).

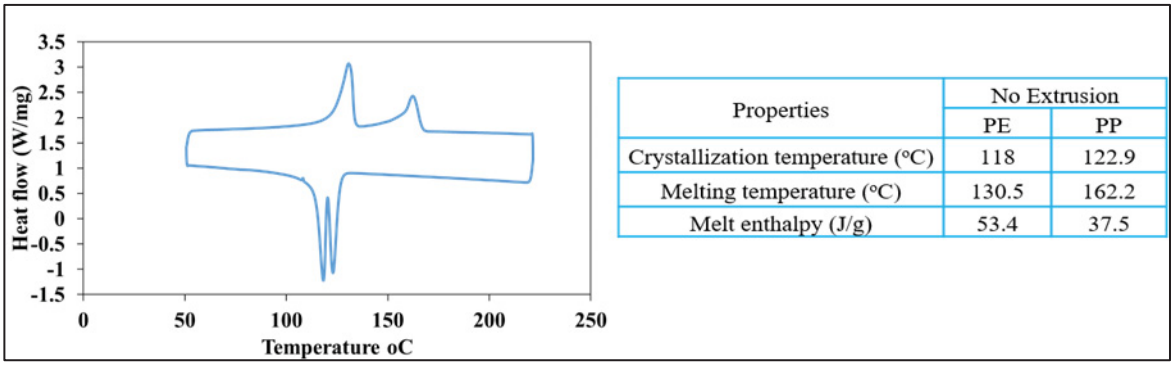

Properties	No Extrusion	
	PE	PP
Crystallization temperature (°C)	118	122.9
Melting temperature (°C)	130.5	162.2
Melt enthalpy (J/g)	53.4	37.5

Figure-A II-1 DSC analysis of unfilled R-(PE/PP)

The area under the melt peak (melting enthalpy, ΔH_m) of the components and blend compositions are linearly correlated in DSC analysis of semi-crystalline polymer blends (Kazemi et al., 2015). However, this method cannot be directly used to quantify the polyethylene (PE)/ polypropylene (PP) composition in recycled blends as the PE and PP grades

are not identified. Nevertheless, this approach can be adopted to estimate the composition of mixed polyolefin waste stream. According to this approach and the respective melt enthalpy values (depicted from Figure-A II-1) of PE and PP indicate that PE consists of 59 wt.% of the blend.

Melt flow index (MFI) of Type 1 and Type 3 composites

Figure-A II-2 (a) shows the MFI results of Type 1 composites (comprised of R-(PE/PP) and FLG) as a function of the concentration of FLG and Figure-A II-2 (b) presents the MFI values of Type 3 composites (comprised of R-(PE/PP), FLG and prime polymer) as a function of the type of prime polymer.

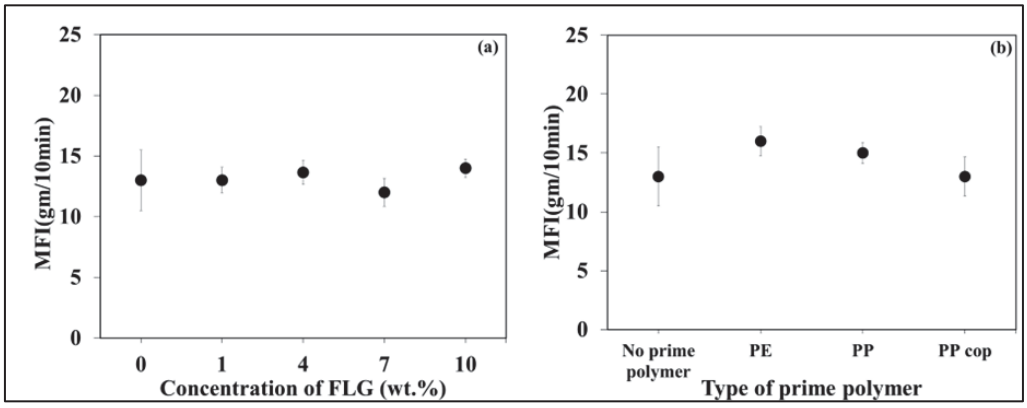

Figure A-II-2 MFI of (a) R-(PE/PP)/FLG composites as a function of the concentration of FLG and (b) R-(PE/PP)/prime polymer/FLG composites as a function of the type of prime polymer

ANNEX III
SUPPORTING ELECTRONIC INFORMATION OF ARTICLE 3

THE INFLUENCE OF A COMMERCIAL FEW-LAYER GRAPHENE ON THE PHOTODEGRADATION RESISTANCE OF A WASTE POLYOLEFINS STREAM AND PRIME POLYOLEFIN BLENDS

S. M. Nourin Sultana [a] , Emna Helal [a,b] , Giovanna Gutiérrez [b], Eric David [a], Nima Moghimian [b] and Nicole R. Demarquette [a]

[a] Mechanical Engineering Department, Ecole de Technologie Superieure, 1100 Notre-Dame Street West, Montreal, Quebec, Canada H3C 1K3
[b] NanoXplore Inc., 4500 Thimens Blvd, Saint-Laurent, QC H4R 2P2, Canada

Paper published in *Recycling*, April 2024
DOI: 10.3390/recycling9020029

Surface appearance of MPWS/FLG composites with higher concentrations of FLG

The SEM images in Figure-A III-1 (a, b) depict the surface finish of MPWS/FLG composites, with 7, and 10 wt.% of FLG, respectively, after 4 weeks of exposure to UV radiation. The MPWS composite filled with 7 wt.% of FLG exhibits a few small cracks along with surface delamination after UV exposure. Interestingly, the UV exposed MPWS/FLG - 90/10 composite displays fewer cracks but more surface delamination. It has been observed that a lower concentration of FLG demonstrates a reduction in crack formation in the UV exposed MPWS composites, while a higher concentration of FLG effectively prevents crack formation but cannot mitigate the surface delamination phenomenon in MPWS composites during UV exposure. Based on the surface finish of the UV samples, it can be said that the presence of FLG slows down the UV degradation of mixed polyolefin waste stream and further retardation of UV degradation is possible with a higher concentration of FLG.

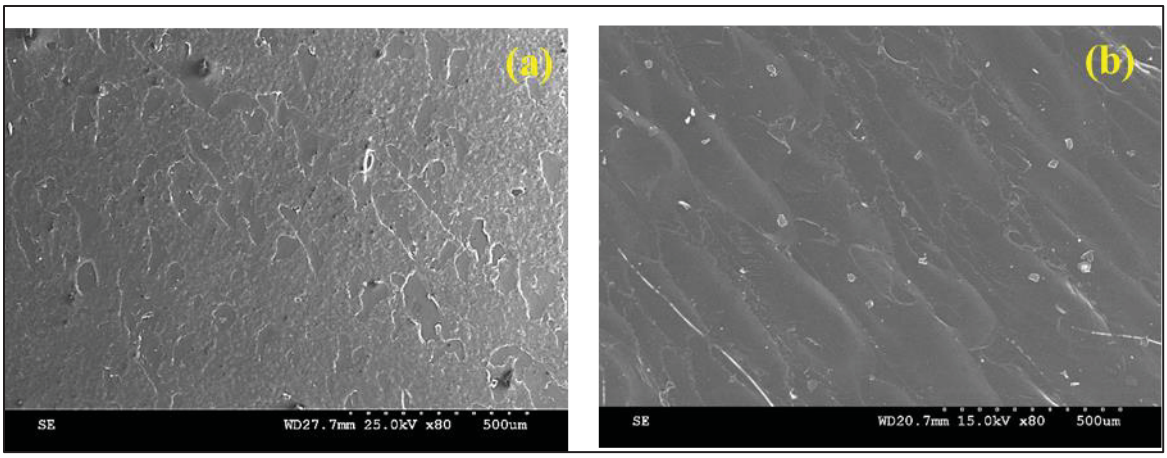

Figure-A III-1 SEM images of the surfaces of MPWS blend compounds with (a) 7 wt.% FLG and, (b) 10 wt.% of FLG; after 4 weeks of UV exposure

Retention of tensile strength and tensile modulus of MPWS/FLG composites after 4 weeks of UV exposure

Figure-A III-2 (a) and A III-2 (b) show that retention of tensile strength and tensile modulus for each of the exposed MPWS/FLG samples are well above 90%. This indicates that these properties of the polymeric materials have been less sensitive to UV exposure, at least for the irradiation duration, adopted in this study.

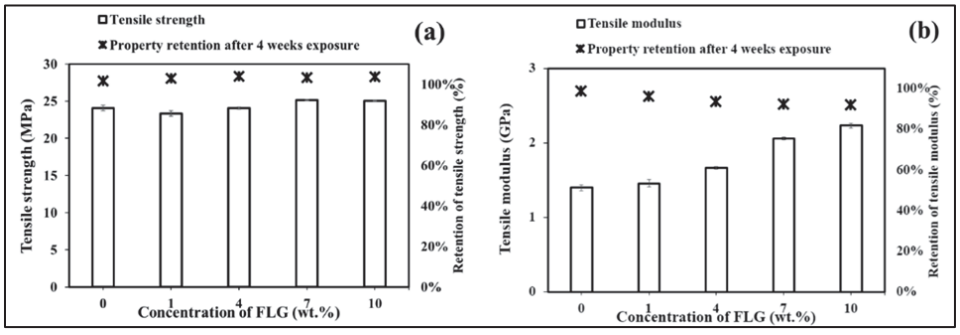

Figure-A III-2 (a) tensile strength and retention of tensile strength, and (b) tensile modulus and retention of tensile modulus of UV-exposed MPWS/FLG composites as a function of FLG concentration, present in the composites

APPENDIX VITA

EDUCATION

- *Doctor of Philosophy* in Mechanical Engineering, École de Technologie Supérieure (ÉTS), Montréal, QC, Canada; February 2019 to July 2024. Supervisor: Prof. Nicole R. Demarquette & Co-supervisor: Prof. Eric David.
- *Master of Science* in Chemical Engineering, University of Calgary, Calgary, AB, Canada; September 2016 to February 2019. Supervisor: Prof. U. T. Sundararaj.
- *Bachelor of Science* in Chemical Engineering, Bangladesh University of Engineering and Technology; Dhaka, Bangladesh; January 2008 to February 2013.

AWARDS AND SCHOLARSHIPS

- Québec Circular Economy Research Network (RRECQ) fund, February 2023
- Fonds de recherche du Québec – Nature et technologies (FRQNT), 2022
- Travel Award, University of Calgary, 2018
- Schulich Student Activity Fund, 2018
- Entrance Award at University of Calgary, 2016
- University Merit Scholarship for academic excellence in undergraduate study at BUET, 2012 Board Scholarships in Bangladesh, 2007

JOURNAL PUBLICATIONS

- "The influence of a commercial few-layer graphene on the photodegradation resistance of a waste polyolefins stream and prime polyolefin blends"; SMN Sultana, E Helal, G Gutiérrez, E David, N Moghimian, NR Demarquette; Recycling, 9 (2), 29, 2024. https://doi.org/10.3390/recycling9020029
- "Effect of few-layer graphene on the properties of mixed polyolefin waste stream"; SMN Sultana, E Helal, G Gutiérrez, E David, N Moghimian, NR Demarquette; Crystals 13 (2), 358, 2023. https://doi.org/10.3390/cryst13020358
- “Tailoring MWCNT Dispersion, Blend Morphology and EMI Shielding Properties by Sequential Mixing Strategy in Immiscible PS/PVDF Blends”; SMN Sultana, SP Pawar, M

Kamkar, U Sundararaj; Journal of Electronic Materials, 1-13, 2019. https://doi.org/10.1007/s11664-019-07371-8

- "Effect of Processing Techniques on EMI SE of Immiscible PS/PMMA Blends Containing MWCNT: Enhanced Intertube and Interphase Scattering"; SMN Sultana, SP Pawar, U Sundararaj; Industrial & Engineering Chemistry Research, 58 (26), 11576-11584, 2019. https://doi.org/10.1021/acs.iecr.8b05957
- "The key role of processing in tuning nonlinear viscoelastic properties and microwave absorption in CNT-based polymer nanocomposites"; M Kamkar, SMN Sultana, SP Pawar, A Eshraghian, E Erfanian, U Sundararaj; Materials Today Communications, 24, 101010, 2020. https://doi.org/10.1016/j.mtcomm.2020.101010

CONFERENCE PRESENTATIONS

- "Investigation of Polyethylene (PE)/ Polypropylene (PP) blend compatibilization by graphene" in 92nd Society of Rheology Conference, 2021.
- "Effect of Processing Techniques on Microwave Screening Ability of Immiscible PS/PMMA Blends Containing MWCNT: Enhanced Intertube and Interphase Scattering" in 68th Canadian Chemical Engineering Conference (CSChE conference), 2018 in Toronto, Canada.
- "Tailoring MWCNT Dispersion, Blend Morphology and Electrical Properties by Sequential Mixing Strategy in Immiscible PS/PVDF Blend" 68th CSChE conference, 2018 in Toronto, Canada.
- "Effect of MWCNT Loading and Blend Components Ratio on Morphology, Electrical Conductivity and Electromagnetic Interference Shielding" in 67th CSChE conference, 2018 in Toronto, Canada.

LIST OF BIBLIOGRAPHICAL REFERENCES

Abbasi, F., Shojaei, D. A., & Bellah, S. M. (2019). The compatibilization effect of exfoliated graphene on rheology, morphology, and mechanical and thermal properties of immiscible polypropylene/polystyrene (PP/PS) polymer blends. *Journal of Thermoplastic Composite Materials*, *32*(10), 1378–1392. https://doi.org/10.1177/0892705718797153

Afzal, A., Kausar, A., & Siddiq, M. (2016). Perspectives of Polystyrene Composite with Fullerene, Carbon Black, Graphene, and Carbon Nanotube: A Review. *Polymer - Plastics Technology and Engineering*, *55*(18), 1988–2011. https://doi.org/10.1080/03602559.2016.1185632

Al-Saleh, M. H. (2016). Electrical, EMI shielding and tensile properties of PP/PE blends filled with GNP:CNT hybrid nanofiller. *Synthetic Metals*, *217*, 322–330. https://doi.org/10.1016/j.synthmet.2016.04.023

Al-Saleh, M. H., Al-Anid, H. K., & Hussain, Y. A. (2013). Electrical double percolation and carbon nanotubes distribution in solution processed immiscible polymer blend. *Synthetic Metals*, *175*, 75–80. https://doi.org/10.1016/j.synthmet.2013.05.004

Al-Salem, S. M., Al-Dousari, N. M., Joseph Abraham, G., D'souza, M. A., Al-Qabandi, O. A., & Al-Zakri, W. (2016). Effect of Die Head Temperature at Compounding Stage on the Degradation of Linear Low Density Polyethylene/Plastic Film Waste Blends after Accelerated Weathering. *International Journal of Polymer Science*, *2016*, 1–16. https://doi.org/10.1155/2016/5147209

Alig, I., Pötschke, P., Lellinger, D., Skipa, T., Pegel, S., Kasaliwal, G. R., & Villmow, T. (2012). Establishment, morphology and properties of carbon nanotube networks in polymer melts. *Polymer*, *53*(1), 4–28. https://doi.org/10.1016/j.polymer.2011.10.063

Alotaibi, M. D., McKinley, A. J., Patterson, B. M., & Reeder, A. Y. (2015). Benzotriazoles in the Aquatic Environment: A Review of Their Occurrence, Toxicity, Degradation and Analysis. *Water, Air, and Soil Pollution*, *226*(7), 1–20. https://doi.org/10.1007/s11270-015-2469-4

Aprianti, N., Kismanto, A., Supriatna, N. K., Yarsono, S., Nainggolan, L. M. T., Purawiardi, R. I., Fariza, O., Ermada, F. J., Zuldian, P., Raksodewanto, A. A., & Alamsyah, R. (2023). Prospect and challenges of producing carbon black from oil palm biomass: A review. *Bioresource Technology Reports*, *23*, 1–16. https://doi.org/10.1016/j.biteb.2023.101587

Arjmand, M., Apperley, T., Okoniewski, M., & Sundararaj, U. (2012). Comparative study of electromagnetic interference shielding properties of injection molded versus compression molded multi-walled carbon nanotube/polystyrene composites. *Carbon*, *50*(14), 5126–5134. https://doi.org/10.1016/j.carbon.2012.06.053

Ashenai Ghasemi, F., Daneshpayeh, S., & Ghasemi, I. (2017). Multi-response optimization of impact strength and elongation at break of nanocomposites based on polypropylene/polyethylene binary polymer matrix in the presence of titanium dioxide nanofiller. *Journal of Elastomers and Plastics*, *49*(8), 633–649. https://doi.org/10.1177/0095244316681834

ASTM D256, Standard Test Methods for Determining the Izod Pendulum Impact Resistance of Plastics. (2023). In *ASTM International: Vol. 08.01* (p. 20). https://doi.org/DOI: 10.1520/D0256-23

ASTM D638, Standard Test Method for Tensile Properties of Plastics. (2015). In *ASTM International* (p. 17). https://doi.org/10.1520/D0638-14

ASTM International. (2010). ASTM D1238, Standard Test Method for Melt Flow Rates of Thermoplastics by Extrusion Plastometer. In *ASTM International* (p. 15). https://doi.org/10.1520/D1238-10.the

ASTM International. (2023). ASTM G154, Standard Practice for Operating Fluorescent Ultraviolet (UV) Lamp Apparatus for Exposure of Materials. In *ASTM International* (p. 12). https://doi.org/10.1520/G0154-23

Batista, N. L., Helal, E., Kurusu, R. S., Moghimian, N., David, E., Demarquette, N. R., & Hubert, P. (2019). Mass-produced graphene—HDPE nanocomposites: Thermal, rheological, electrical, and mechanical properties. *Polymer Engineering and Science*, *59*(4), 675–682. https://doi.org/10.1002/pen.24981

Bertin, S., & Robin, J.-J. (2002). Study and characterization of virgin and recycled PE/PP blends. *European Polymer Journal*, *38*, 2255–2264.

Bijarimi, M., Amirul, M., Norazmi, M., Ramli, A., Desa, M. S. Z. M. A., Desa, M. S. Z. M. A., & Abu Samah, M. A. (2019). Preparation and characterization of poly (lactic acid) (PLA)/polyamide 6 (PA6)/graphene nanoplatelet (GNP) blends bio-based nanocomposites. *Materials Research Express*, *6*(5), 1–8. https://doi.org/10.1088/2053-1591/ab05a3

Blom, H. P., Teh, J. W., & Rudin, A. (1996). I-PP/HDPE blends. III. Characterization and compatibilization at lower i-PP contents. *Journal of Applied Polymer Science*, *61*(6), 959–968. https://doi.org/10.1002/(sici)1097-4628(19960808)61:6<959::aid-app10>3.0.co;2-q

Bouhfid, R., Arrakhiz, F. Z., & Qaiss, A. (2016). Effect of graphene nanosheets on the mechanical, electrical, and rheological properties of Polyamide 6/Acrylonitrile-Butadiene-Styrene blends. *Polymer Composites*, *37*(4), 998–1006. https://doi.org/10.1002/pc.23259

Cetiner, B., Sahin Dundar, G., Yusufoglu, Y., & Saner Okan, B. (2023). Sustainable

Engineered Design and Scalable Manufacturing of Upcycled Graphene Reinforced Polylactic Acid/Polyurethane Blend Composites Having Shape Memory Behavior. *Polymers*, *15*(5), 1–17. https://doi.org/10.3390/polym15051085

Chakraborty, M., & Hashmi, M. S. J. (2018). Wonder material graphene: properties, synthesis and practical applications. *Advances in Materials and Processing Technologies*, *4*(4), 573–602. https://doi.org/10.1080/2374068X.2018.1484998

Chaudhuri, I., Fruijtier-Pölloth, C., Ngiewih, Y., & Levy, L. (2017). Evaluating the evidence on genotoxicity and reproductive toxicity of carbon black: a critical review. *Critical Reviews in Toxicology*, *48*(2), 143–169. https://doi.org/10.1080/10408444.2017.1391746

Chiu, F. C., Behera, K., Cai, H. J., & Chang, Y. H. (2021). Polycarbonate/poly(Vinylidene fluoride)-blend-based nanocomposites—effect of adding different carbon nanofillers/organoclay. *Polymers*, *13*, 1–15. https://doi.org/10.3390/polym13162626

Choi, W., Lahiri, I., Seelaboyina, R., & Kang, Y. S. (2010). Synthesis of graphene and its applications: A review. *Critical Reviews in Solid State and Materials Sciences*, *35*(1), 52–71. https://doi.org/10.1080/10408430903505036

Christensen, P. A., Egerton, T. A., Martins-Franchetti, S. M., Jin, C., & White, J. R. (2008). Photodegradation of polycaprolactone/poly(vinyl chloride) blend. *Polymer Degradation and Stability*, *93*(1), 305–309. https://doi.org/10.1016/j.polymdegradstab.2007.08.008

Cui, Y., Kundalwal, S. I., & Kumar, S. (2016). Gas barrier performance of graphene/polymer nanocomposites. *Carbon*, *98*, 313–333. https://doi.org/10.1016/j.carbon.2015.11.018

Dash, G. N., Pattanaik, S. R., & Behera, S. (2014). Graphene for electron devices: The panorama of a decade. *IEEE Journal of the Electron Devices Society*, *2*(5), 77–104. https://doi.org/10.1109/JEDS.2014.2328032

Davidson, M. G., Furlong, R. A., & McManus, M. C. (2021). Developments in the life cycle assessment of chemical recycling of plastic waste – A review. *Journal of Cleaner Production*, *293*, 1–12. https://doi.org/10.1016/j.jclepro.2021.126163

Dikobe, D. G., & Luyt, A. S. (2017). Thermal and mechanical properties of PP/HDPE/wood powder and MAPP/HDPE/wood powder polymer blend composites. *Thermochimica Acta*, *654*(April), 40–50. https://doi.org/10.1016/j.tca.2017.05.002

dos Anjos, E. G. R., de Souza Vieira, L., Marini, J., Brazil, Tayra Rodrigues Gomes, N. A., Santos, & Rezende, Mirabel Cerqueira Passador, F. R. (2022). Influence of graphene nanoplates and ABS-g-MAH on the thermal, mechanical, and electromagnetic properties of PC/ABS blend. *Journal of Applied Polymer Science*, *139*(3), 1–15. https://doi.org/10.1002/app.51500

dos Anjos, E. G. R., Marini, J., Gomes, N. A. S., Rezende, M. C., & Passador, F. R. (2022). Synergistic effect of adding graphene nanoplates and carbon nanotubes in polycarbonate/acrylonitrile-styrene-butadiene copolymer blend. *Journal of Applied Polymer Science*, *139*(37), 1–15. https://doi.org/10.1002/app.52873

dos Anjos, E. G. R., Moura, N. K., Antonelli, E., Baldan, M. R., Gomes, N. A., Braga, N. F., Santos, A. P., Rezende, M. C., Pessan, L. A., & Passador, F. R. (2022). Role of adding carbon nanotubes in the electric and electromagnetic shielding behaviors of three different types of graphene in hybrid nanocomposites. *Journal of Thermoplastic Composite Materials*, *0*(0), 1–27. https://doi.org/10.1177/08927057221124483

Du, B. X., Hou, Z. H., Li, J., & Li, Z. L. (2018). Effect of graphene nanoplatelets on space charge and breakdown strength of PP/ULDPE blends for HVDC cable insulation. *IEEE Transactions on Dielectrics and Electrical Insulation*, *25*(6), 2405–2412. https://doi.org/10.1109/TDEI.2018.007271

Elias, L., Cassagnau, P., Fenouillot, F., & Majeste, J. C. (2007). Morphology and rheology of immiscible polymer blends Filled with silica nanoparticles. *Polymer*, *48*(20), 6029–6040. https://doi.org/10.1016/j.polymer.2007.07.061

Fang, C., Nie, L., Liu, S., Yu, R., An, N., & Li, S. (2013). Characterization of polypropylene-polyethylene blends made of waste materials with compatibilizer and nano-filler. *Composites: Part B*, *55*, 498–505. https://doi.org/10.1016/j.compositesb.2013.06.046

Feng, Y., Yuan, Z., Sun, H., He, H., & Zhang, G. (2020). Toughening and reinforcing wood flour/polypropylene composites with high molecular weight polyethylene under elongation flow. *Composites Science and Technology*, *200*(381), 1–8. https://doi.org/10.1016/j.compscitech.2020.108395

Ferdous, W., Manalo, A., Siddique, R., Mendis, P., Zhuge, Y., Wong, H. S., Lokuge, W., Aravinthan, T., & Schubel, P. (2021). Recycling of landfill wastes (tyres, plastics and glass) in construction – A review on global waste generation, performance, application and future opportunities. *Resources, Conservation and Recycling*, *173*(May), 1–13. https://doi.org/10.1016/j.resconrec.2021.105745

Fernandes, L. ., Freitas, C. A., Demarquette, N. r., & Fechine, G. J. M. (2010). Photodegradation of Thermodegraded Polypropylene/ High-Impact Polystyrene Blends: Mechanical Properties. *Journal of Applied Polymer Science*, *120*, 770–779. https://doi.org/DOI 10.1002/app.33096

Ferreira, E. H. C., Andrade, R. J. E., & Fechine, G. J. M. (2019). The “superlubricity state” of carbonaceous fillers on polyethylene-based composites in a molten state. *Macromolecules*, *52*(24), 9620–9631. https://doi.org/10.1021/acs.macromol.9b01746

Ferreira Junior, J. C., Moghimian, N., Gutiérrez, G., Helal, E., Ajji, A., Barra, G. M. de O., &

Demarquette, N. R. (2022). Effects of an industrial graphene grade and surface finishing on water and oxygen permeability, electrical conductivity, and mechanical properties of high-density polyethylene (HDPE) multilayered cast films. *Materials Today Communications*, *31*, 1–8. https://doi.org/10.1016/j.mtcomm.2022.103470

Fortelný, I., Michálková, D., & Kruliš, Z. (2004). An efficient method of material recycling of municipal plastic waste. *Polymer Degradation and Stability*, *85*, 975–979. https://doi.org/10.1016/j.polymdegradstab.2004.01.024

Galindo, B., Alcolea, S. G., Gómez, J., Navas, A., Murguialday, A. O., Fernandez, M. P., & Puelles, R. C. (2014). Effect of the number of layers of graphene on the electrical properties of TPU polymers. *IOP Conference Series: Materials Science and Engineering*, *64*(1). https://doi.org/10.1088/1757-899X/64/1/012008

Garofalo, E., Claro, M., Scarfato, P., Di Maio, L., & Incarnato, L. (2015). Upgrading of recycled plastics obtained from flexible packaging waste by adding nanosilicates. *AIP Conference Proceedings*, *1695*, 1–9. https://doi.org/10.1063/1.4937331

Genoyer, J., Helal, E., Gutierrez, G., Moghimian, N., David, E., & Demarquette, N. R. (2023). Graphene and Nanoclay as Processing Aid Agents: A Study on Rheological Behavior in Polystyrene. *C-Journal of Carbon Research*, *9*(4), 1–17. https://doi.org/10.3390/c9040096

Ghosh, A. (2021). Performance modifying techniques for recycled thermoplastics. *Resources, Conservation and Recycling*, *175*, 1–26. https://doi.org/10.1016/j.resconrec.2021.105887

Gijsman, P., Jan, H., Daan, T., Hennekens, J., & Tummers, D. (1993). The mechanism of action of hindered amine light stabilizers. *Polymer Degradation and Stability*, *39*(2), 225–233. https://doi.org/https://doi.org/10.1016/0141-3910(93)90099-5

Gijsman, P., Meijers, G., & Vitarelli, G. (1999). Comparison of the UV-degradation chemistry of polypropylene, polyethylene, polyamide 6 and polybutylene terephthalate. *Polymer Degradation and Stability*, *65*(3), 433–441. https://doi.org/10.1016/S0141-3910(99)00033-6

Göldel, A., Kasaliwal, G., & Pötschke, P. (2009). Selective localization and migration of multiwalled carbon nanotubes in blends of polycarbonate and poly(styrene-acrylonitrile). *Macromolecular Rapid Communications*, *30*(6), 423–429. https://doi.org/10.1002/marc.200800549

Goodwin, D. G., Shen, S. J., Lyu, Y., Lankone, R., Barrios, A. C., Kabir, S., Perreault, F., Wohlleben, W., Nguyen, T., & Sung, L. (2020). Graphene/polymer nanocomposite degradation by ultraviolet light: The effects of graphene nanofillers and their potential for release. *Polymer Degradation and Stability*, *182*, 1–14. https://doi.org/10.1016/j.polymdegradstab.2020.109365

Grace, H. P. (1982). Dispersion phenomena in high viscosity immiscible fluid systems and application of static mixers as dispersion devices in such systems. *Chemical Engineering Communications*, *14*(3–6), 225–277. https://doi.org/10.1080/00986448208911047

Graziano, A., Dias, O. A. T., Garcia, C., Jaffer, S., Tjong, J., & Sain, M. (2020). Impact of Reduced Graphene Oxide on structure and properties of polyethylene rich binary systems for performance-based applications. *Polymer*, *202*, 1–10. https://doi.org/10.1016/j.polymer.2020.122622

Graziano, A., Garcia, C., Jaffer, S., Tjong, J., & Sain, M. (2020). Novel functional graphene and its thermodynamic interfacial localization in biphasic polyolefin systems for advanced lightweight applications. *Composites Science and Technology*, *188*(July 2019), 321–329. https://doi.org/10.1016/j.compscitech.2019.107958

Graziano, A., Garcia, C., Jaffer, S., Tjong, J., Yang, W., & Sain, M. (2020). Functionally tuned nanolayered graphene as reinforcement of polyethylene nanocomposites for lightweight transportation industry. *Carbon*, *169*, 99–110. https://doi.org/10.1016/j.carbon.2020.07.040

Grigore, M. E. (2017). Methods of recycling, properties and applications of recycled thermoplastic polymers. *Recycling*, *2*(4), 1–11. https://doi.org/10.3390/recycling2040024

Gubbels, F., Blacher, S., Vanlathem, E., Jerome, R., Deltour, R., Brouers, F., & Teyssibt, P. (1995). Design of Electrical Conductive Composites : Key Role of the Morphology on the Electrical Properties of Carbon Black Filled Polymer Blends. *Macromolecules*, *28*, 1559–1566.

Gubbels, Frédéric, & Jérôme, R. (1998). Kinetic and Thermodynamic Control of the Selective Localization of Carbon Black at the Interface of Immiscible Polymer Blends. *Chemistry of Materials*, *10*(7), 1227–1235. https://doi.org/10.1021/cm970594d

Gubbels, Frédéric, Jérôme, R., Teyssié, P., Vanlathem, E., Deltour, R., Calderone, A., Parenté, V., Brédas, J. L., Bredas, J.-L., & Brédas, J. L. (1994). Selective Localization of Carbon Black in Immiscible Polymer Blends: A Useful Tool To Design Electrical Conductive Composites. *Macromolecules*, *27*(7), 1972–1974. https://doi.org/10.1021/ma00085a049

Guo, Y., Zuo, X., Xue, Y., Tang, J., Gouzman, M., Fang, Y., Zhou, Y., Wang, L., Yu, Y., & Rafailovich, M. H. (2020). Engineering thermally and electrically conductive biodegradable polymer nanocomposites. *Composites Part B*, *189*, 1–9. https://doi.org/10.1016/j.compositesb.2020.107905

Gutiérrez-Villarreal, M. H., & Zavala-Betancourt, S. A. (2017). A Comparative Study of the Photodegradation of Two Series of Cyclic Olefin Copolymers. *International Journal of Polymer Science*, 1–10. https://doi.org/https://doi.org/10.1155/2017/1870814

Haghnegahdar, M., Naderi, G., & Ghoreishy, M. H. R. (2017). Electrical and thermal properties of a thermoplastic elastomer nanocomposite based on polypropylene/ethylene propylene diene monomer/graphene. *Soft Materials*, *15*(1), 82–94. https://doi.org/10.1080/1539445X.2016.1268622

Halina, K. (1995). Photodegradation of Polystyrene and Poly(vinyl acetate) Blends-I. Irradiation of PS/PVAc blends by Polychromatic Light. *European Polymer Journal*, *31*(11), 1037–1042.

Hasani, M., Mahdavian, M., Yari, H., & Ramezanzadeh, B. (2018). Versatile protection of exterior coatings by the aid of graphene oxide nano-sheets; comparison with conventional UV absorbers. *Progress in Organic Coatings*, *116*(August 2017), 90–101. https://doi.org/10.1016/j.porgcoat.2017.11.020

Helal, E., Kurusu, R. S., Moghimian, N., Gutierrez, G., David, E., & Demarquette, N. R. (2019). Correlation between morphology, rheological behavior, and electrical behavior of conductive cocontinuous LLDPE/EVA blends containing commercial graphene nanoplatelets. *Journal of Rheology*, *63*(6), 961–976. https://doi.org/10.1122/1.5108919

Hocker, S. J. A., Kim, W. T., Schniepp, H. C., & Kranbuehl, D. E. (2018). Polymer crystallinity and the ductile to brittle transition. *Polymer*, *158*(June), 72–76. https://doi.org/10.1016/j.polymer.2018.10.031

Horrocks, A. R., Mwila, J., Miraftab, M., Liu, M., & Chohan, S. S. (1999). Influence of carbon black on properties of orientated polypropylene 2. Thermal and photodegradation. *Polymer Degradation and Stability*, *65*(1), 25–36. https://doi.org/10.1016/S0141-3910(98)00213-4

Hsieh, C. T., Pan, Y. J., & Lin, J. H. (2017). Polypropylene/high-density polyethylene/carbon fiber composites: Manufacturing techniques, mechanical properties, and electromagnetic interference shielding effectiveness. *Fibers and Polymers*, *18*(1), 155–161. https://doi.org/10.1007/s12221-017-6371-0

Im, J. S., Kim, J. G., & Lee, Y. S. (2009). Fluorination effects of carbon black additives for electrical properties and EMI shielding efficiency by improved dispersion and adhesion. *Carbon*, *47*(11), 2640–2647. https://doi.org/10.1016/j.carbon.2009.05.017

Jia, L. C., Yan, D. X., Cui, C. H., Ji, X., & Li, Z. M. (2016). A unique double percolated polymer composite for highly efficient electromagnetic interference shielding. *Macromolecular Materials and Engineering*, *301*(10), 1232–1241. https://doi.org/10.1002/mame.201600145

Johra, F. T., Lee, J. W., & Jung, W. G. (2014). Facile and safe graphene preparation on solution based platform. *Journal of Industrial and Engineering Chemistry*, *20*(5), 2883–2887. https://doi.org/10.1016/j.jiec.2013.11.022

Juan, L. (2020). Simultaneous improvement in the tensile and impact strength of polypropylene reinforced by graphene. *Journal of Nanomaterials*, *2020*, 1–5. https://doi.org/10.1155/2020/7840802

Jubinville, D., Esmizadeh, E., Saikrishnan, S., Tzoganakis, C., & Mekonnen, T. (2020). A comprehensive review of global production and recycling methods of polyolefin (PO) based products and their post-recycling applications. *Sustainable Materials and Technologies*, *25*, e00188. https://doi.org/10.1016/j.susmat.2020.e00188

Karaagac, E., Koch, T., & Archodoulaki, V.-M. (2021). The effect of PP contamination in recycled high-density polyethylene (rPE-HD) from post-consumer bottle waste and their compatibilization with olefin block copolymer (OBC). *Waste Management*, *119*, 285–294. https://doi.org/10.1016/j.wasman.2020.10.011

Karimi, S., Helal, E., Gutierrez, G., David, E., Samara, M., & Demarquette, N. (2023). Photo-stabilization mechanisms of high-density polyethylene (HDPE) by a commercial few-layer graphene. *Polymer Engineering and Science*, *July*, 3879–3890. https://doi.org/10.1002/pen.26493

Karimi, S., Helal, E., Gutierrez, G., Moghimian, N., Madinehei, M., David, E., Samara, M., & Demarquette, N. (2021). A review on graphene ' s light stabilizing effects for reduced photodegradation of polymers. *Crystals*, *11*(3), 1–22. https://doi.org/https://dx.doi.org/10.3390/cryst11010003

Karlsson, S. (2004). Recycled polyolefins. Material properties and means for quality determination. *Advances in Polymer Science*, *169*, 201–229. https://doi.org/10.1007/b94173

Kasaliwal, G. R., Göldel, A., Pötschke, P., & Heinrich, G. (2011). Influences of polymer matrix melt viscosity and molecular weight on MWCNT agglomerate dispersion. *Polymer*, *52*(4), 1027–1036. https://doi.org/10.1016/j.polymer.2011.01.007

Kazemi, Y., Kakroodi, A. R., & Rodrigue, D. (2015). Compatibilization Efficiency in Post-Consumer Recycled Polyethylene/Polypropylene Blends: Effect of Contamination. *Polymer Engineering and Science*, 2368–2376. https://doi.org/https://doi.org/10.1002/pen.24125

Khadri Diallo, A., Helal, E., Gutiérrez, G., Madinehei, M., David, E., Demarquette, N., & Moghimian, N. (2022). Graphene: A multifunctional additive for sustainability. *Sustainable Materials and Technologies*, *33*, 1–6. https://doi.org/10.1016/j.susmat.2022.e00487

Koodehi, A. V., & Dadvand Koohi, A. (2018). Optimization of Thermal Stability of High-Density Polyethylene Composite Using Antioxidant, Carbon Black and Nanoclay Addition by a Central Composite Design Method: X-ray Diffraction and Rheological Characterization. *Journal of Macromolecular Science, Part B: Physics*, *57*(10), 660–678.

https://doi.org/10.1080/00222348.2018.1511030

Kuilla, T., Bhadra, S., Yao, D., Kim, N. H., Bose, S., & Lee, J. H. (2010). Recent advances in graphene based polymer composites. *Progress in Polymer Science*, *35*(11), 1350–1375. https://doi.org/10.1016/j.progpolymsci.2010.07.005

Kurusu, R. S., Helal, E., Moghimian, N., David, E., & Demarquette, N. (2018). The Role of Selectively Located Commercial Graphene Nanoplatelets in the Electrical Properties, Morphology, and Stability of EVA/LLDPE Blends. *Macromolecular Materials and Engineering*, *303*(9), 1–9. https://doi.org/10.1002/mame.201800187

Lago, E., Cagnin, E., Boaretti, C., Roso, M., Lorenzetti, A., & Modesti, M. (2020). Influence of different carbon-based fillers on electrical and mechanical properties of a PC/ABS blend. *Polymers*, *12*(29), 1–16. https://doi.org/10.3390/polym12010029

Larsen, Å. G., Olafsen, K., & Alcock, B. (2021). Determining the PE fraction in recycled PP. *Polymer Testing*, *96*, 1–11. https://doi.org/10.1016/j.polymertesting.2021.107058

Liebscher, M., Domurath, J., Saphiannikova, M., Müller, M. T., Heinrich, G., & Pötschke, P. (2020). Dispersion of graphite nanoplates in melt mixed PC/SAN polymer blends and its influence on rheological and electrical properties. *Polymer*, *200*, 1–10. https://doi.org/10.1016/j.polymer.2020.122577

López-Martínez, E. D., Martínez-Colunga, J. G., Ramírez-Vargas, E., Sanchez-Valdes, S., Ramos-de Valle, L. F., Benavides-Cantu, R., Rodríguez-Gonzalez, J. A., Mata-Padilla, J. M., Cruz-Delgado, V. J., Borjas-Ramos, J. J., & Da Silva, L. (2022). Influence of carbon structures on the properties and photodegradation of LDPE/LLDPE films. *Polymers for Advanced Technologies*, *33*(5), 1727–1741. https://doi.org/https://doi.org/10.1002/pat.5635

Lou, C. W., Huang, C. L., Pan, Y. J., Lin, Z. I., Song, X. M., & Lin, J. H. (2016). Crystallization, mechanical, and electromagnetic properties of conductive polypropylene/SEBS composites. *Journal of Polymer Research*, *23*(5), 1–9. https://doi.org/10.1007/s10965-016-0979-4

Ma, T., Liu, Z., Wen, J., Gao, Y., Ren, X., Chen, H., Jin, C., Ma, X. L., Xu, N., Cheng, H. M., & Ren, W. (2017). Tailoring the thermal and electrical transport properties of graphene films by grain size engineering. *Nature Communications*, *8*, 1–9. https://doi.org/10.1038/ncomms14486

Madi, N. K. (2013). Thermal and mechanical properties of injection molded recycled high density polyethylene blends with virgin isotactic polypropylene. *Materials and Design*, *46*, 435–441. https://doi.org/10.1016/j.matdes.2012.10.004

Mailhot, B., Morlat, S., & Gardette, J. L. (2000). Photooxidation of blends of polystyrene and

poly(vinyl methyl ether): FTIR and AFM studies. *Polymer*, *41*(6), 1981–1988. https://doi.org/10.1016/S0032-3861(99)00204-9

Mak, K. F., Ju, L., Wang, F., & Heinz, T. F. (2012). Optical spectroscopy of graphene: From the far infrared to the ultraviolet. *Solid State Communications*, *152*(15), 1341–1349. https://doi.org/10.1016/j.ssc.2012.04.064

Mantia, F. P. La, Morreale, M., Botta, L., Mistretta, M. C., Ceraulo, M., & Scaffaro, R. (2017). Degradation of polymer blends : A brief review. *Polymer Degradation and Stability*, *145*, 79–92. https://doi.org/10.1016/j.polymdegradstab.2017.07.011

Maris, J., Bourdon, S., Brossard, J. M., Cauret, L., Fontaine, L., & Montembault, V. (2018). Mechanical recycling: Compatibilization of mixed thermoplastic wastes. *Polymer Degradation and Stability*, *147*, 245–266. https://doi.org/10.1016/j.polymdegradstab.2017.11.001

Martikka, O., & Kärki, T. (2019). Promoting recycling of mixed waste polymers in wood-polymer composites using compatibilizers. *Recycling*, *4*(1), 1–15. https://doi.org/10.3390/recycling4010006

Mistretta, M. C., Botta, L., Vinci, A. D., Ceraulo, M., & Mantia, F. P. La. (2019). Photo-oxidation of polypropylene / graphene nanoplatelets composites. *Polymer Degradation and Stability*, *160*, 35–43. https://doi.org/10.1016/j.polymdegradstab.2018.12.003

Mofokeng, T. G., Ray, S. S., & Ojijo, V. (2018). Structure–property relationship in PP/LDPE blend composites: The role of nanoclay localization. *Journal of Applied Polymer Science*, *135*(17), 1–12. https://doi.org/10.1002/app.46193

Moghimian, N., & Nazarpour, S. (2020). The future of carbon: An update on graphene's dermal, inhalation, and gene toxicity. *Crystals*, *10*(9), 1–6. https://doi.org/10.3390/cryst10090718

Moghimian, N., Saeidlou, S., Lentzakis, H., Rosi, G. F., Song, N., & David, E. (2017). Electrical conductivity of commercial graphene polyethylene nanocomposites. *17th IEEE International Conference on Nanotechnology*, 757–761. https://doi.org/10.1109/NANO.2017.8117344

Moon, Y., Yun, J., Kim, H., & Lee, Y. (2011). Effect of graphite oxide on photodegradation behavior of poly (vinyl alcohol)/ graphite oxide composite hydrogels. *Carbon Letters*, *12*(3), 138–142. https://doi.org/http://carbonlett.org/ 10.5714/CL.2011.12.3.138

More Recycling for the Canadian Plastics Industry Association. (2018). 2016 post-consumer plastics recycling in Canada

Mun, S. C., Kim, M. J., Cobos, M., Gu, L., & Macosko, C. W. (2019). Strategies for interfacial

localization of graphene/polyethylene-based cocontinuous blends for electrical percolation. *AIChE Journal*, *65*(6), 1–12. https://doi.org/10.1002/aic.16579

Najafi, S. K., Hamidinia, E., & Tajvidi, M. (2006). Mechanical properties of composites from sawdust and recycled plastics. *Journal of Applied Polymer Science*, *100*(5), 3641–3645. https://doi.org/10.1002/app.23159

Navas, I. O., Arjmand, M., & Sundararaj, U. (2017). Effect of carbon nanotubes on morphology evolution of polypropylene/polystyrene blends: Understanding molecular interactions and carbon nanotube migration mechanisms. *RSC Advances*, *7*(85), 54222–54234. https://doi.org/10.1039/c7ra11390k

Nirmalraj, P. N., Lutz, T., Kumar, S., Duesberg, G. S., & Boland, J. J. (2011). Nanoscale mapping of electrical resistivity and connectivity in graphene strips and networks. *Nano Letters*, *11*(1), 16–22. https://doi.org/10.1021/nl101469d

Nunes, M. A. B. S., de Matos, B. R., Silva, G. G., Ito, E. N., de Melo, T. J. A., & Fechine, G. J. M. (2021). Hybrids nanocomposites based on a polymer blend (linear low-density polyethylene/poly(ethylene-co-methyl acrylate) and carbonaceous fillers (graphene and carbon nanotube). *Polymer Composites*, *42*(2), 661–677. https://doi.org/10.1002/pc.25856

Nuraje, N., Khan, S. I., Misak, H., & Asmatulu, R. (2013). The Addition of Graphene to Polymer Coatings for Improved Weathering. *Polymer Science*, *2013*, 1–8. https://doi.org/10.1155/2013/514617

Ojeda, T., Freitas, A., Birck, K., Dalmolin, E., Jacques, R., Bento, F., & Camargo, F. (2011). Degradability of linear polyolefins under natural weathering. *Polymer Degradation and Stability*, *96*(4), 703–707. https://doi.org/10.1016/j.polymdegradstab.2010.12.004

Ołdak, D., Kaczmarek, H., Buffeteau, T., & Sourisseau, C. (2005). Photo- and bio-degradation processes in polyethylene, cellulose and their blends studied by ATR-FTIR and raman spectroscopies. *Journal of Materials Science*, *40*(16), 4189–4198. https://doi.org/10.1007/s10853-005-2821-y

Oliveira, Y. D. C. de, Amurin, L. G., Valim, F. C. F., Fechine, G. J. M., & Andrade, R. J. E. (2019). The role of physical structure and morphology on the photodegradation behaviour of polypropylene-graphene oxide nanocomposites. *Polymer*, *176*, 146–158. https://doi.org/10.1016/j.polymer.2019.05.029

Otero-Navas, I., Arjmand, M., & Sundararaj, U. (2017). Carbon nanotube induced double percolation in polymer blends: Morphology, rheology and broadband dielectric properties. *Polymer*, *114*(February), 122–134. https://doi.org/10.1016/j.polymer.2017.02.082

Paben, J. (2016). *DuPont announces compatibilizer for mixed PP, PE streams*. Resource Recycling. https://resource-recycling.com/plastics/

Pan, Y., Liu, X., Hao, X., Starý, Z., & Schubert, D. W. (2016). Enhancing the electrical conductivity of carbon black-filled immiscible polymer blends by tuning the morphology. *European Polymer Journal*, *78*, 106–115. https://doi.org/10.1016/j.eurpolymj.2016.03.019

Parameswaranpillai, J., Elamon, R., Sanjay, M. R., & Siengchin, S. (2019). Synergistic effects of ethylene propylene diene copolymer and carbon nanofiber on the thermo-mechanical properties of polypropylene/high-density polyethylene composites. *Materials Research Express*, *6*(8), 2–13. https://doi.org/10.1088/2053-1591/ab1d37

Parameswaranpillai, J., Joseph, G., Shinu, K. P., Jose, S., Salim, N. V., & Hameed, N. (2015). Development of hybrid composites for automotive applications: Effect of addition of SEBS on the morphology, mechanical, viscoelastic, crystallization and thermal degradation properties of PP/PS-xGnP composites. *RSC Advances*, *5*(33), 25634–25641. https://doi.org/10.1039/c4ra16637j

Parameswaranpillai, J., Pulikkalparambil, H., Sanjay, M. R., & Siengchin, S. (2019). Polypropylene/high-density polyethylene based blends and nanocomposites with improved toughness. *Materials Research Express*, *6*(7), 2–12. https://doi.org/10.1088/2053-1591/ab18cd

Parameswaranpillai, J., Sanjay, M. R., Varghese, S. A., Siengchin, S., Jose, S., Salim, N., Hameed, N., & Magueresse, A. (2019). Toughened PS/LDPE/SEBS/xGnP ternary composites: morphology, mechanical and viscoelastic properties. *International Journal of Lightweight Materials and Manufacture*, *2*(1), 64–71. https://doi.org/10.1016/j.ijlmm.2018.12.003

Peng, Y., Guo, X., Cao, J., & Wang, W. (2017). Effects of two staining methods on color stability of wood flour/polypropylene composites during accelerated UV weathering. *Polymer Composites*, *38*(6), 1194–1205. https://doi.org/10.1002/pc.23683

Petigny, J., Ménigault, C., Luisce, T., Harscoët, E., David, A., Mitsios, A., Laberge, M., Lysenko, D., Moore, P., Dimoff, A., & Solly, J. (2019). *Economic study of the Canadian plastic industry, markets and waste : summary report to Environment and Climate Change Canada*.

Phuong, N. N., Zalouk-Vergnoux, A., Poirier, L., Kamari, A., Châtel, A., Mouneyrac, C., & Lagarde, F. (2016). Is there any consistency between the microplastics found in the field and those used in laboratory experiments? *Environmental Pollution*, *211*, 111–123. https://doi.org/10.1016/j.envpol.2015.12.035

Pötschke, P., Pegel, S., Claes, M., & Bonduel, D. (2008). A novel strategy to incorporate

carbon nanotubes into thermoplastic matrices. *Macromolecular Rapid Communications*, *29*(3), 244–251. https://doi.org/10.1002/marc.200700637

Pour, R. H., Hassan, A., Soheilmoghaddam, M., & Bidsorkhi, H. C. (2016). Mechanical, thermal, and morphological properties of graphene reinforced polycarbonate/acrylonitrile butadiene styrene nanocomposites. *Polymer Composites*, *37*(6), 1633–1640. https://doi.org/10.1002/pc.23335

Qiu, G. X., Ehrenstein, G. W., & Raue, F. (2002). Mechanical properties and morphologies of PP/mPE/filler composites. *Journal of Applied Polymer Science*, *83*(14), 3029–3035. https://doi.org/10.1002/app.2333

Rabek, J. F. (1995). *Polymer Photodegradation: Mechanisms and Experimental Methods*. Chapman & Hall.

Rafeie, O., Razavi Aghjeh, M. K., Tavakoli, A., Salami Kalajahi, M., & Jameie Oskooie, A. (2018). Conductive poly(vinylidene fluoride)/polyethylene/graphene blend-nanocomposites: Relationship between rheology, morphology, and electrical conductivity. *Journal of Applied Polymer Science*, *135*(23), 1–13. https://doi.org/10.1002/app.46333

Ragaert, K., Delva, L., & Van Geem, K. (2017). Mechanical and chemical recycling of solid plastic waste. *Waste Management*, *69*, 24–58. https://doi.org/10.1016/j.wasman.2017.07.044

Ragaert, K., Huysveld, S., Vyncke, G., Hubo, S., Veelaert, L., Dewulf, J., & Du Bois, E. (2020). Design from recycling: A complex mixed plastic waste case study. *Resources, Conservation and Recycling*, *155*, 1–9. https://doi.org/10.1016/j.resconrec.2019.104646

Ramos, M. A., & Belmontes, F. A. (1991). Polypropylene/Low Density Polyethylene Blends With Short Glass Fibers. II: Effect of Compounding Method on Mechanical Properties. *Polymer Composites*, *12*(1), 1–6. https://doi.org/https://doi.org/10.1002/pc.750120102

Ran, C., Wang, M., Gao, W., Ding, J., Shi, Y., Song, X., Chen, H., & Ren, Z. (2012). Study on photoluminescence quenching and photostability enhancement of MEH-PPV by reduced graphene oxide. *Journal of Physical Chemistry C*, *116*(43), 23053–23060. https://doi.org/10.1021/jp306631y

Ranby, B. (1989). Photodegradation and photo-oxidation of synthetic polymers. *Journal of Analytical and Applied Pyrolysis*, *15*, 237–247.

Rivaton, A., Serre, F., & Gardette, J. L. (1998). Oxidative and photooxidative degradations of PP/PBT blends. *Polymer Degradation and Stability*, *62*(1), 127–143. https://doi.org/10.1016/S0141-3910(97)00271-1

Rostami, A., Masoomi, M., Fayazi, M. J., & Vahdati, M. (2015). Role of multiwalled carbon nanotubes (MWCNTs) on rheological, thermal and electrical properties of PC/ABS blend. *RSC Advances*, *5*(41), 32880–32890. https://doi.org/10.1039/c5ra04043d

Sadeghi, A., Moeini, R., & Yeganeh, J. K. (2019). Highly conductive PP/PET polymer blends with high electromagnetic interference shielding performances in the presence of thermally reduced graphene nanosheets prepared through melt compounding. *Polymer Composites*, *40*(S2), E1461–E1469. https://doi.org/10.1002/pc.25051

Sarfraz, M., Liaqat, W. A., Ali, M., & Qaiser, A. A. (2022). Graphene-integrated thermoplastic vulcanizates: Effects of in-situ vulcanization on structural, thermal, mechanical and electrical properties. *Progress in Rubber, Plastics and Recycling Technology*, *39*(2), 181–194. https://doi.org/10.1177/14777606221147928

Schyns, Z. O. G., & Shaver, M. P. (2020). Mechanical Recycling of Packaging Plastics: A Review. *Macromolecular Rapid Communications*, *2000415*, 1–27. https://doi.org/10.1002/marc.202000415

Siddiqui, J., & Pandey, G. (2013). A Review of Plastic Waste Management Strategies. *International Research Journal of Environment Sciences*, *2*(12), 84–88. www.isca.me

Silva, D. J., & Wiebeck, H. (2020). Current options for characterizing, sorting, and recycling polymeric waste. *Progress in Rubber, Plastics and Recycling Technology*, *36*(4), 284–303. https://doi.org/10.1177/1477760620918603

Singh, M. K., Mohanty, A. K., & Misra, M. (2023). Upcycling of waste polyolefins in natural fiber and sustainable filler-based biocomposites: A study on recent developments and future perspectives. *Composites Part B: Engineering*, *263*(May), 110852. https://doi.org/10.1016/j.compositesb.2023.110852

Strapasson, R., Amico, S. C., Pereira, M. F. R., & Sydenstricker, T. H. D. (2005). Tensile and impact behavior of polypropylene/low density polyethylene blends. *Polymer Testing*, *24*(4), 468–473. https://doi.org/10.1016/j.polymertesting.2005.01.001

Strugova, D., David, É., & Demarquette, N. R. (2023). Effect of steady shear deformation on electrically conductive PP/PS/MWCNT composites. *Journal of Rheology*, *67*(5), 977–993. https://doi.org/10.1122/8.0000647

Strugova, D., Ferreira Junior, J. C., David, É., & Demarquette, N. R. (2021). Ultra-low percolation threshold induced by thermal treatments in co-continuous blend-based PP/PS/MWCNTs nanocomposites. *Nanomaterials*, *11*(6), 2–18. https://doi.org/10.3390/nano11061620

Sultana, S. M. N., Helal, E., Gutiérrez, G., David, E., Moghimian, N., & Demarquette, N. R.

(2023). Effect of Few-Layer Graphene on the Properties of Mixed Polyolefin Waste Stream. *Crystals*, 1–14. https://doi.org/https://doi.org/10.3390/cryst13020358

Sultana, S. M. N., Pawar, S. P., & Sundararaj, U. (2019). Effect of Processing Techniques on EMI SE of Immiscible PS/PMMA Blends Containing MWCNT: Enhanced Intertube and Interphase Scattering. *Industrial and Engineering Chemistry Research*, 1–9. https://doi.org/10.1021/acs.iecr.8b05957

Sumita, M., Sakata, K., Hayakawa, Y., Asai, S., Miyasaka, K., & Tanemura, M. (1992). Double percolation effect on the electrical conductivity of conductive particles filled polymer blends. *Colloid & Polymer Science*, *270*(2), 134–139. https://doi.org/10.1007/BF00652179

Sumita, Masao, Sakata, K., Asai, S., Miyasaka, K., & Nakagawa, H. (1991). Dispersion of fillers and the electrical conductivity of polymer blends filled with carbon black. *Polymer Bulletin*, *25*(2), 265–271. https://doi.org/10.1007/BF00310802

Sun, X., Huang, C., Wang, L., Liang, L., Cheng, Y., Fei, W., & Li, Y. (2021). Recent Progress in Graphene / Polymer Nanocomposites. *Advance Materials*, *33*, 1–28. https://doi.org/10.1002/adma.202001105

Thareja, P., Moritz, K., & Velankar, S. S. (2010). Interfacially active particles in droplet/matrix blends of model immiscible homopolymers: Particles can increase or decrease drop size. *Rheologica Acta*, *49*(3), 285–298. https://doi.org/10.1007/s00397-009-0421-5

Tipton, D. A., & Lewis, J. W. (2008). Effects of a hindered amine light stabilizer and a UV light absorber used in maxillofacial elastomers on human gingival epithelial cells and fibroblasts. *Journal of Prosthetic Dentistry*, *100*(3), 220–231. https://doi.org/10.1016/S0022-3913(08)60182-1

Tu, C., Nagata, K., & Yan, S. (2017a). Influence of melt-mixing processing sequence on electrical conductivity of polyethylene/polypropylene blends filled with graphene. *Polymer Bulletin*, *74*(4), 1237–1252. https://doi.org/10.1007/s00289-016-1774-4

Tu, C., Nagata, K., & Yan, S. (2017b). Morphology and electrical conductivity of polyethylene/polypropylene blend filled with thermally reduced graphene oxide and surfactant exfoliated graphene. *Polymer Composites*, *38*(10), 2098–2105. https://doi.org/10.1002/pc.23782

Tu, C., Nagata, K., & Yan, S. (2022). Dependence of Electrical Conductivity on Phase Morphology for Graphene Selectively Located at the Interface of Polypropylene/Polyethylene Composites. *Nanomaterials*, *12*, 1–12. https://doi.org/10.3390/nano12030509

Tucker III, C. L., & Moldenaers, P. (2002). Microstructural evolution in polymer blends.

Annual Review of Fluid Mechanics, *34*(1), 177–210. https://doi.org/10.1146/annurev.fluid.34.082301.144051

Vandebril, S., Vermant, J., & Moldenaers, P. (2010). Efficiently suppressing coalescence in polymer blends using nanoparticles: Role of interfacial rheology. *Soft Matter*, *6*(14), 3353–3362. https://doi.org/10.1039/b927299b

Verma, P., Saini, P., Malik, R. S., & Choudhary, V. (2015). Excellent electromagnetic interference shielding and mechanical properties of high loading carbon-nanotubes/polymer composites designed using melt recirculation equipped twin-screw extruder. *Carbon*, *89*, 308–317. https://doi.org/10.1016/j.carbon.2015.03.063

Volder, M. F. L. De, Tawfick, S. H., Baughman, R. H., & Hart, A. J. (2013). CNTs: Present and Future Commercial Applications. *Science*, *339*(6119), 535–539. http://citeseerx.ist.psu.edu/viewdoc/download?doi=10.1.1.703.4188&rep=rep1&type=pdf

Vranjes, N., & Rek, V. (2007). Effect of EPDM on morphology, mechanical properties, crystallization behavior and viscoelastic properties of iPP+HDPE blends. *Macromolecular Symposia*, *258*, 90–100. https://doi.org/10.1002/masy.200751210

Waldman, W. R., & De Paoli, M. A. (2008). Photodegradation of polypropylene/polystyrene blends: Styrene-butadiene-styrene compatibilisation effect. *Polymer Degradation and Stability*, *93*(1), 273–280. https://doi.org/10.1016/j.polymdegradstab.2007.09.003

Wang, C. qing, Wang, H., Fu, J. gang, & Liu, Y. nian. (2015). Flotation separation of waste plastics for recycling-A review. *Waste Management*, *41*, 28–38. https://doi.org/10.1016/j.wasman.2015.03.027

Wang, F., Zhang, Y., Zhang, B. B., Hong, R. Y., Kumar, M. R., & Xie, C. R. (2015). Enhanced electrical conductivity and mechanical properties of ABS/EPDM composites filled with graphene. *Composites Part B*, *83*, 66–74. https://doi.org/10.1016/j.compositesb.2015.08.049

Wei, Z., Hou, Y., Jiang, C., Liu, H., Chen, X., Zhang, A., & Liu, Y. (2019). Graphene Enhanced Electrical Properties of Polyethylene Blends for High-Voltage Insulation. *Electronic Materials Letters*, *15*(5), 582–594. https://doi.org/10.1007/s13391-019-00158-3

Wirth-Lima, A. J., & Bezerra-Fraga, W. (2021). Graphene-based BPSK and QPSK modulators working at a very high bit rate (up Tbps range). *Optical and Quantum Electronics*, *53*(5), 1–16. https://doi.org/10.1007/s11082-021-02928-6

Wu, D., Lin, D., Zhang, J., Zhou, W., Zhang, M., Zhang, Y., Wang, D., & Lin, B. (2011). Selective localization of nanofillers: Effect on morphology and crystallization of PLA/PCL blends. *Macromolecular Chemistry and Physics*, *212*(6), 613–626.

https://doi.org/10.1002/macp.201000579

Wu, S. (1971). Calculation of interfacial tension in polymer systems. In *Journal of Polymer Science: Part C* (Vol. 34, Issue 1, pp. 19–30). https://doi.org/10.1002/polc.5070340105

Yang, M., Wang, K., Ye, L., Mai, Y. W., & Wu, J. (2003). Low density polyethylene-polypropylene blends Part 2 - Strengthening and toughening with copolymer. *Plastics, Rubber and Composites*, *32*(1), 27–31. https://doi.org/10.1179/146580103225009095

Yi, X.-S., Wu, G., & Ma, D. (1998). Property balancing for polyethylene-based carbon black-filled conductive composites. *Journal of Applied Polymer Science*, *67*(1), 131–138. http://dx.doi.org/10.1002/(SICI)1097-4628(19980103)67:1%3C131::AID-APP15%3E3.0.CO;2-4

Yoo, B. M., Shin, H. J., Yoon, H. W., & Park, H. B. (2014). Graphene and graphene oxide and their uses in barrier polymers. *Journal of Applied Polymer Science*, *131*(1), 1–23. https://doi.org/10.1002/app.39628

Yousefi, A. A., Ait-Kadi, A., & Roy, C. (1998). Effect of elastomeric and plastomeric tougheners on different properties of recycled polyethylene. *Advances in Polymer Technology*, *17*(2), 127–143. https://doi.org/10.1002/(SICI)1098-2329(199822)17:2<127::AID-ADV4>3.0.CO;2-V

Yousif, E., & Haddad, R. (2013). Photodegradation and photostabilization of polymers , especially polystyrene : review. *Springer Plus*, *2*, 1–32. https://doi.org/10.1186/2193-1801-2-398

Yui, H., Wu, G., Sano, H., Sumita, M., & Kino, K. (2006). Morphology and electrical conductivity of injection-molded polypropylene/carbon black composites with addition of high-density polyethylene. *Polymer*, *47*(10), 3599–3608. https://doi.org/10.1016/j.polymer.2006.03.064

Zaikin, A. E., Zharinova, E. A., & Bikmullin, R. S. (2007). Specifics of localization of carbon black at the interface between polymeric phases. *Polymer Science Series A*, *49*(3), 328–336. https://doi.org/10.1134/S0965545X07030145

Zhong, Y. L., Tian, Z., Simon, G. P., & Li, D. (2015). Scalable production of graphene via wet chemistry: Progress and challenges. *Materials Today*, *18*(2), 73–78. https://doi.org/10.1016/j.mattod.2014.08.019